Quench Protection System of Superconducting Quadrupole Magnet: Simulation and Experimental Studies

Arman Mohaddin Nadaf

Department of Mechanical Engineering

National Institute of Technology Rourkela

Quench Protection System of Superconducting Quadrupole Magnet: Simulation and Experimental Studies

Thesis submitted in partial fulfillment of the requirements for the degree of

Master of Technology (M.Tech.)

In

MECHANICAL ENGINEERING

(Cryogenic & Vacuum Technology)

By

Arman Mohaddin Nadaf

Roll No. 214ME5331

Under the guidance of

Prof. Sunil Kumar Sarangi

NIT, Rourkela

Dr. Soumen Kar

IUAC, New Delhi

Department of Mechanical Engineering

National Institute of Technology, Rourkela

May, 2016

Dedication

To

My Parents

Julekha Mohaddin Nadaf

&

Mohaddin Miraso Nadaf

Declaration of Originality

I, *Arman Mohaddin Nadaf*, Roll Number *214ME5331* hereby declare that this dissertation entitled *Quench Protection System of Superconducting Quadrupole Magnet: Simulation and Experimental Studies* presents my original work carried out as a M Tech student of NIT Rourkela and, to the best of my knowledge, contains no material previously published or written by another person, nor any material presented by me for the award of any degree or diploma of NIT Rourkela or any other institution. Any contribution made to this research by others, with whom I have worked at NIT Rourkela or elsewhere, is explicitly acknowledged in the dissertation. Works of other authors cited in this dissertation have been duly acknowledged under the sections “Reference” or “Bibliography”.

I am fully aware that in case of any non-compliance detected in future, the Senate of NIT Rourkela may withdraw the degree awarded to me on the basis of the present dissertation.

May 30, 2016

Arman Mohaddin Nadaf
NIT Rourkela

Acknowledgment

For successful completion of every work, there is requirement of continuous efforts of many people and to be motivated throughout the time period needs support from positive environment. After dipping my hands into the reservoir of knowledge, now I would like to pay their credits forever.

First I am thankful to Dr. Kanjilal, who allowed me to use the India's finest research facilities and given me an exposure to carry out the project work at IUAC with dynamic and intellect family. I take immense pleasure in thanking my supervisors Mr. Soumen Kar (Scientist-F, IUAC) and Prof. Sunil Kumar Sarangi (Director, NIT Rourkela) for their excellent guidance with regular assessment, innovative suggestions and endless efforts which leads to successful completion of project work.

I would also express my sincere gratitude to Dr. R.G. Sharma (Ex. NPL), Dr. T. S. Datta (Scientist-H), Dr. Anup Choudhury (Scientist-F), Mr. Rajesh Kumar (Engineer-E), Mr. Manoj Kumar (JE) and Mr. Suresh Babu (JE), for their continuous encouragement, support and understanding, without which, this project work would not have been possible.

I record my deepest gratitude to Mr. Sankar Ram (RS), Mr. Vijay Soni (RS), Mr. Navneet Suman (RS), Mr. Mukesh Kumar (RS) and Mr. Santosh Sahu (Engineer-C) for their valuable suggestions and encouragement for the accomplishment of my project work. Finally, I would like to express my heartfelt thanks to my beloved parents for their blessings, my friends (Lokesh Posa and Visakh A C) for their help and wishes for the successful completion of this project.

Arman Mohaddin Nadaf

Roll No.- 214ME5331

Abstract

The main motivation behind this thesis is to design an efficient quench protection system (QPS) for the superconducting quadrupole magnet system under development at IUAC. A detailed the magneto-static simulations have been done for the quadrupole magnet using OPERA-3D software to analyse the field profile and the magnet bore, fringe field and peak field in the conductor of the magnet system. Quench simulation with different QPS circuit configurations using OPERA-QUENCH code for a single NbTi coil and a quadrupole singlet is one of the major objectives of the thesis. One of the configurations of the protection circuit for single NbTi coil has been tested at 4.2K in a test rig. Single superconducting quadrupole coil is simulated in QUENCH package with adiabatic boundary condition for same circuit operated at current of 80A and 100A, it results in linear increment of final maximum temperature and resistance of coil after quenching. Depending on the protection circuit such as only resistor, back-to-back diode and back-to-back diode with resistor across the coil. The final temperature varies in between 38 to 47 K. The purpose of the heater power to initiate the quench in the magnet analysed and experimentally validated from the single coil experiment in LHe cryostat. The effect of dumping resistors of 0.91 and 2.5 Ω results into the decrement in original time constant ($\tau_C = 1.5\ s$) to decay the remaining current from 1 s and 0.667 s respectively is characterized. Simulation study is extended to superconducting quadrupole singlet with many combinations of circuits and get an idea about mutual coupling between the coils during quench. A helium cryostat has been designed for testing of the QPS of the superconducting quadrupole doublet structure (QDS). And optimized it mechanically for minimum heat load of 21.4 W.

Keywords :– Magneto-static simulation, Quench Protection System, Maximum temperature rise, peak voltage.

Abbreviations

IUAC	Inter-University Accelerator Centre
HYRA	Hybrid Recoil Mass Analyser
LTS	Low Temperature Superconductor
HTS	High Temperature Superconductor
SQC	Superconducting Quadrupole Structure
B2B	Back-to-back
QPS	Quench Protection System
B2B D + R	Back-to-back diode plus resistor
STC	Superconducting Test Cryostat
MSLD	Mass Spectrometry Leak Detector
QSS	Quadrupole Singlet Structure
QDS	Quadrupole Doublet Structure
MLI	Multi-Layer Insulation
NbTi	Niobium Titanium
Nb_3Sn	Niobium Tin

Symbols

I	Current
L	Inductance
E_{Total}	Stored energy
T_c	Critical temperature
J_c	Critical current density
B_c	Magnetic flux density
t	Time
V_m	Maximum voltage
E_O	Initial stored-energy in the magnet
i_0	Initial current
j_0	Conductor current density to time t = 0
T	Temperature
$F^*(T)$	Function of temperature
r	Copper to superconductor ratio

ρ	Matrix resistivity
$C(T)$	Volume specific heat
$j(t)$	Conductor current density as a function of the time t
B_0	Total field
B_x	Field in x direction
B_y	Field in y direction
B_z	Field in z direction
R_Q	Coil quench resistor
R_D	Dump resistor
E_d	Energy dumped in dump resistor
τ_c	Time constant
V_L	Inductive voltage
R_{sh_D}	Shunt resistor in series with dump resistor
σ	Hoop stress
P_i	Internal pressure
r_i	Inner radius

t_c	Thickness of cylindrical CAN of LHe vessel
S_{yt}	Yield strength
P_{cr}	Critical pressure
μ	Poisson's ratio
E_e	Modulus of elasticity
f	Factor for homogeneity
M	Bending moment
e	Eccentricity
σ_{max}	Maximum permissible stress
t_1	Thickness of bottom plate
W	Total load of assembly
t_2	Thickness of upper lid
σ_t	Tensile stress
q_{1-2}	Radiative heat transfer from surface 1 to 2
q	Heat flux density
$A_{surface}$	Surface area

H_1	Heat load due to radiation
k	Thermal conductivity
A	Cross section area
H_{21}	Conduction load from each port
H_{22}	Conduction load through G10 support
H_2	Heat load through conduction
H_3	Heat load through vapour cooled current leads
H_T	Total thermal load
m	Molecular weight
A_{vent}	Vent area
ρ_{vap}	Vapour density
h_{fg}	Latent heat of vaporization
R	Gas constant
γ	Adiabatic index
V_{LHe}	Volume of LHe required
$V_{1.1\,m}$	Volume of LHe bath up to 1.1 m length

$V_{structure}$	Volume of QDS
M_{LHe}	Mass of LHe
ρ_{LHe}	Density of LHe

TABLE OF CONTENTS

LIST OF FIGURES

LIST OF TABLES

Chapter 1

1 INTRODUCTION

Inter-University Accelerator Centre (IUAC) is one of the premier heavy ion accelerator laboratory in India. The basic objective of (IUAC) is to provide front ranking accelerator based research facilities to create possibilities for internationally competitive research within the university system. The Centre has been playing a very special role of a research institute within the University system where the scientific and technical staff have dual responsibilities of facilitating research for a large user community as well as conducting their own research. Emphasis is put on encouraging group activities and sharing of the facilities at the Centre in synergy with those existing elsewhere. The Centre has established sophisticated accelerator systems and experimental facilities in project mode involving several universities for internationally competitive research in the areas of Nuclear Physics, Materials Science, Atomic Physics, Radiation Biology, Radiation Physics and Accelerator Mass Spectrometry [1]. Accelerators at IUAC produces high energy ion beams for the characterization material properties of different materials and basic studies of nuclear physics. Hybrid recoil mass analyser (HYRA) is a unique, dual-mode spectrometer designed to carry out nuclear reaction and structure studies in heavy and medium-mass nuclei using gas-filled and vacuum modes respectively and has the potential to address newer domains in nuclear physics accessible using high energy, heavy-ion beams from superconducting LINAC accelerator (being commissioned) and ECR-based high current injector system (planned) at IUAC [2]. The first stage is commissioned with normal quadrupole doublet (Q1 & Q2). Figure 1.1 shows the schematic of the HYRA installation. The first stage of HYRA is operational and initial experiments have been carried out. To guide the particle from source to the target, there is requirement of uniform magnetic field along the beam length.

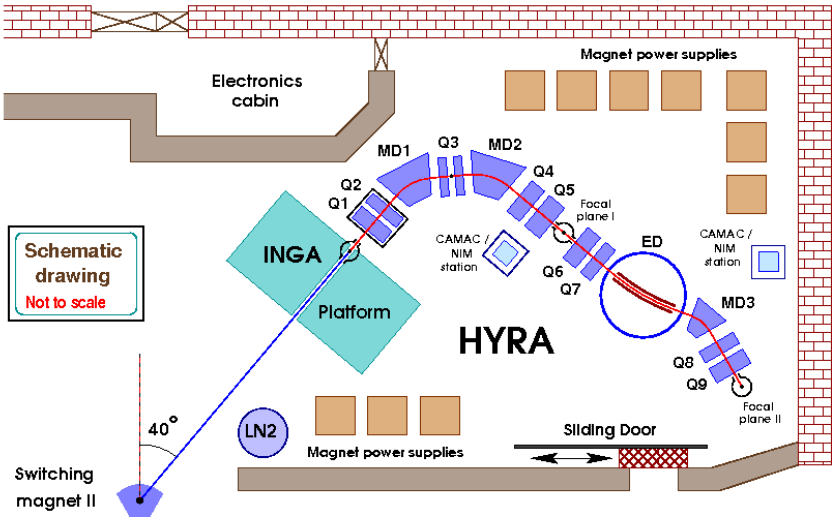

Figure 1.1 Schematic of the HYRA installation at IUAC [1]

Normal quadrupole coils are integrated on iron pole pieces. To enhance the magnetic field gradient in Q1 and Q2 with the existing space available in the beam line, Normal quadrupole doublets (Q1 & Q2) will later be replaced with superconducting quadrupole doublets. Superconducting quadrupole will provide higher field gradient (18-20T/m) which eventually enhance the separation of nuclei with higher masses. Though the superconducting coils will also be integrated with the iron pole pieces to shape the magnetic field at the centre of the bore. Hence shape of the coil will have less significant role in deciding the field profile at the central bore. Shape of the iron pole tip will have major role in determining the field profile. Iron will also be used to minimize the fringe field outside the magnet.

A Single Quadrupole will be able to focus the beam only in one axis. That is, if one is focusing in horizontal axis, it is defocusing in vertical axis. Hence in beam lines, two quadrupole singlets, with their fields focussing the beam in two perpendicular directions, are used. The normal and rotated quadrupoles are respectively shown in Figure 1.2 a) and b) [3].

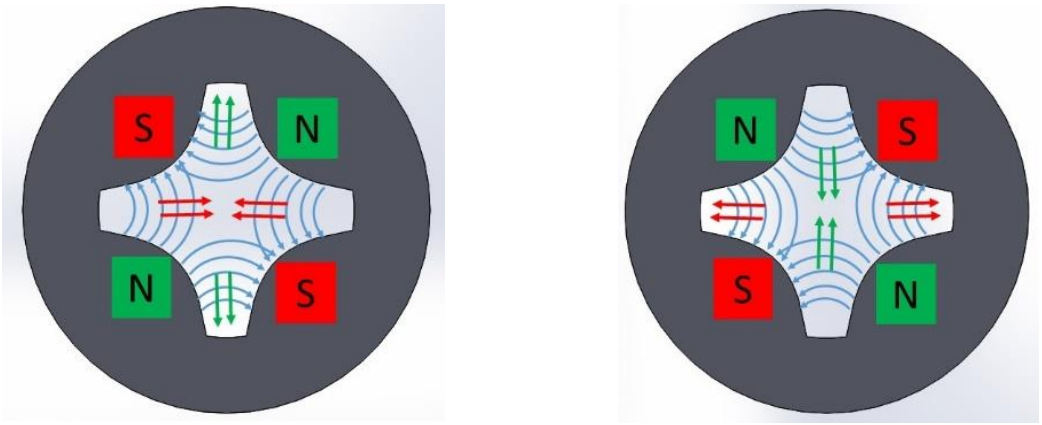

a) Rotated Normal Quad Horizontal focusing- "Focusing"

b) Normal Quad Vertical focusing- “Defocusing”

Figure 1.2 normal and rotated quadrupoles

The alternate use of focusing and defocusing is called FODO technique and is widely used in particle accelerators. To keep the accelerated ion beam in a confined central region, the vertically focusing quadrupole is followed by a horizontally focusing quadrupole whose effect is similar to ‘a pinched straw’ as shown in Figure 1.3 [3]. The FODO is analogous to the converging diverging lenses uses in optical purpose.

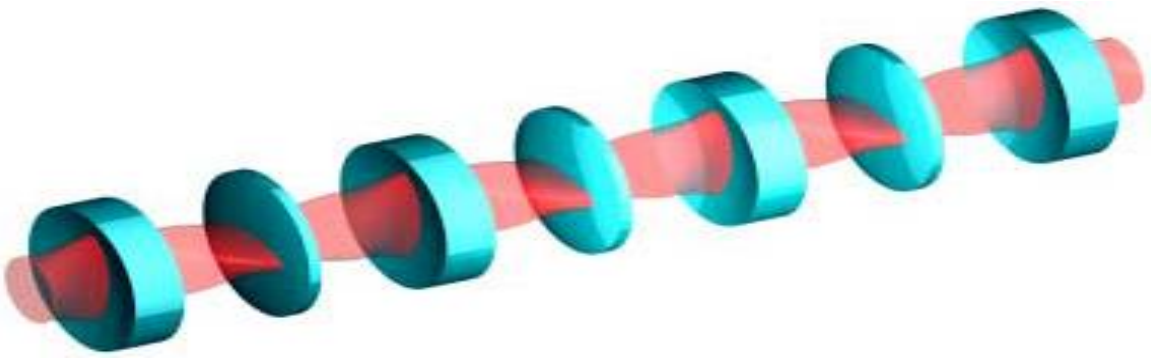

Figure 1.3 Pinched Straw Analogy with Convex and concave lens

1.1 Superconductivity

The helium cryogenics and superconductivity were respectively discovered in 1908 and 1911 by Prof. H. Kammerlingh Onnes at Leiden University. The evolution of superconductivity is

started after these main two discovery. He first observed the phenomenon of the transition of metal below its critical temperature turns into the zero resistive material called as superconducting state. Figure 1.4 shows the resistivity versus temperature behaviour of superconductor and normal conductor. The Meissner's effect comes with field expulsion from the material when cooled below its critical temperature in magnetic environment, and material started acting like perfectly diamagnetic in nature.

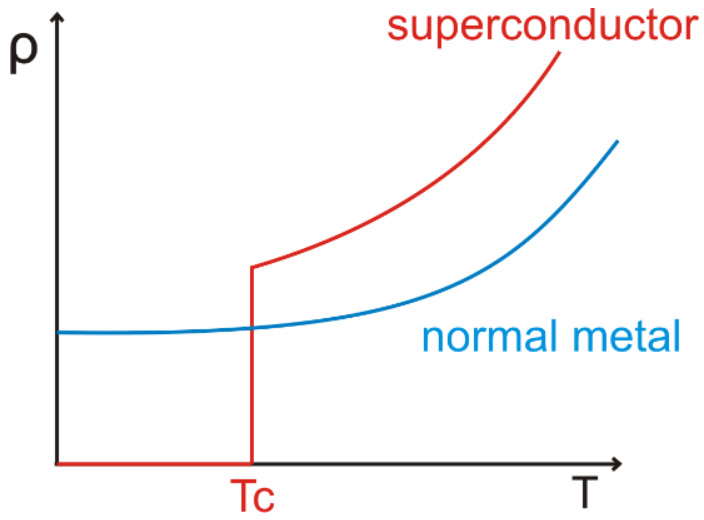

Figure 1.4 Resistivity (ρ) Vs Temperature (T) behaviour of superconductor and normal metal [4].

Based on their response in the external magnetic field, the superconductors are broadly classified into two groups; Type I & Type II. Figure 1.5 shows the magnetic field response of Type I and Type II superconductors. Type-I superconductors are pure metals like Pb, Hg, Sn, Nb and V etc. They show a sharp transition from superconducting state to the normal state with only one critical field limit called as Hc even its temperature is well below the critical limit. Type II superconductors are mostly alloys and compounds like NbTi, Nb3Sn etc shows that after certain critical field strength of Hc1, there is an existence of the mixed state form Hc1 to Hc2, in which the magnetic flux lines are passing as well as expulsing through the material is called as the mixed state.

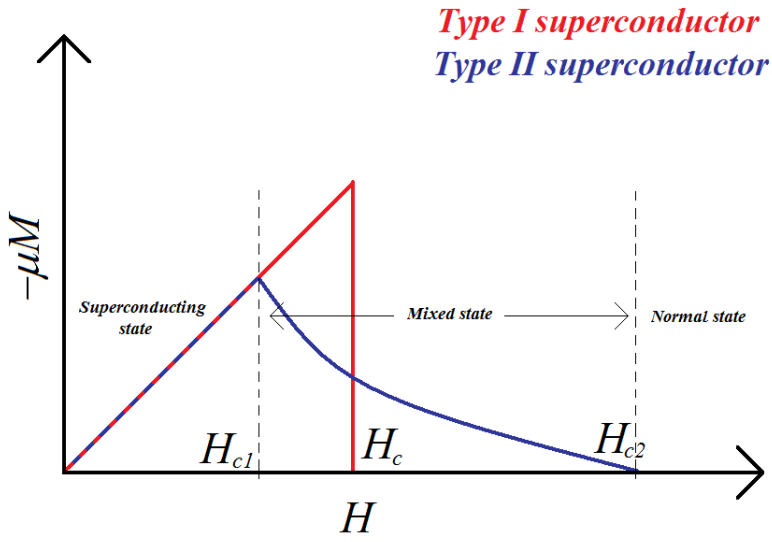

Figure 1.5 Magnetization curve of Type-I and Type-II superconductor.

Thus a type II superconductor behaves like a type I superconductor and remains perfect diamagnetic only up to the lower critical field (H_{c1}). Beyond, the material though remains superconducting but is no longer a perfect diamagnetic. At H_{c2}, the material turns normal.

On the basis of the working temperature range which is decided by the dominant fluids used for the reaching that temperature. The liquid helium (4.2K) cooled superconductors are called as low temperature superconductors (LTS) such as NbTi, Nb3Sn etc. Similarly, liquid nitrogen (77K) cooled superconductors are called as high temperature superconductors (HTS) such as BSSCO, YBCO etc. Figure 1.6 shows the LTS and HTS in terms of the cryogen (i.e. coolant) used to make them superconductor.

For high field magnet application, type-I superconductors are ruled out because their current carrying capacity is very small since the current flow is restricted to a thin surface layer and their critical field is less than few tenths of a Tesla. The higher value of upper critical field of many type-II superconductors make them very attractive for building magnets for generating high magnetic field. However, type-II superconducting wire needs to carry large current in the presence of high magnetic field. Apparently, type–II superconductors appear quite suitable on first sight because of their large upper critical field but pure type II superconductors are found to have rather low current density in presence of magnetic field.

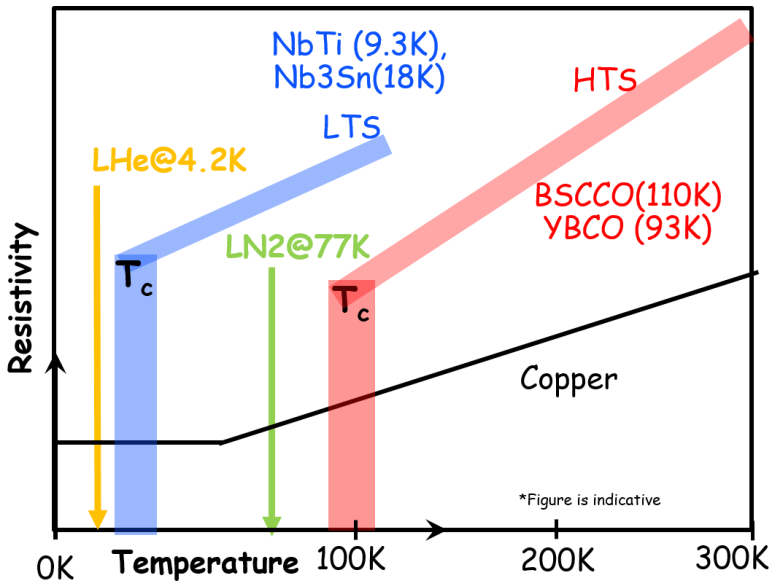

Figure 1.6 LTS and HTS superconductors and corresponding coolant diagram [6].

Figure 1.7 shows the critical magnetic field versus the critical current density of 0.8mm wire of NbTi , Nb3Sn and BSCCO at 4.2K and NbTi at 1.8K [Ref Ramesh Gupta's Lecture].

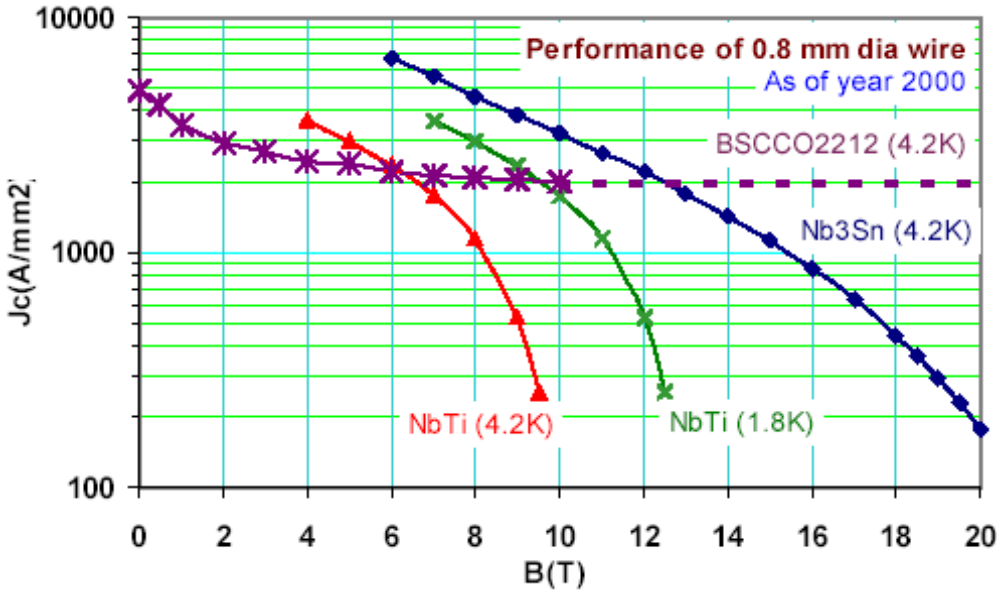

Figure 1.7 Critical field versus critical current density of different practical superconductors at different temperature [7].

The applications of the both LTS and HTS are as per field requirement for the user. The NbTi are best option for the lower field application up to 8T and the Nb3Sn can be used up to 15 T for the application like Magnetic Resonance Imaging (MRI), superconducting dipole and quadrupole and Superconducting Quantum Interface Device (SQUID) etc. HTS application are for the higher field such as Nuclear Magnetic Resonance (NMR) Spectroscopy, Superconducting Magnetic Energy Storage (SMES) and Low temperature physics experiment purpose where high field is required for characterization of the material.

1.2 Quench in Superconducting magnet

A superconductor undergoes a transition from its superconducting state to a normal conducting state beyond a critical value of temperature ($\boldsymbol{T_c}$), current density ($\boldsymbol{J_c}$) and the magnetic flux density ($\boldsymbol{B_c}$). Just the same way in a superconducting (SC) magnet, the moment any of these parameters exceeds its critical value, it too turns normal. This transition from superconducting state to resistive state in a magnet is known as a quench. Quench is one of the crucial phenomena for any superconducting magnet. The stored energy (E_{Total}) in a solenoid magnet at a current (I) is given by [8],

$$E = \frac{1}{2} L I^2 \qquad (1.1)$$

where, $\boldsymbol{L}$ is the inductance of the solenoid magnet.

During quench, the stored energy of the magnet is adiabatically converted into the heat energy which eventually may raise the temperature of the magnet to dangerous level. This heat dissipation is not uniform around the magnet winding. The localized heating causes growth of normal zone which eventually decay the magnet current. The maximum temperature occurs at the initiating point, called as hot spot, will always suffer the highest temperature rise, due to longest joule heating time. The excessive rise in hot spot temperature causes insulation failure and even melting of the conductor, further driving the conductor to an irreversible damaged condition [8].

Even if we bind the temperature within a safety limit, the most prominent issues are the voltages developed between turn-to-turn, layer-to-layer and coil-to-ground during the quench process.

These excessive voltages can cause voltage breakdowns and arcing. The arc provides path for the stored energy to dissipate at the location where arcing occurs and causes the coil to melt [9]. The reduction in overall current density J of the conductor will rapidly reduce the maximum temperature by extending dissipation time, will also reduce Vm. The method to reduce J is to add more copper so that overall resistivity will decrease, as superconductors having much higher resistivity then copper at room temperature.

To avoid above mentioned problems related to quenching of superconducting magnet, a Quench Protection System (QPS) is necessary across the magnet.

1.3 Objective of Thesis

1. One of the major objective of the thesis is the magneto-static simulation of superconducting quadrupole with super- ferric iron core using OPERA-3D FEA Code.
2. Quench Simulation of Superconducting quadrupole magnets using OPERA-3D FEA code.
3. Quench Simulation of single superconducting coil using OPERA-3D code and experimental validation of quench in 4K test rig
4. Design of the 4K rig for testing of the superconducting quadrupole doublet

Chapter 2

2 LITERATURE SURVEY

First studies related to simulation of quench phenomena in superconducting magnets was done by Dr. M. N. Wilson at RHEL in 1968 [8]. He developed a 'quench' computer simulation programme at RHEL to simulate the current decay and energy dissipation in the magnet during quench. A circuit breaker was used to disconnect the magnet from the power supply as quench happens and a parallel external dump resistor was used as protection scheme to dissipate the quench energy away from the cryogenic environment (figure 2.1). A test solenoid was used to verify the results obtained from the programme and it was confirmed that the use of the external resistor for energy dumping, reduces the boil-off of liquid helium from 400 litres to 16 litres. It was also seen that the use of a protection circuit also helps to limits the open circuit peak temperature in range of 35 – 40 K when a 1Ω was used while it was as high as 150 K when no protection circuit was employed.

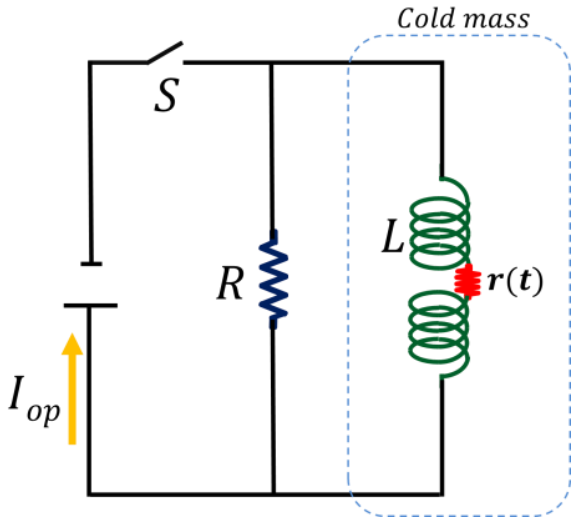

Figure 2.1 Protection by means of a switched external dump resistor

In ISABELLE project [10] the protection circuit consists of room temperature diodes connected across each magnet having high enough forward voltage to prevent any leakage current during charging or operation. When magnet quenches, the voltage across the coil increases above the bias voltage of diode and after that diode acts as a closed switch

bypassing the magnet current. But the use of room temperature diode pose some problems, the number of expensive diodes used increases since the forward bias voltage of diodes are lower at room temperature compared to cold conditions. In case of individual protection circuit for each coil the leads of the diodes represent a considerable heat load to the helium vessel. These problems were overcome by installing the diodes directly on the magnets in the cryogenic condition. (Figure 2.2) shows that there was an increment in bias voltage from 0.7 V to 1 V is seen as temperature decreases from room temperature to 30 K, below 30 K the bias voltage shoots high and at 4.2 K exceeds 20 V for cold silicon diodes. The diodes are anchored with a copper mass of 7 kg, which allows using the diode to maintain constant forward bias voltage by staying at a constant temperature.

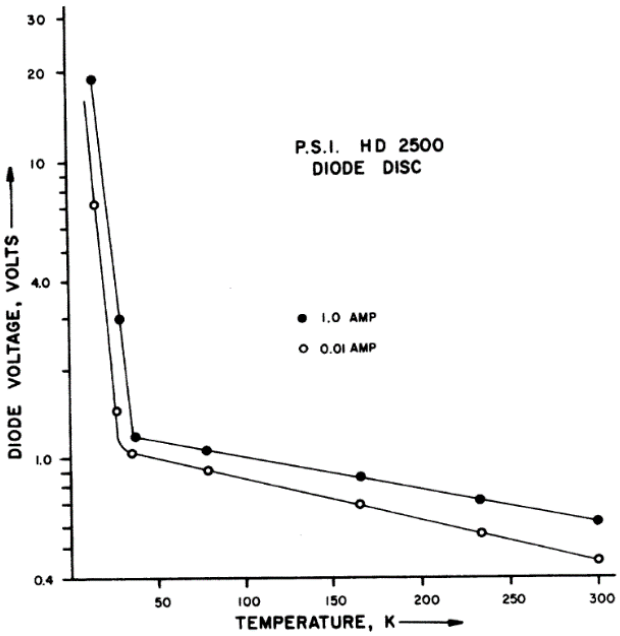

Figure 2.2 Forward bias voltage for a high current silicon diode as a function of temperature

The resistors when used as dump resistors are not a good choice in superconducting magnets since at time of energizing the resistor creates an alternating path for the current to flow thus producing helium boil-off due to joule heating. To avoid this problem, the non-linear components such as power diodes, which shows high resistances during charging and low resistance during quench condition are used in the resistance circuit as shown in (figure 2.3). At 4.2 K, when the diode is acting as an open switch, it offers a forward bias voltage of 9 V, but as soon that voltage is crossed and the diode starts conducting the voltage drops reduces to

1.4 V thus acting as good conducting path. The response time of the diode was seen to be around 1 ms to protect the persistent switch (PCS) which was connected across racetrack coil [11].

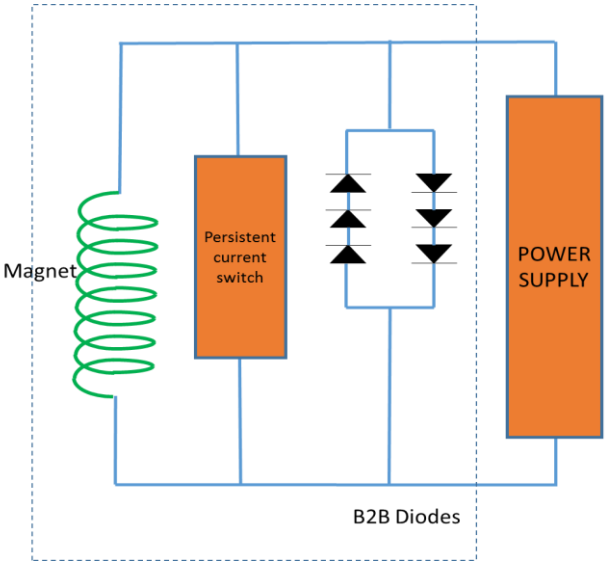

Figure 2.3 A general circuit for protectio of the PCS

The maximum voltage (V_m) across the coil [12] is given by the following equation

$$V_M = \frac{E_0 j_0^2}{F^*(T) i_0} \frac{r+1}{r} \tag{2.1}$$

where E_O is initial stored-energy in the magnet, j_0 is the conductor current density to time = 0, i_0 is the initial current, r is the copper to superconductor ratio of the conductor and $F^*(T)$ is function of temperature which is given as

$$F^*(T) = \int_0^{T_M} \frac{C(T)}{\rho(T)} dT = \frac{r+1}{r} \int_0^{\infty} j(t)^2 dt \tag{2.2}$$

where, $C(T)$ is the volume specific heat; r is the matrix resistivity; T is temperature; $j(t)$ is the conductor current density as a function of the time t during the quench. The subdivision mechanism reduces the maximum possible voltage across the coil as the energy associated with each subdivision almost reduces with factor of subdivision.

The protection circuit used at MICE coupling magnet [9] consists of a pair of back-to-back diodes with a shunt resistor across each subdivision of the coil. A Semi-empirical model was

developed which fetches both coil subdivision as well as quench-back from the mandrel. Adiabatic boundary condition is used to determine the temperature from the joule heating in the quenching volume. Without shunt resistors across the coil peak temperature of ~135 K was produced and ground-to-voltage of 2.7 kV was developed. A shunt resistor of 5Ω reduces the peak temperature to ~100 K and peak-to-ground voltage to 1.35 kV. The following (figure 2.4) shows the subdivision circuit used for the MICE coupling magnet.

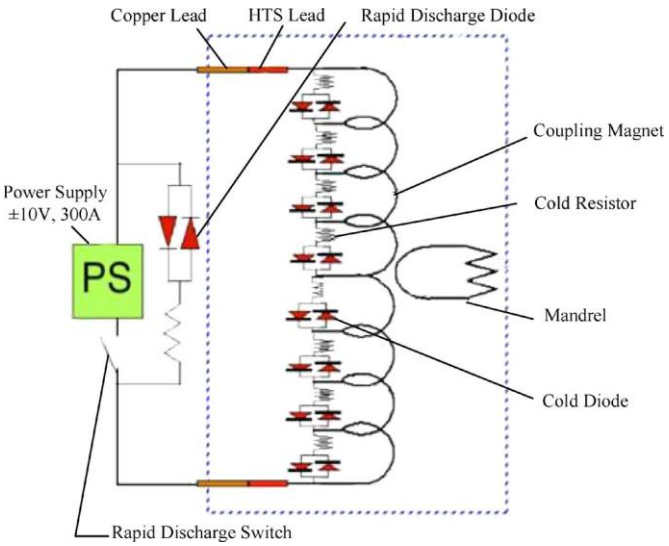

Figure 2.4 Protection of the MICE coupling magnet

The 9.4 T MRI superconducting magnet at CAS, Beijing [13] uses two passive quench protection circuits are used across the main coil after subdivision and other four coils are combined into one section which is them connected to a third protection circuit (as shown in figure 2.5). Quench heaters are also used in this case to spread the quench faster. These heaters are basically resistors and powered through split current due to voltage generation across the quenching section. The peak voltage of 600 V with maximum hoop stress of 150 MPa in case of coil 12 ensures safety of the magnet.

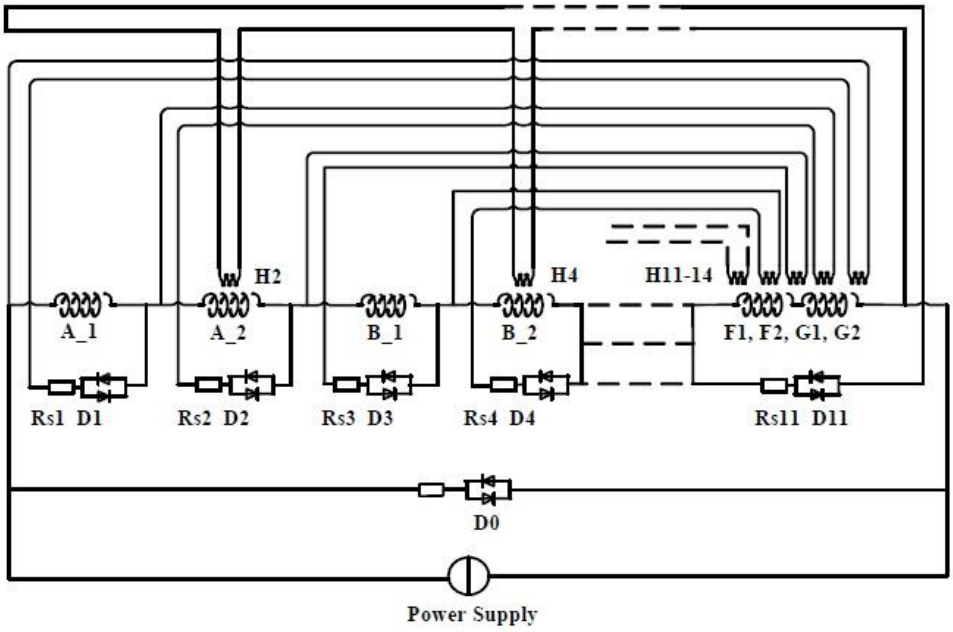

Figure 2.5 Configuration of the heater network used for 9.4 T MRI magnet at CAS

During charging and discharging the voltage developed across the diode should be less than 80 % of the diode forward voltage at 4.2 K. The power diodes R620 (as shown in figure 2.6) and R7HC series shows no orientation effect on the forward voltage when place in the magnetic environment [14]. Whereas, Normal silicon diodes which are used for the temperature measurements shows strong anisotropy with both the magnetic field and orientation of the diode [15].

Figure 2.6 A Powerex R6201250xx diode rated at 500 A with a backward voltage of 1200 V

2.1 Superconducting Quadrupole at IUAC

Superconducting Quadrupole Structure (SQC) for ion focusing purpose for Hybrid Recoil Mass Analyser (HYRA) is under development at IUAC, New Delhi. It will consist of 8 superconducting NbTi coils of racetrack type. The coils will be mounted on soft super ferric iron structure which confine the magnetic field lines within its volume by allowing high permeable magnetic path. The ideal quadrupole develops a zero field at centre. To get minimum residual field at the centre in any quadrupole configuration, four iron pole pieces should ideally be exactly symmetric. The details of the SQC are shown in figure 2.7

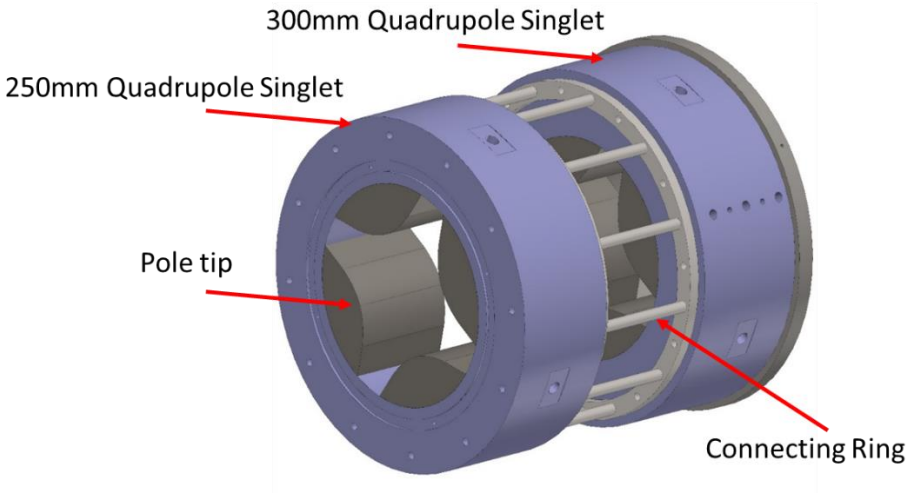

Figure 2.7 Superconducting Quadrupole Doublet Structure

The setup consist of doublet arrangement of quadrupoles separated by 300mm spacing in between them. The two singlets used are identical in all aspects expect the axial length of the racetrack coil, which are different for the two singlets. The pole tips and yoke are made up of super-ferric iron (AISI-1010). The yoke of iron structure have inner diameter (ID) & outer diameter (OD) 590 & 780 mm respectively. Each pole tip is placed at 450 from each other, having diametrically opposite fitted coils on it. The connecting ring of 300 mm length in between these two singlet is made of stainless steel to separate them from each other.

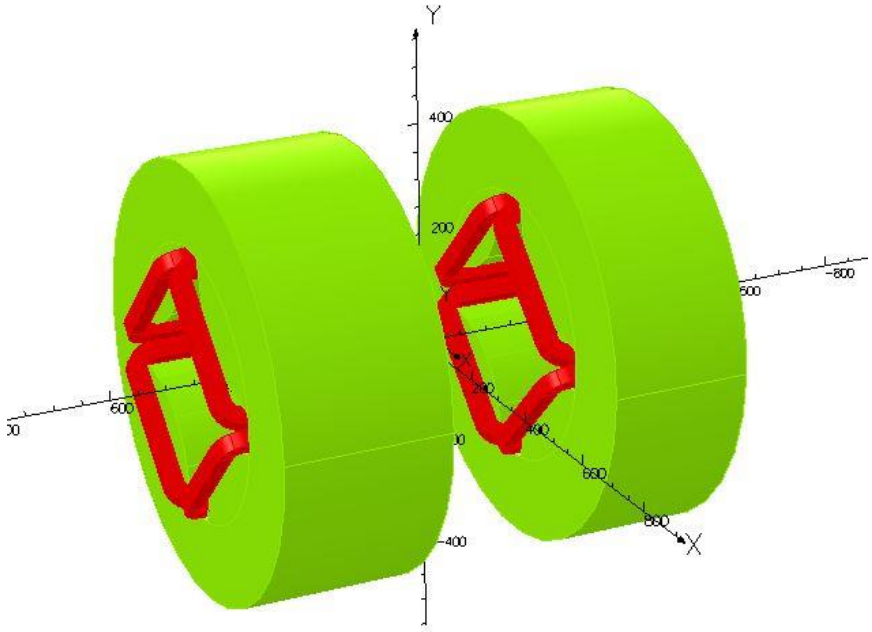

Figure 2.8 SQDS quadrupole, IUAC design [Red: superconducting NbTi coils and Green: iron yoke]

Figure 2.8 shows that, there would be total eight numbers of NbTi coils in the quadrupole doublet; four coils are of 300mm of length (nomenclature: SQC-300) and another four coils are of 250mm (SQC-250) length. Each coil configuration is similar to the racetrack. Individual racetrack coils from each singlet is shown in figure 2.9. The coils are made of multi-filamentary NbTi wire. The specification of the NbTi wire is shown in the Table 2.1.

Table 2.1 Specification of NbTi wire

Parameter	Value
Bare Dia	0.7mm
Cu:Sc	8:1
Ic@Bc	150A@3T
Ic@ Bc	85A@6T

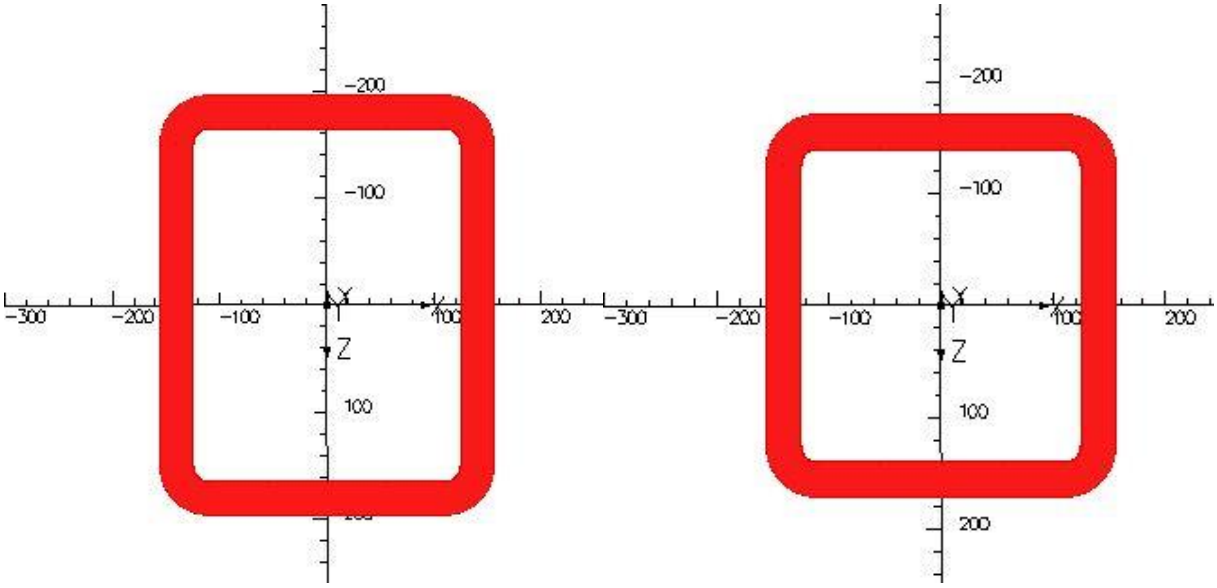

a. SQC-300 coil of 300mm of length b. SQC-250 coil of 250 mm of length

Figure 2.9 Racetrack coils from individual singlets

The diameter of the wire with Formvar insulation is 0.75mm with 8:1 copper to superconducting ratio. Figure 2.10 shows the critical current versus critical magnetic field of the multi-filamentary NbTi wire used for the coils.

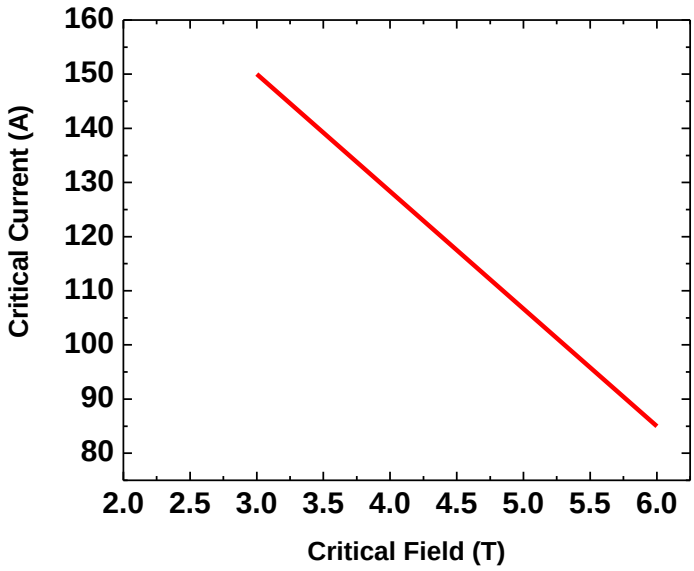

Figure 2.10 Critical current versus critical field curve of the NbTi conductor used for racetrack coil

All the 8 coils are random windings using NbTi wire ϕ0.75mm and have 1600 turns. After winding the coils are wrapped with glass cloth and impregnated using stycast epoxy.

Each singlet have 4 NbTi superconducting coils with alternate coils having opposite current direction. This causes to cancel out the central field at axis of the singlet structure. Each coil has 1600 turns. Each singlet will be energized through separate power supplies. The inductance of each SQC-300 and SQC-250 coil is measured to be respectively 1.35 H and 1.5H respectively. When placed in the iron structure the respective inductances increases to 1.6H and 1.8H. In case of individual singlets, the 250mm and 300mm singlets shows total inductances of 8.4 H and 9.1 H respectively. This non-linear increase in the inductance of the four coils combined is due to the presence of mutual coupling of the coils with each other.

The co-ordinates of the mid –point of the 300 mm singlet centres is (0, 0, 300) and of 250mm singlet is (0, 0, -275). The pole tips are hyperbolic in profile with centre (95.459415, 95.459415, 300) for the 300mm pole tip and (95.459415, 95.459415, -275) for the 250mm pole as shown in figure 2.5. The centre co-ordinates of the pole tips are changes its sign as the quadrant changes.

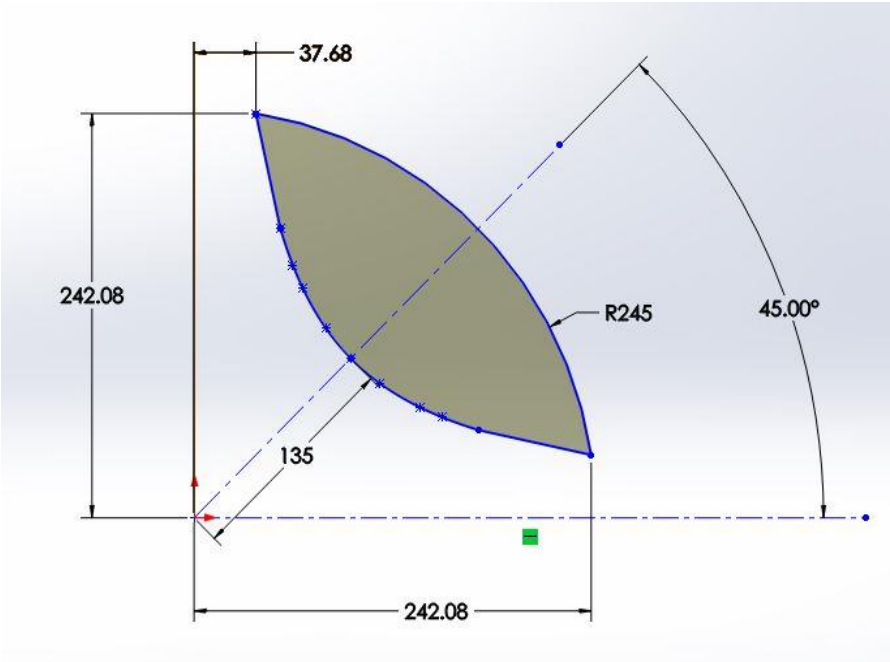

Figure 2.11 Pole tip of the Superconducting Quadrupole

Chapter 3

3 THE MAGNETO-STATIC SIMULATION OF SUPERCONDUCTING QUADRUPOLE DOUBLET STRUCTURE

The main aim in performing magneto-static simulations is to get an idea about the field profile inside the magnet and super-ferric iron structure and the electromagnetic forces that are produced from these fields. These forces act on the superconducting magnets during both normal operation and also quench state. During quenching the unbalanced current flow causes unbalanced electromagnetic force can produce considerable coil motions and the coil strains [16]. To enhance the magnetic field in the coil centres, soft iron pole tips of low carbon iron (AISI-1010) is used. This material which has high permeability, can shape the field by providing a low resistance path for the magnetic flux to flow while restricting the field into core structure of the magnet thus reducing the fringe field outside of doublet structure [17].

3.1 3D model of the Superconducting Quadrupole Doublet Structure in OPERA

The non-linear magneto-static problem is solved using TOSCA module available in OPERA-3D by Vector Fields. The module uses a formulation involving reduced and total scalar potentials. The Ferric Iron structure is modelled in a CAD software and imported into the module while the 8 Biot-sarvat conductors present in the doublet structure are modelled in the software environment (Figure 3.1). A 20 mm mesh is used for meshing the model while a smaller mesh of 10 mm size is used in critical areas such as pole tip. Other parameters such as current density, boundary conditions etc. are also given before the model is solved to find the magnetic field.

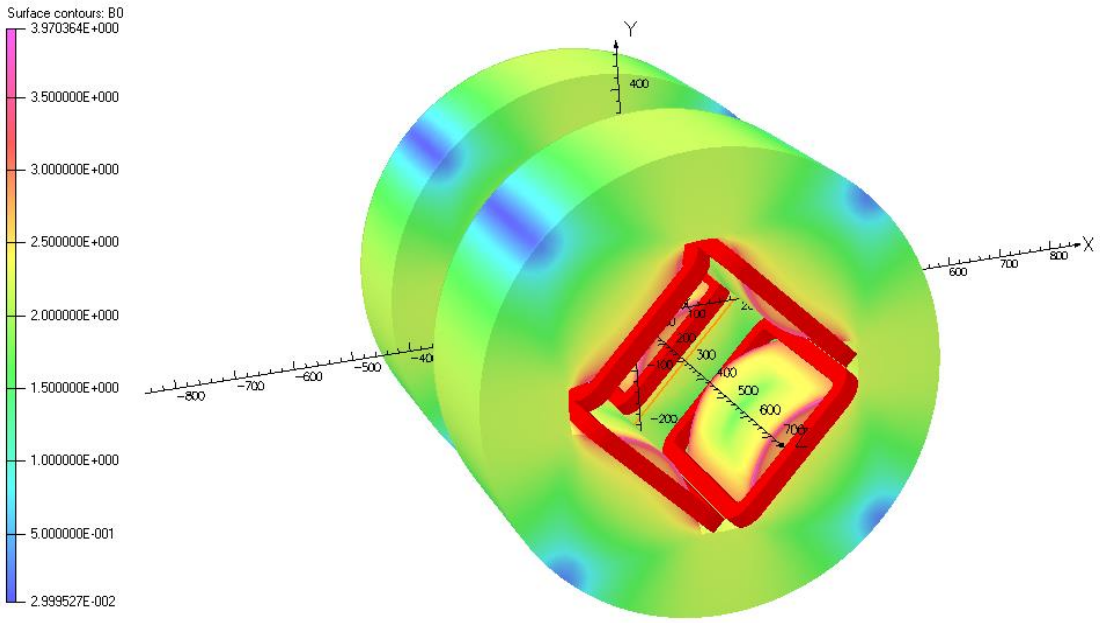

Figure 3.1 Magneto-static simulation of Quadrupole Doublet Structure

3.1.1 300mm Singlet quadrupole

Figures 4.2 shows the variation of total field and three components of the fields from one pole tip to the diametrically opposite pole tip it can be seen from figure 3.1 that B0 is linearly decreasing from the pole tip to the centre and further increasing with same gradient up to the next pole tip. The 14 Gauss residual field obtained at the centre is not an issue as per the focusing requirement concern. In figure 3.2 b) and c), it can be seen that $B_x$and B_y are showing same behaviour both in terms of magnitude and polarity. The X and Y component of the magnetic field in the pole tips are of the same magnitude but changes their polarity when moving from one pole to another and both components become zero near to the centre. The B_z in figure 3.2 d) is showing random variation between two pole tip, and component is contributing in the residual field at centre. The field values at the pole tips of the 300 mm singlet, calculated using OPERA are given in table 3.1.

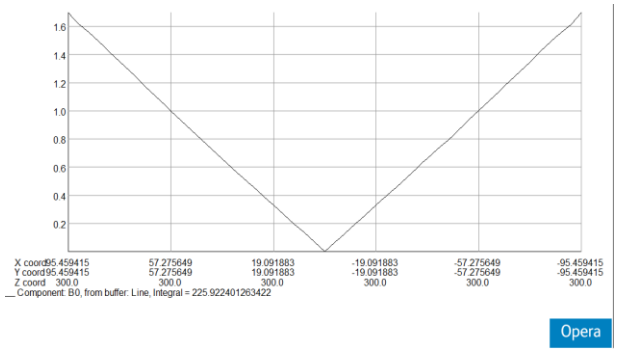

a) Variation of Total field (B_0),T from one pole tip to opposite pole tip

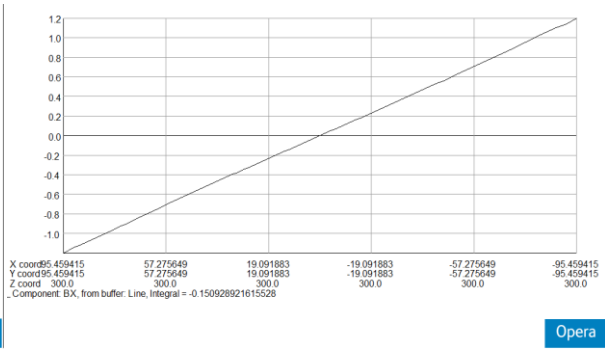

b) Variation of B_x,T from one pole tip to opposite pole tip

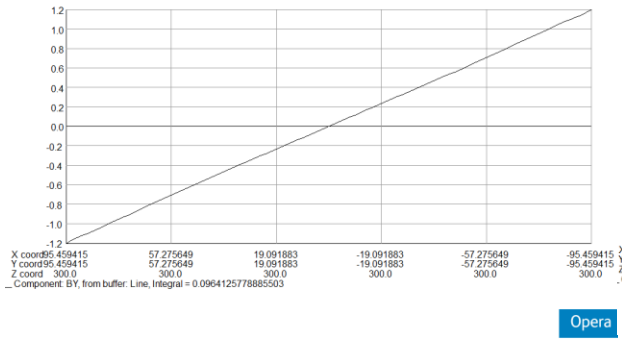

c) Variation of B_y,T from one pole tip to opposite pole tip

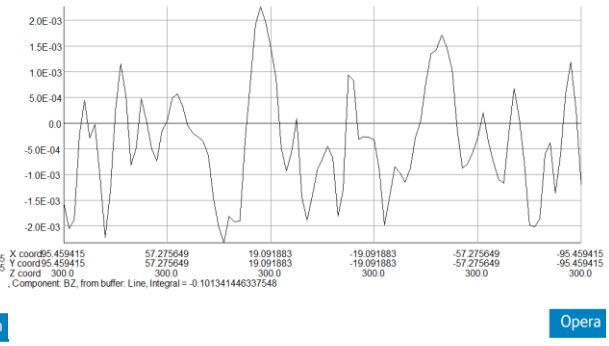

d) Variation of B_z,T from one pole tip to opposite pole tip

Figure 3.2 Variation of field from one pole tip to opposite pole tip

Table 3.1 Fields at pole tips and at centre

Field location	Co-ordinates, mm	Field , T
I Quadrant pole tip	95.459415, 95.459415, 300	1.699
II Quadrant pole tip	-95.459415, 95.459415, 300	1.711
III Quadrant pole tip	-95.459415, -95.459415, 300	1.699
IV Quadrant pole tip	95.459415, -95.459415, 300	1.701
Residual field at centre	0, 0, 300	1.37×10^{-3}

3.1.2 250 mm singlet quadrupole

The graphs plotted for the field variation are in below figure 3.3 from one pole tip to other pole tip. The 250mm singlet also showing the same behaviour as that of the 300mm singlet with residual field value of 22 Gauss at the centre. Hence the criteria of the magnetic centre matching with geometric centre is fulfilled to get higher focusing power. The field values calculated in OPERA are given in the following table 3.2 on the pile tips of the 250mm singlet iron structure.

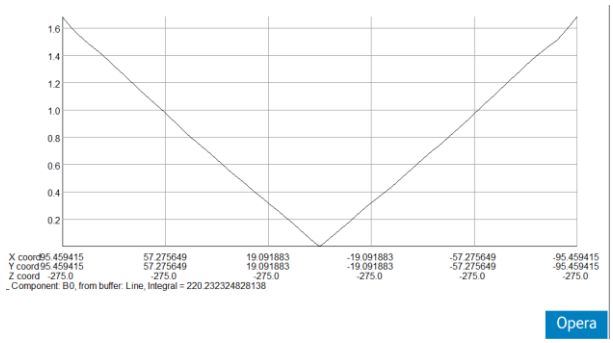

a) Variation of B_0,T from one pole tip to opposite pole tip

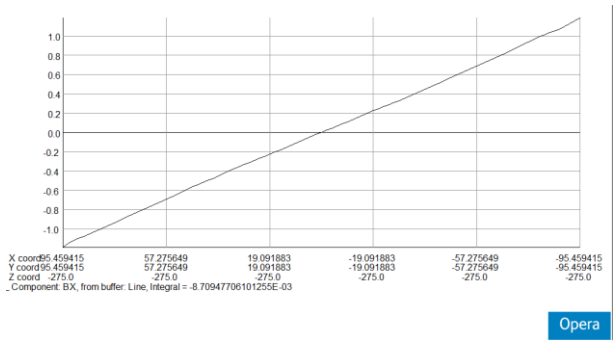

b) Variation of B_x,T from one pole tip to opposite pole tip

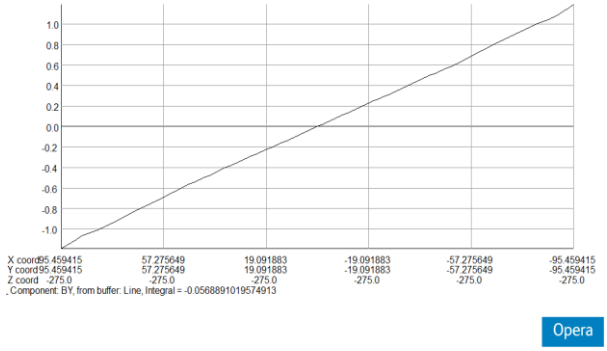

c) Variation of B_y,T from one pole tip to opposite pole tip

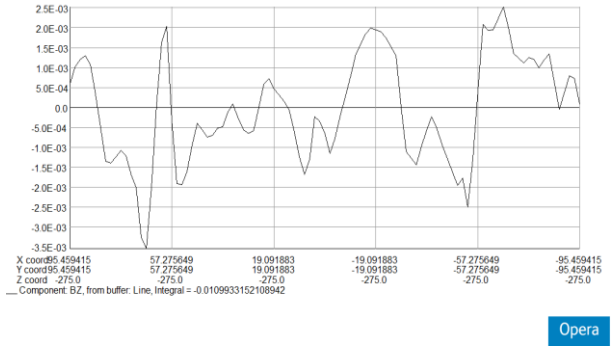

d) Variation of B_z,T from one pole tip to opposite pole tip

Figure 3.3 Variation of field from one pole tip to opposite pole tip

Table 3.2 Fields at pole tips and at centre

Field location	Coordinates, mm	Field, T
I Quadrant pole tip	95.459415, 95.459415, -275	1.68140694
II Quadrant pole tip	-95.459415, 95.459415, -275	1.67901388
III Quadrant pole tip	-95.459415, 95.459415, -275	1.68541027
IV Quadrant pole tip	95.459415, -95.459415, -275	1.68655209

Residual field at centre	0,	0,	-275	2.1829 x 10^{-3}

3.2 Axial Variation of magnetic field $B_{(y)}$ at different radial positions

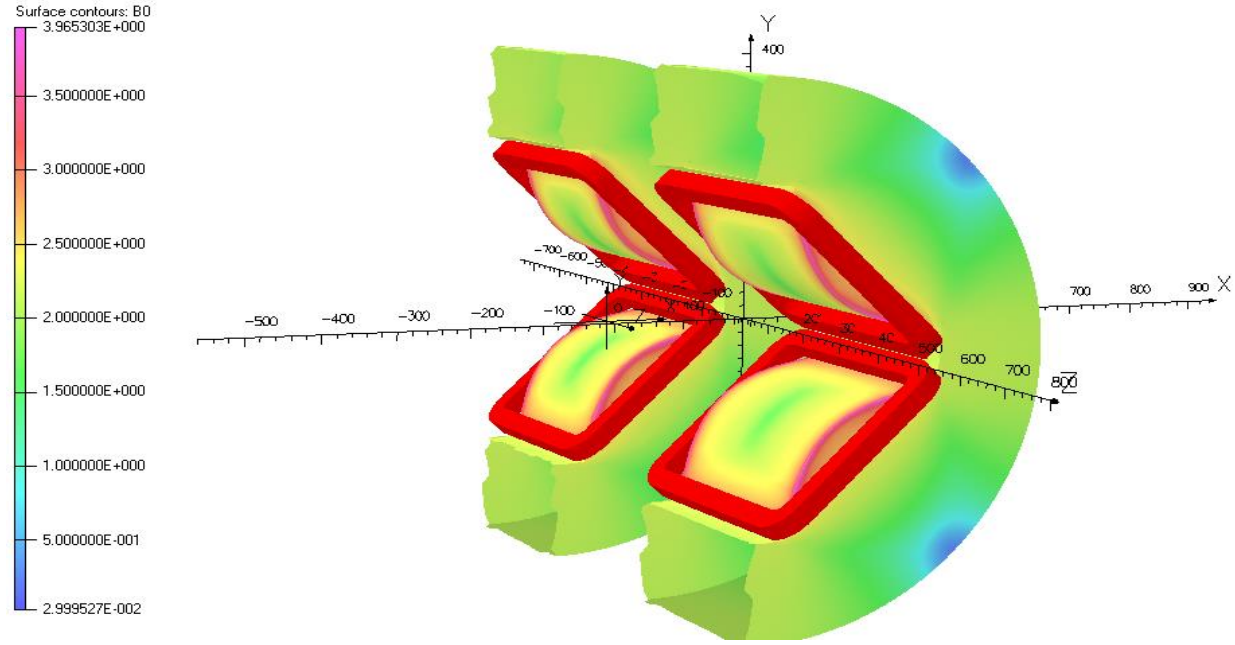

Figure 3.4 a contour of field concentration at the pole tip

The figure 3.4 shows that the field variation in the pole tips and yoke. It can be seen that there is field concentration happening at the sharp edges of pole tip. The figure 3.5 a)-d) shows the variation of B_y in x direction at different positions in Y axis. It can be seen that there is linear variation of field in the air domain up to pole tips. After that as X increases the field peak jumps rapidly within the pole tip and further increases in the yoke region. The field concentration at pole edges subjects the coils to be operated at an higher field than that of the coil centre field, which may push the coil above its the critical field limit. Further at the time of the charging / discharging or during quench the coil can experience higher stresses due to higher field force. The iron yoke provides a minimum resistance path for the magnetic flux to flow through because of its higher permeability while also increasing the pole tip field 3 to 3.5 times thus providing a higher field gradient.

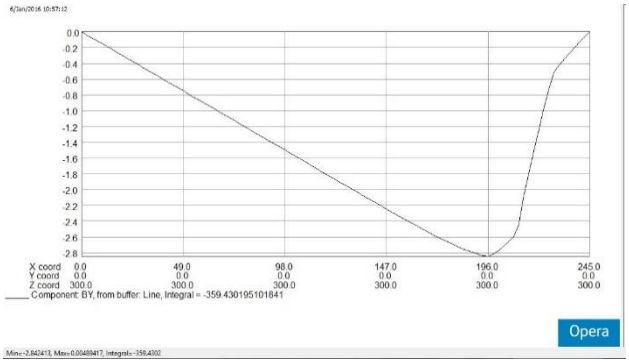

a) B_y Vs X at y=0mm

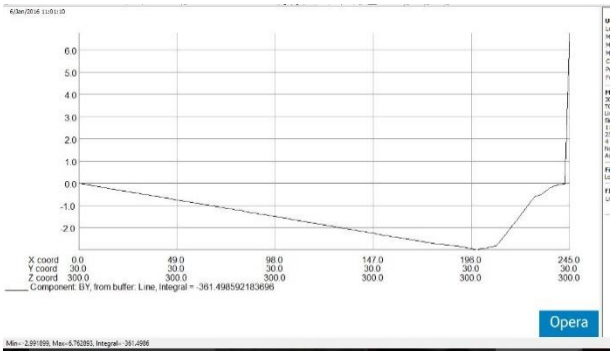

b) B_y Vs X at y=30mm

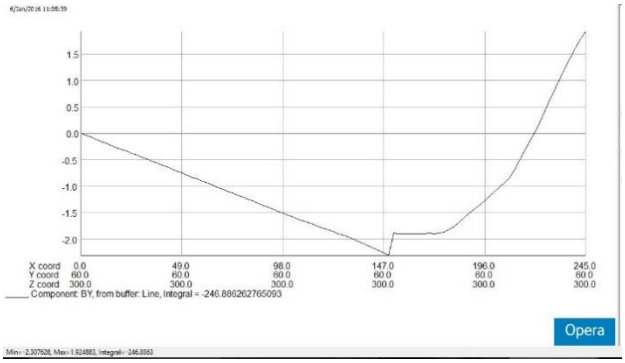

c) B_y Vs X at y=60mm

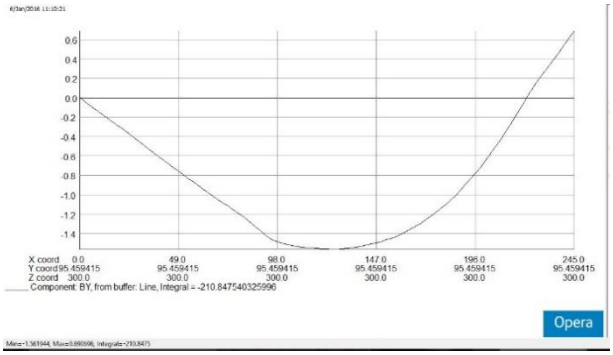

d) B_y Vs X at pole tip centre

Figure 3.5 Axial Variation of magnetic field $B_{(y)}$ at different radial positions

3.3 Field Variation (B_0), T outside the super-ferric iron structure

The field variation outside doublet structure is also an important concern from the design point of view of the cryostat which encloses the magnet during operation. The fringe fields created by the magnet can induce additional forces and eddy currents in the cryostat during operation. The YZ-plane in figure 3.6 shows the field map outside the doublet structure.

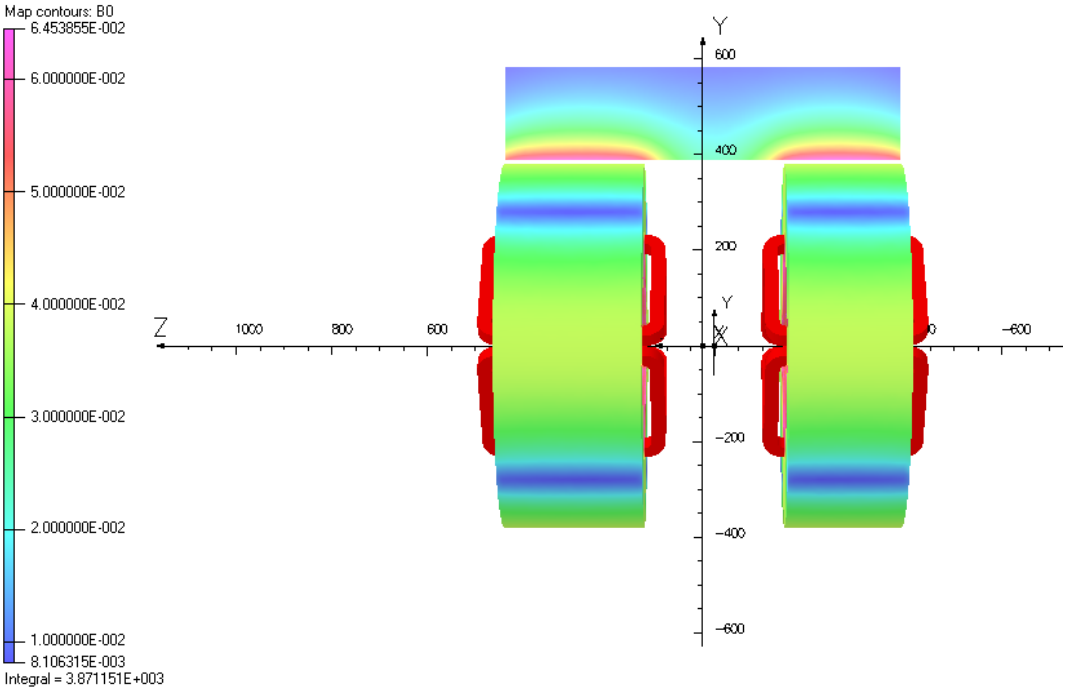

Figure 3.6 Field Variation of B_0 (T) outside the super-ferric iron structure

Because of the above reasons shielding of the magnet so as to minimize the field outside the yoke structure is also an important concern. The field values outside the doublet structure are tabulated in table 3.3, which is showing that iron yoke is capable to shape the field within it by creating large field gradient with the outer environment.

Table 3.3 Fields outside the iron structure

Co-ordinate(x,y,z in mm)	Field (in T)
(0,0,0)	1.34×10^{-3}
(0,100,0)	0.0835
(0,200,0)	0.0185
(0,300,0)	0.0267
(0,400,0)	0.0240
(0,600,0)	8.91×10^{-3}
(0,400,300)	0.0629
(0,600,300)	9.96×10^{-3}
(0,400,-275)	0.0644
(0,600,-275)	9.78×10^{-3}

Chapter 4

4 QUENCH PROTECTION SYSTEM

The basic principle of the protection system is to reroute the stored energy of the magnets once a quench appears by adding a device (diode, SCR) operating at ambient or low temperatures connected in series to the coils [18]. The conventional method of quench protection is putting a resistor across the coil to extract the magnet energy that otherwise can produce high voltages to ground when the hot-spot temperatures are made low. The best method to protect the magnet is quench the entire coil quickly, so that there is uniform distribution of the stored energy over the entire coil. The quick quenching of magnets results in low hot-spot temperature but it may increase the voltage to ground and the layer-to-layer voltage [19].

In superconducting magnet protection circuits, metallic resistors are widely used due to their constant resistance over large temperature range. But it is not a very effective way of protection since during charging, the resistance offered by the coil is comparable to that of the shunt resistor causing some current to flow through the resistor. If resistor is place inside the helium vessel, then the current flowing through the resistor evaporates a small amount of liquid helium increasing the operational costs [11].

The combination of cold diodes and resistor at low temperature were used as protection circuit. The cold diodes don’t allow the current to flow in the protection circuit during charging condition and eliminates the problem of liquid helium boil-off until a quench happens.

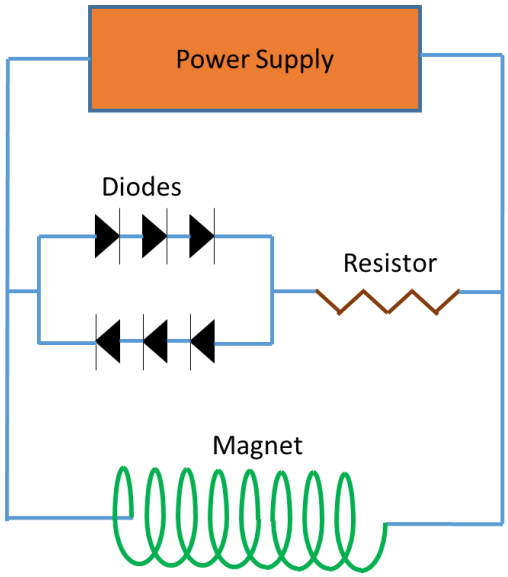

Figure 4.1 the schematic of a B2B diode + resistor quench protection system for a superconducting magnet

In above figure 4.1, the back-to-back (B2B) diode plus resistor circuitry is used as protection circuit for a superconducting magnet. The upper set of diodes is required, while the magnet is energized, the voltage across the magnet rises above the forward voltage of diode then diode bypasses the current through the resistor. The stored energy of the magnet starts to act as a battery after the quenching of the magnet. To dissipate this energy, another set of diodes is required to flow the current [14].

The above mentioned ways are all passive quench protection system which does not need a quench detector for the coils to quench, safely by controlling the critical parameters (T_C, B_C and I_C). Active protection system uses the quench heaters and quench detection circuits. As the magnet quenches, the signal detector sends a signal to fire the quench heaters, spreading the quench and reducing the hot spot temperature within the coils. This requires extensive engineering to place the heaters and detection system there by complicating the system. Hence, it is better to go for passive quench protection circuit which inherently provides safety as well as is less expensive to implement [20].

The hot-spot always suffers to through the highest temperature throughout the time of quench. The rise of temperature causes thermal elongation in the winding, which induces thermal stress into

the winding. The differential stain in the coil layers which are subjected to 100 K to 4.2 K temperature gradient from inner to outer should be within 0.1%. The temperature limit of 100 K was normally preferred as permissible hot-spot temperature for the winding material in the magnet. [21]

4.1 Selection of Quench Protection circuit

The passive quench protection circuit can be one of following configuration placed across each coil

i. Dump resistor
ii. Back-to-back diode
iii. Back-to-back diode with dump resistor

Figure 4.2 shows the above mentioned circuitry elements. The placement of these circuits can be inside the cryostat in cold condition or outside in warm condition. User has to decide to go the best suitable option as per operating condition requirement.

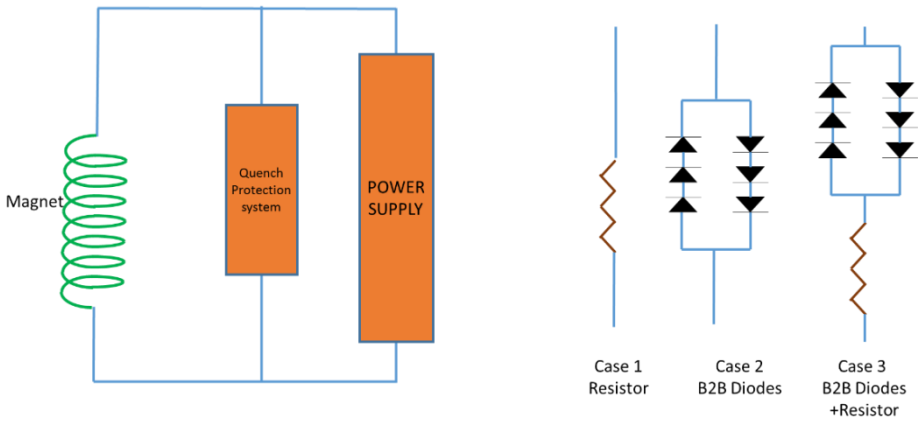

Figure 4.2 the different quench protection circuit options 1) Resistor, 2) B2B Diodes & 3) B2B Diodes +Resistor

4.2 Selection of the resistor for Quench Protection Circuit

The resistor is a passive element which helps to decay the quench current rapidly, hence its selection plays important role in terms of maximum allowable voltage rise and maximum

temperature in coil. To select the correct value of resistance for the quench protection system, one has to find an optimum condition between maximum voltage generated across the coil terminal and maximum temperature rise during quench. The magnetic energy stored in the coil is given by the inductance of the coil and the current flowing in the coil and is given by governs the current decay and is given by

$$E = \frac{1}{2} * LI^2 \qquad (4.1)$$

Where, E= magnetic stored energy, L is inductance of the coil, I is the current.

During quench the stored energy is dissipated over both the coil and over the dump resistor. The energy dissipation if given by

$$E = i^2 * R_Q + i^2 * R_D \qquad (4.2)$$

Where, R_Q is coil quench resistance and R_D is resistance across the coil. The percentage of energy dumped in the dump resistor is given by

$$E_d = \frac{R_D}{R_D + R_Q} \qquad (4.3)$$

i) If the value of dumping resistance is low, then the respective time constant (τ_c) will be more. The time constant of current decay in an inductive coil is given by the following equation.

$$\tau_c = \frac{L}{R} \qquad (4.4)$$

In one time constant the current will decay by 63% of its initial value. Approximately ($5\tau_c$) five time constants are required for complete decay of the current. If the resistance is low, the time constant will be high. Then the current will flow through the coil for a longer duration resulting in more joule heating, In turn causing higher temperature rise in the coil. Also lower value of dumping resistance produces low voltage development across the coil terminals. But At the time of charging it generates more amount heat than a high resistance circuit, which evaporates more amount of liquid helium if resistor is placed inside the cryogenic vessel.

ii) If the resistor value (R_D) is higher, then after quench the voltage developed across the coil will be higher. The current decay is shared by dumping resistor and the coil resistance. The sharing of energy allows coil to reach normal state in less period of time with less temperature increment compared to low dumping resistor circuit. The higher value of resistance also produces lower joule heating and thus evaporates less liquid helium at the time of energizing.

Considering an example in which operating current for superconducting coil is 100 A and coil resistance at normal state of R_Q=10 Ω. For different values of resistance following data has been obtained as given in table 4.1.

Table 4.1 Selection of the resistor for Quench Protection Circuit

Case No.	$R_{D,}$ Ω	T_{max}	V_{max}, V	Percentage of energy dumped in resistor
1	0.1	↑↑↑	10	0.99
2	1	↑↑	100	9.09
3	5	↑	500	33.33

In case of persistent current operation mode, the position of the dumping resistor is also important factor. Both room temperature and cryogenic temperature mounting of resistor has there inherent problems. The room temperature resistor always carries some amount of heat load via the current leads while in case of liquid helium dipped resistor evaporates considerable amount liquid helium at the time of charging.

In our case we are using continuous power supply mode with vapour-cooled current leads, which allows us to place the resistor at room temperature.

4.3 Selection of the Diodes for the Quench Protection circuit

The diode can be used at cold side or room temperature side as per requirement and is decided by the ramping rate while energizing the magnet. Diodes are used to prevent any current from flowing through the dump resistor. This is achieved by keeping the forward bias voltage of the diode higher

than that of the voltage developed during charging. During quench the coil voltage will be higher than the forward voltage of the diodes and the current will flow through the diodes and decay through the dump resistors. To achieve the higher forward voltage, multiple diodes in series can be used. The back-to-back configuration is always preferred to protect the magnet since it can act independent of the polarity.

The cryogenic mounting of diodes provides an increment in forward bias voltage than the room temperature mounting. Not only it reduces the requirement of number of diodes but also it allows user to energize the magnet with higher ramping rate. If only back-to-back diode circuitry is used as the Quench Protection Circuit, it means that the magnet will reach the highest temperature as well as high peak profile rise of voltage in coil due to full dumping of magnet stored energy in it.

Hence, it is preferred to use both back-to-back diode plus resistor across the coil to reduce the maximum temperature and voltage rise after quenching.

4.3.1 Advantages of the Back-to-back diode plus resistor circuitry

The back-to-back diode plus resistor across the coil is a preferable quench protection circuit due to its inherent advantages as follows

1. It disconnects the QPS at the time of charging through back-to-back circuitry by which charging can be done at faster rate with zero boil-off the liquid helium due to blocking of current flow through the dumping resistor while charging.
2. If magnet quenches, then the diode will start conducting and will provide a current decay path through the dumping resistor.
3. Due to combined effect of back-to-back diodes and resistor, the maximum temperature and voltage peak in the coil can be limited.

Chapter 5

5 QUENCH SIMULATIONS OF SINGLE COIL

The passive quench protection circuit may be of only resistor, only back-to-back diodes or combination of back-to-back diodes plus resistor across the coil. Depending upon the circuit components the quench exhibits different results such as the maximum temperature rise, voltage profile, current decay time and resistances increment with respect to growth of normal zone. These parameters are simulated in the QUENCH module of OPERA to study the effect of different quench protection circuits.

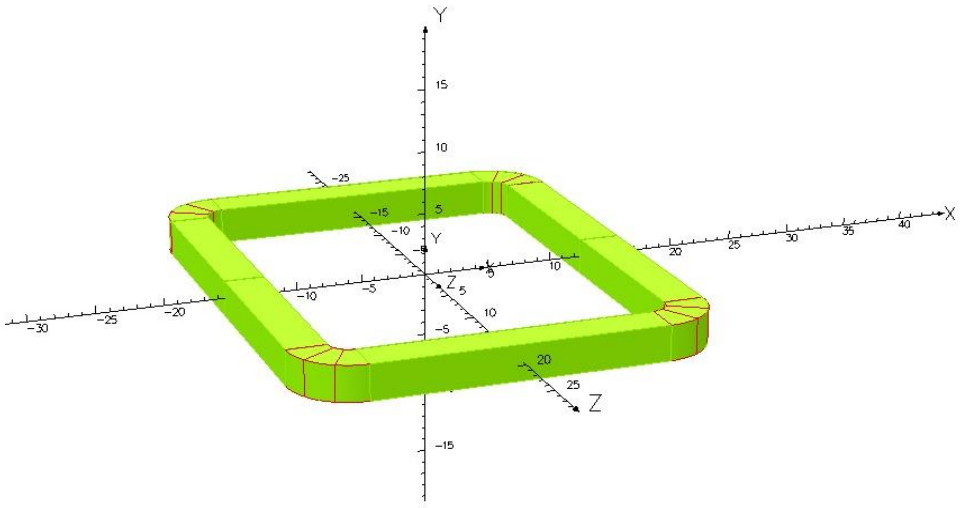

Figure 5.1 Coil modelling in Opera-QUENCH code

5.1 Input to QUENCH analysis

The quench simulation is performed in the quench module of OPERA. QUENCH module, unlike the TOSCA module provides a more complex analysis of the situation. This demands more number of inputs such as material properties, coil parameters etc. Main inputs for the QUENCH module are listed in Table 5.1.

Table 5.1 Inputs for the QUENCH module

Coil Dimension	28 x 30 mm^2
Cu : SC ratio	7.6 : 1
Number of Turns	1600
Wire diameter	0.75 mm

The NbTi is a type-II superconductor and shows non-linear material properties. The temperature dependent non-linear material and electrical properties for Copper, Niobium-Titanium etc. are already available for the non-linear materials. By pointing the software to the appropriate files, the program can access the property data at the run time. To initiate the quench in the coil, a heat-flux of 50 W/m^2 boundary condition is given on the surface of the coil. An area of 2 x 2 mm^2 on the inner surface of the coil was selected as the heater and quench was initiated with an energy pulse of 2W for a duration of 0.1 second.

5.2 Electrical circuitry

In order to properly couple the electromagnetic circuit with thermal model, the inductance matrix input is required. The experimental practice of calculating the inductance is through the charging and discharging in which the inductive voltage ($V_L = -L\frac{di}{dt}$) profile across the coil terminal is to be measured with suitable circuitry and measurement instruments. The room temperature resistance of the coil is 100 Ω. With the help of LCR circuit, the measured inductance of the coil was verified to be 1.5 H.

Case 1. Resistor as a Quench Protection circuit across the coil

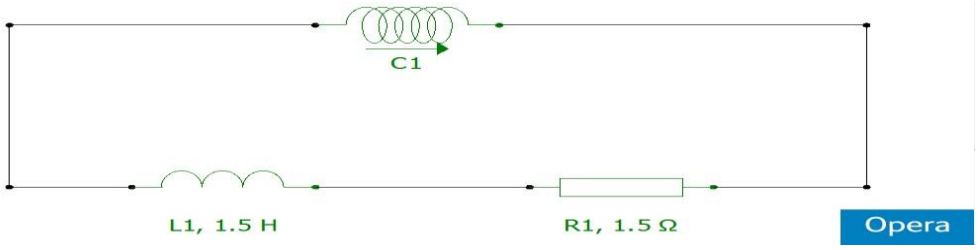

Figure 5.2 Resistor as a Quench Protection circuit for the Single coil

For the Quench Simulation the electrical circuit of resistor as QPS for single coil is shown in figure 5.2, in which coil is protected against the quench through resistor.

a) 100A single coil quench simulation with 2W heater

The heater boundary condition is defined in the Quench model which drives the coil to become resistive from its superconducting state at 4.2 K and 100 A at t=0 sec. Figure 5.3 a) shows that the inner layer is subjected to Quench first because the heat pulse from the heater causes quench at the heat further generated first travels in the inner layer, because of the higher thermal conductivity of copper wire. At 10.56 K coil shows resistance of 8.7 X 10^{-6} Ω with 8.7 mV of voltage generation across the coil terminals. In 'heater on' period coil temperature rises to 33.83 K with 0.41 Ω resistance and current decays at low rate to 89.65 A. After 0.1 sec the figure 5.3-b) & c) shows that the coil temperature decreases to 31.27 K and further increases to highest temperature of 38.5 K in 1sec as normal zone spreads to outer zones.

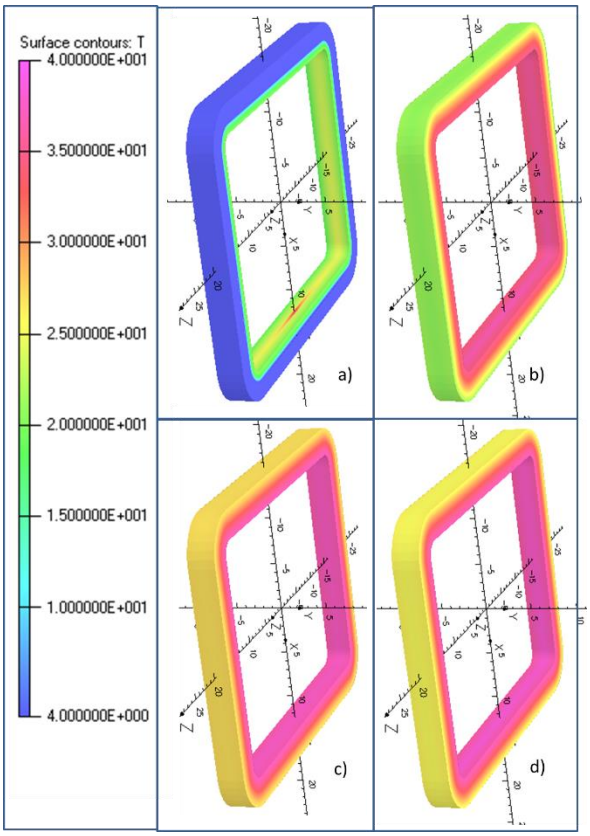

Figure 5.3 Temperature contours of the coil for resistor as Quench Protection circuit at the different time steps a) t=0.1s, b) t=0.5s, c) t=1s and d) t=5sec

The heater pulse of 0.1 sec quenches the coil by bringing the temperature above the critical temperature. As soon as the heater is turned off, the coil temperature lowers by ~2 K due to balancing of the heater power and joule heating with the adiabatic boundary limitation. Further increase in temperature and the final hotspot temperature is governed only by the amount of energy stored in the magnet and its dissipation during quench and not the initiating heat pulse is the temperature variations in the coil is profiled in the figure 5.4-a). The current decays from its initial value of 100 A to 0.00227 A in 5sec in an exponential rate (figure 5.4-c) and the normal zone spreads throughout coil with in 1sec and nearly remains at the same resistance value of 2.22 Ω till the end of 5 sec is shown in figure 5.4-b). The voltage peak of 103.12 V comes at 360 ms and after that it reduces with current decay to a zero value which is plotted in figure 5.4-d).

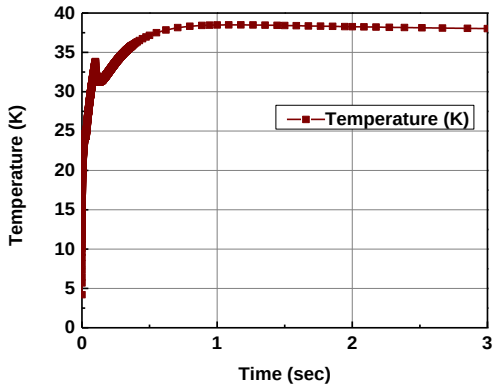

a) Temperature(K) Vs Time(sec)

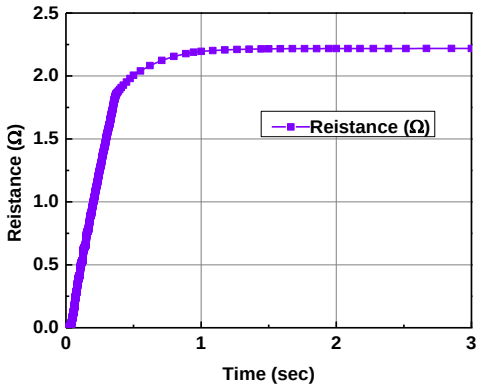

b) Resistance(Ω) Vs Time(sec)

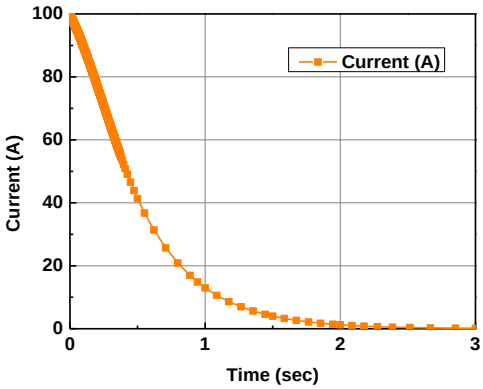

c) Current(A) Vs Time(sec)

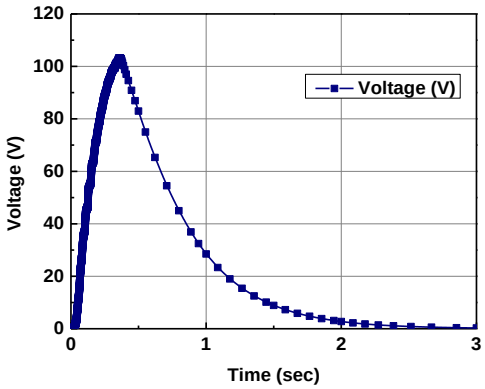

d) Voltage(V) Vs Time(sec)

Figure 5.4 The Quench simulation results of 1.5 Ω resistor as a Quench Protection circuit across the coil.

b) 80A single coil quench simulation with 2W heater

The electrical circuitry is same as figure 100 A single coil protected with resistor across it. The operating temperature is 80 A.

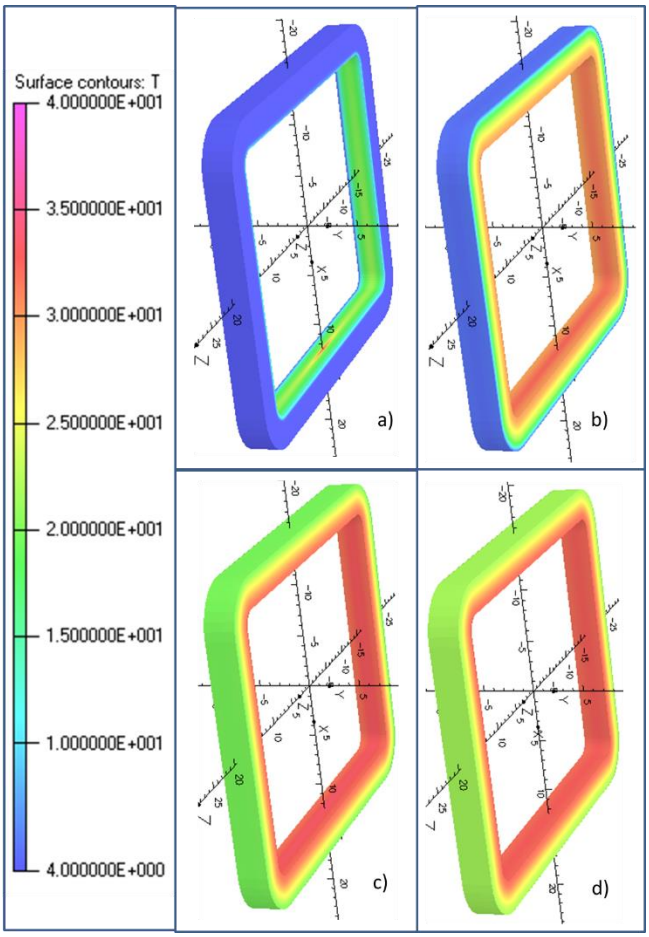

Figure 5.5 Temperature contours of the coil for resistor as Quench Protection circuit at the different time steps

The heater pulse of 2W capacity for initial 0.1s quenches the coil by bringing the temperature above the critical temperature. The resistance of 85 X $10^{-7}\Omega$ at 10.11 K is shown at 0.000229 s. At the of heater input (t=0.1s) temperature reaches to 31.11 K with coil resistance of 0.2047 Ω with almost 10% decay in initial current of 80A. Figure 5.5 a) shows that the inner layer is subjected to heater input and normal zone started spreading in azimuthal direction as cooper having higher thermal conductivity in that direction. After 0.1 s, propagation of normal zone to outer layer the joule heating start dominating over adiabatic boundary condition is shown in figure 5.5 b) and c). Within 5 sec, whole coil becomes resistive in nature is shown in figure 5.5 d).

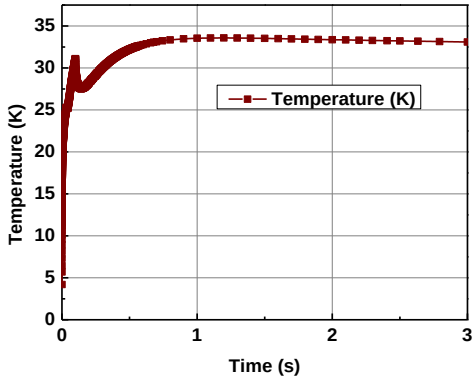

a) Temperature(K) Vs Time(sec)

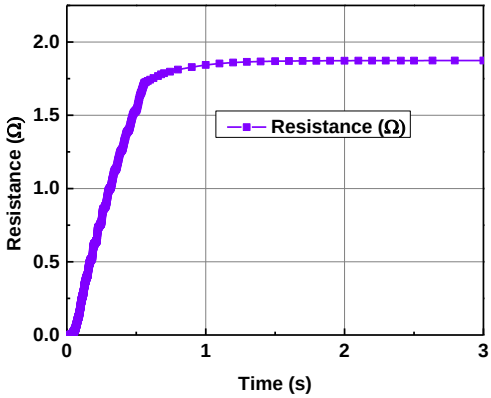

b) Resistance(Ω) Vs Time(sec)

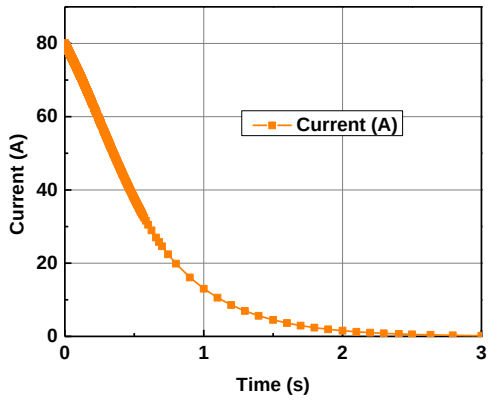

c) Current(A) Vs Time(sec)

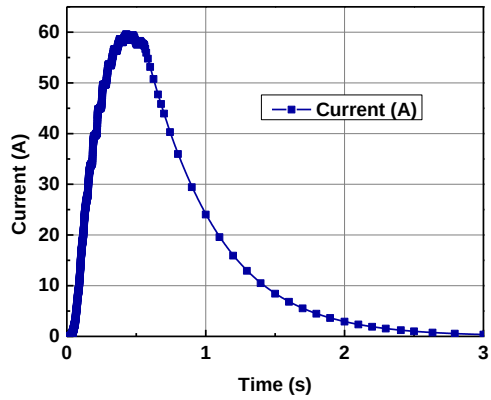

d) Voltage(V) Vs Time(sec)

Figure 5.6 The Quench simulation results of 1.5 Ω resistor as a Quench Protection circuit across the coil.

The dominated initial 0.1 s with temperature 31.11 K as heater switches off, after it decreases to 27.55 s for heat balancing between heat input and joule heating with 4.2 K boundary condition as shown in figure 5.6 a). The peak voltage of 59.56 V appears at 0.426 s with resistance of 1.367 Ω and 31.61 K coil temperature as shown in figure 5.6 d). Within 0.5 sec current decays more than ~50% of initial current. Coil reaches to maximum temperature of 33.58 K at 1.2 sec with final

resistance of 1.87Ω as shown in figure 5.6 b) and c). As coil reaches its maximum temperature and resistance, current and voltage decrease in same manner.

c) 10 W heater at 80A quench simulation

In this case heater input is increased from 2 W to 10 W, for checking the effect of heater on the coil. The electrical circuit same as 100 A with resistance as a QPS.

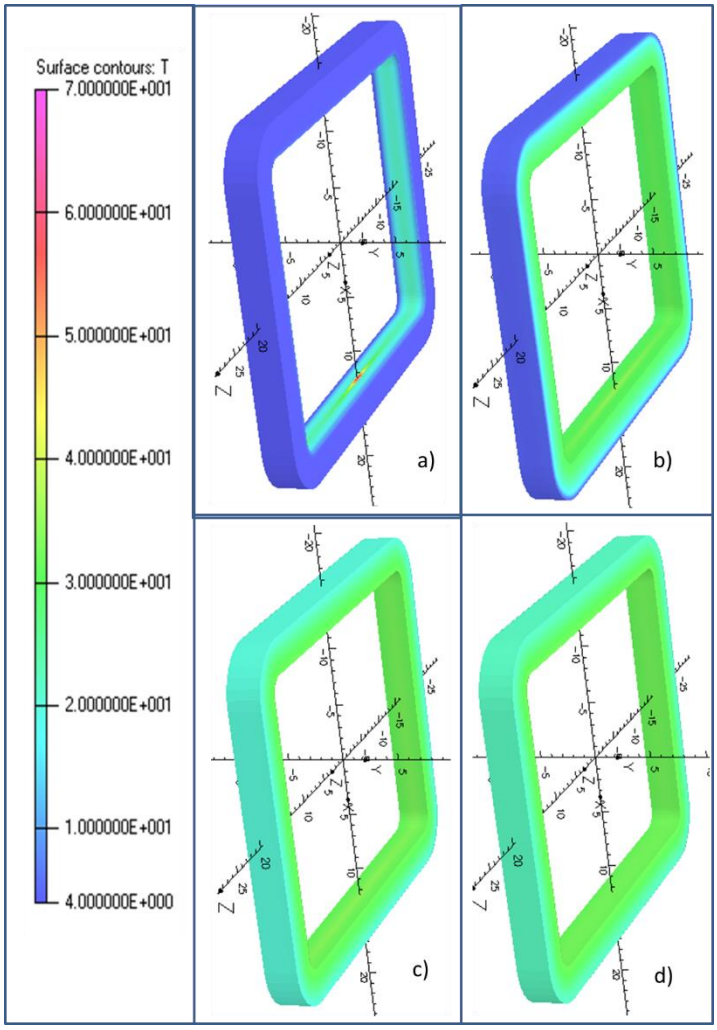

Figure 5.7 Temperature contours of the coil for resistor as Quench Protection circuit at the different time steps

The similar pattern is fooled in this case also. But in initial case 10W of heater pulse, temperature shoots up to 66.04 K at t=0.1sec. Then due to heat balancing it decreases to 34.716 K in 1sec and it reaches to final maximum temperature of 33.27 K at the end of 3sec.The above figure 5.7 a)

shows that heater initiate the quench into inner layer of the coil with resistance of 2.02 X 10^{-6} Ω at 12.467 K within 3 X 10^{-5} s. The heat propagated from inner to outer in further time period with increase in resistance of coil is shown in figure 5.7 b), c) and d). The final coil temperature reaches to 33.27 K with 1.864Ω resistance.

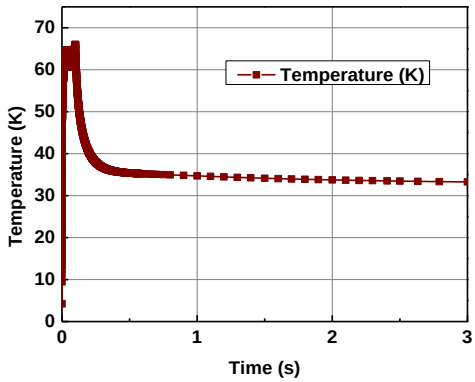

a) Temperature(K) Vs Time(sec)

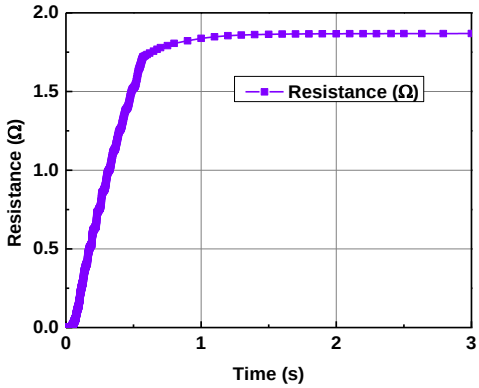

b) Resistance(Ω) Vs Time(sec)

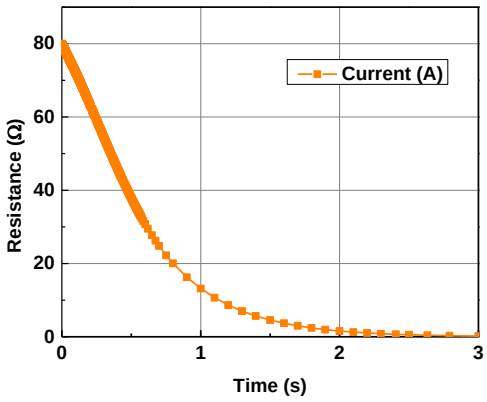

c) Current(A) Vs Time(sec)

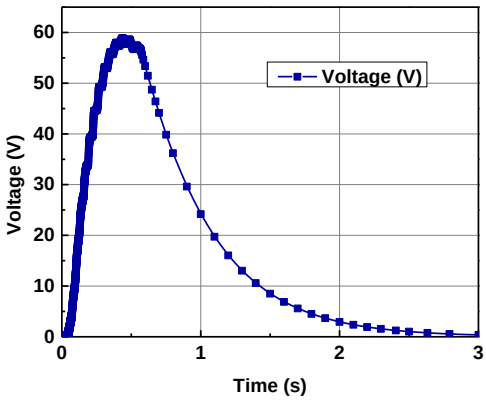

d) Voltage(V) Vs Time(sec)

Figure 5.8 The Quench simulation results of 1.5 Ω resistor as a Quench Protection circuit across the coil

Due to heater pulse, coil reaches to 66.04 K at end of 0.1 s, and further decreases to 33.27 K in next 3sec is plotted in figure 5.8 a). The resistance increase linearly with time till temperature

increment after that it slowly settle with final temperature. As current decays in the coil, the generated peak voltage also decrease with it. Within 3 s both almost comes to zero.

d) Comparison of the of the cases a), b) and c)

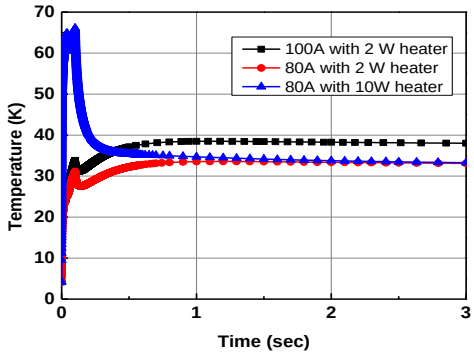

a) Temperature(K) Vs Time(sec)

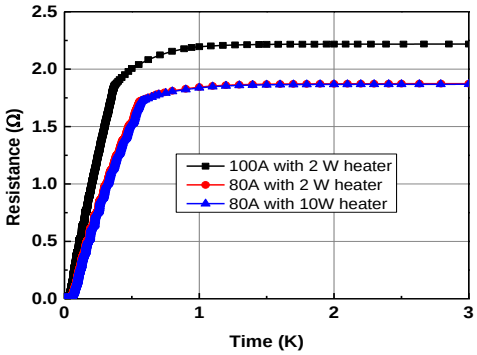

b) Resistance(Ω) Vs Time(sec)

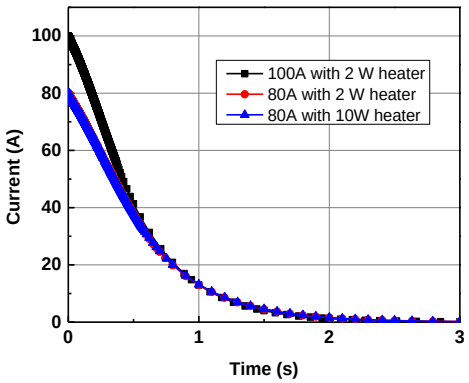

c) Current(A) Vs Time(sec)

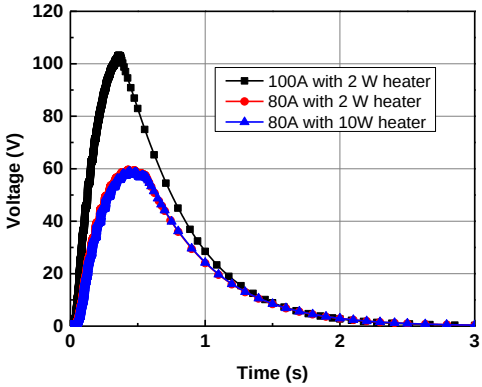

d) Voltage(V) Vs Time(sec)

Figure 5.9 comparison of the results of the 1.a) resistor, 2) B2B Diode and 3) B2B Diode + R as a quench protection circuit

Operating current plays important in controlling parameter which drives the quench parameters.in case of 100A coil reaches to highest final temperature with high resistance value of 38K and 2.2186 Ω respectively. Current decays also faster increase of 100A with highest peak voltage of 103.1 V. Figure 5.9 shows that after 1 s in both cases, current and voltage follows same pattern as coil

reached to its highest resistance respect to maximum temperature. It means that higher operating current will result in high temperature rise as well as more peak voltage. Heater input will be higher 10W instead of 2W, then initially rise temperature at the end of 0.1sec is 66.04 K rather than 31 K in 2W. After 0.1 s coil temperature decreases in case of 10 W till final temperature of 33.27 K. All remaining curves are follows same curve as 2W heater input. It means that heater pulse plays role of quench initiation only.

Case 2. B2B diodes as a Quench Protection circuit across the coil

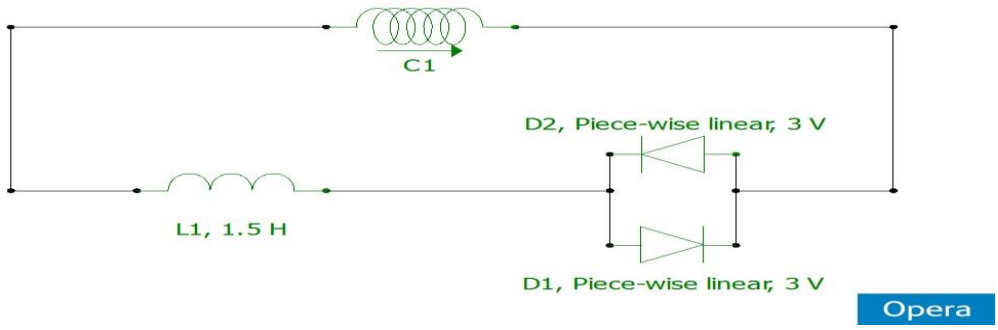

Figure 5.10 B2B Diodes as the Quench Protection Circuit

For the Quench Simulation the electrical circuit of resistor as QPS for single coil is shown in figure 5.10, in which coil is protected against the quench through B2B diodes. The coil starts quenching above 10.1 K with resistance of 3.16 X 10^{-6} Ω and 3mV voltage across the coil terminal. In first 0.1 sec the temperature contour in figure 5.11-a) shows that the heater heats up the inner layer of the coil with temperature rise to 33.88 K from 4.2 K, which is initial temperature of the coil at t=0 sec. Due to the absence of the passive device like resistor to dump the quench energy, the current decays to 98.9 A with much slow rate compared to previous case. The resistance reaches to 0.43Ω in 0.1 sec and after that the normal zone starts propagating throughout the coil from one layer to other layer. The contours from the figure 5.11-b)-d) shows the growth of normal zone with different time steps.

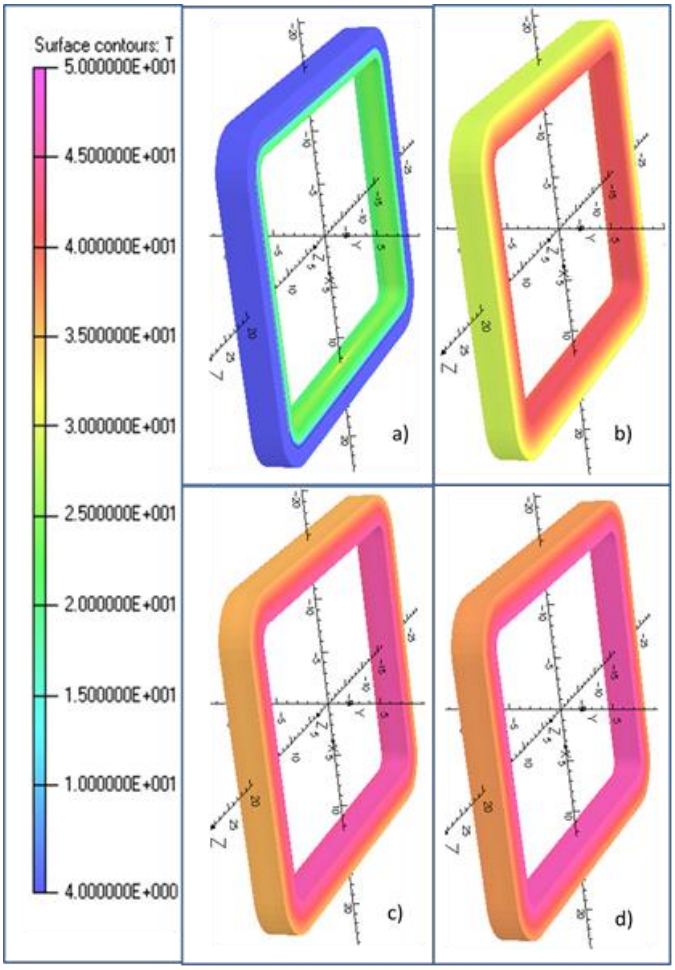

Figure 5.11 Temperature contours of the coil for B2B Diodes as a Quench Protection circuit at the different time steps

After heater is turned off, the temperature of the coil decreases to 31.7 K and further increases to highest temperature of 46.98 K. The resistance of the coil also grows up to 3.10 Ω in 1.5sec and after that remains almost constant in that value. Increment in both the temperature and resistance are plotted in Figure 5.12-a) and 5.12-b) respectively. The whole energy in dumped into the coil is the main reason for the higher temperature. The Figure 5.12-d) profiles the peak voltage shoot up to 165.91 V in 0.3 second and its decrease to zero as current decays. The initial current of 100 A decays to 0.000289A in 2.85 sec and is graphed in the Figure 5.12-c) which appears to be exponential decay rate. The back-to-back diode circuit helps to decide the charging time ramp rate of the coil because at the time charging inductive voltage is generated across the coil terminal.

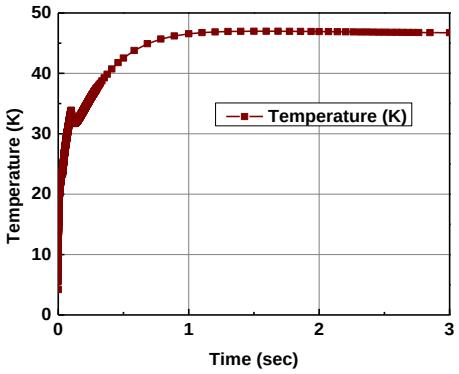

a) Temperature(K) Vs Time(sec)

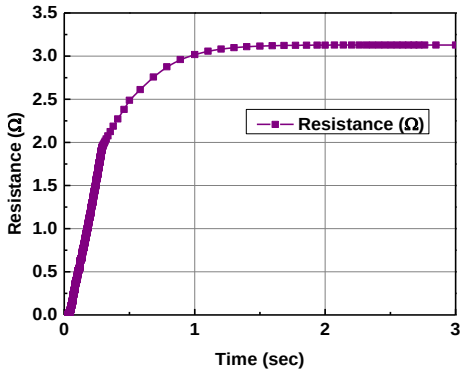

b) Resistance(Ω) Vs Time(sec)

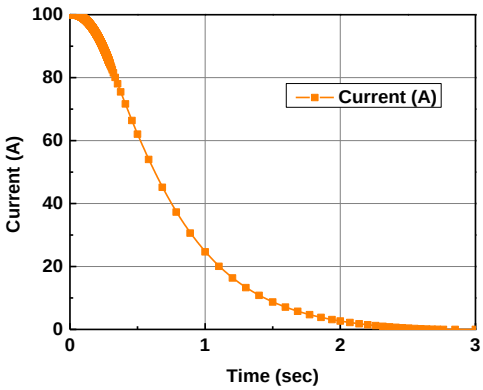

c) Current(A) Vs Time(sec)

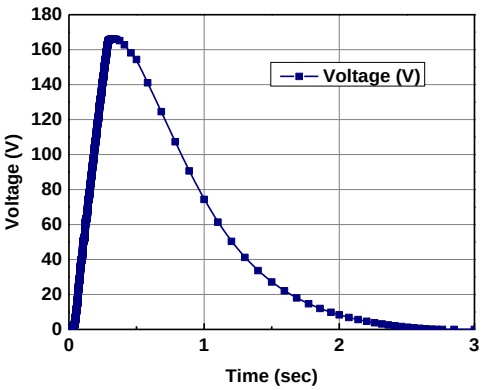

d) Voltage(V) Vs Time(sec)

Figure 5.12 The Quench results of B2B diodes as Quench Protection circuit across the coil

Case 3. B2B diodes plus resistor as a Quench Protection circuit across the coil

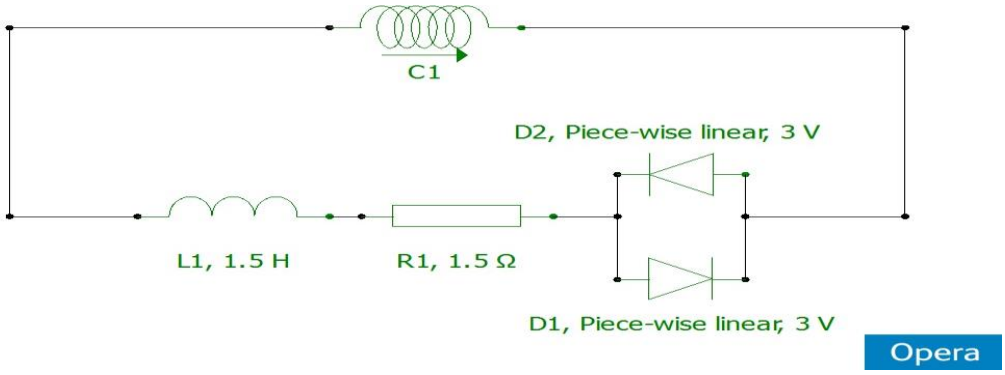

Figure 5.13 B2B Diodes + R as a Quench Protection Circuit

For the Quench Simulation the electrical circuit of resistor as QPS for single coil is shown in figure 5.13, in which coil is protected against the quench through B2B diodes. The initial condition at t=0 sec, the coil temperature is 4.2K. The heater of 2 W capacity in 0.2 X 0.2 cm^2 is initiating the quench into the coil and at 10.5 K the coil started showing the resistive zone creation in the order of 8.7 X 10^{-6} Ω with 8.7 mV of the voltage generation across the coil terminals. Heater is on for the 0.1 sec, up to that time period coil further subjected to growth of the normal zone in the inner layer of the coil which is shown in the figure 5.14-a), with increment in resistance value of 0.41Ω at 33 K. After heater is in the off state, the coil temperature decreases to 31.2 K and again starts rising as the current start decaying with faster rate due to the spreading of the normal zone throughout the coil layers as shown in the figures 5.14-b) & c) for 0.5 sec and 1 sec respectively.

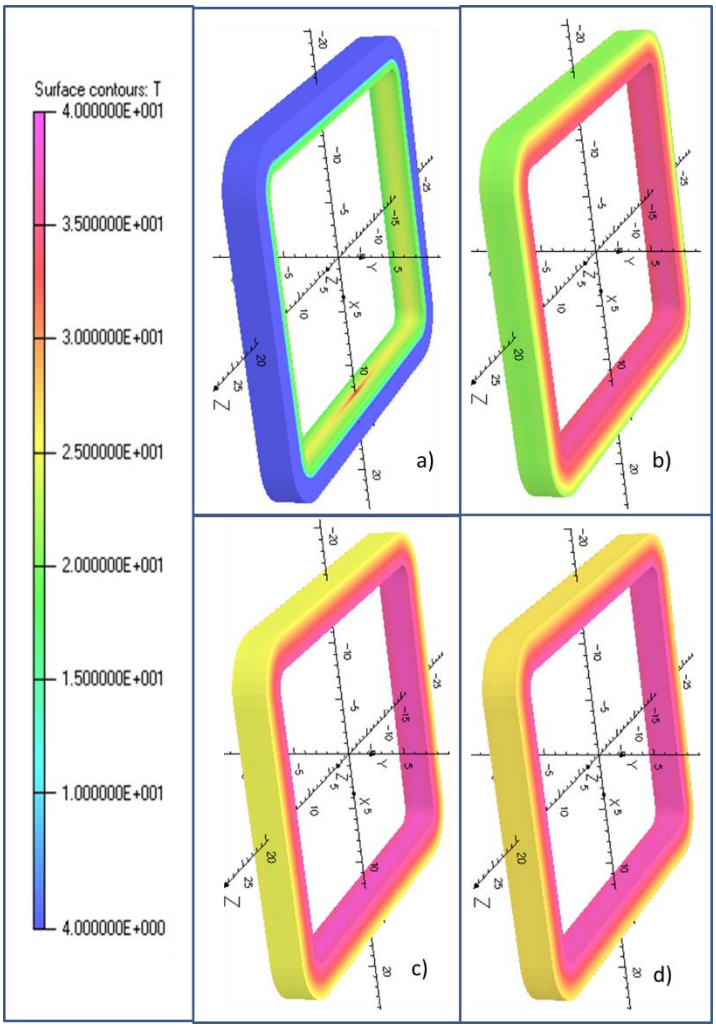

Figure 5.14 Temperature contours of the coil for B2B Diodes as a Quench Protection circuit at the different time steps

At the end of 1 second, the coil reaches its highest temperature of 38.3 K with 2.2Ω resistance as shown in Figure 5.15-a) & b). The voltage profile shows that in graph Figure 5.15-d) voltage rises from the initial condition to peak voltage 101.63 V in 0.360 sec and further decreases as current goes down. The current decay shows exponential decay rate as shown in Figure 5.15-d), the initial current in the coil is 100 A and it decays to 3.54 X 10^{-5} A in 2.3 second. Almost at end of 5 seconds both current and voltage comes to zero values with resistance 2.2 Ω at 37.3 K.

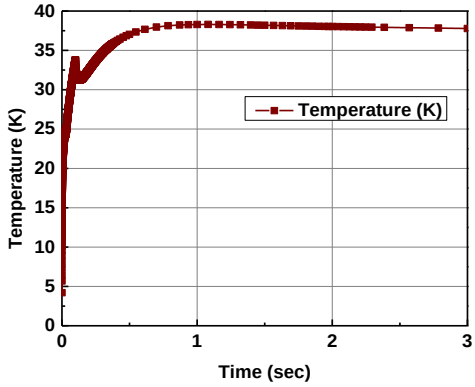

a) Temperature(K) Vs Time(sec)

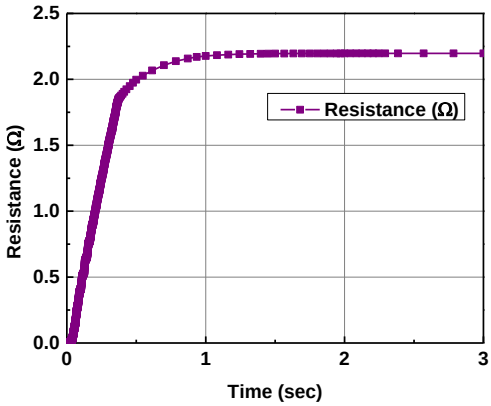

b) Resistance(Ω) Vs Time(sec)

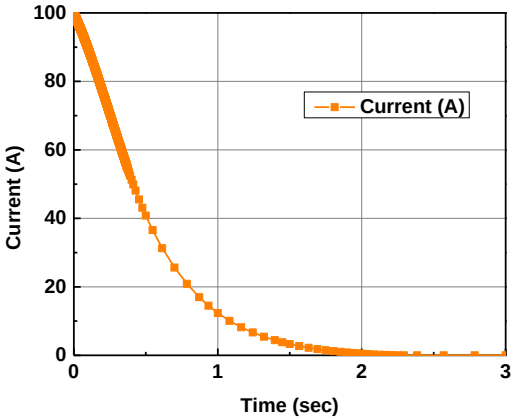

c) Current(A) Vs Time(sec)

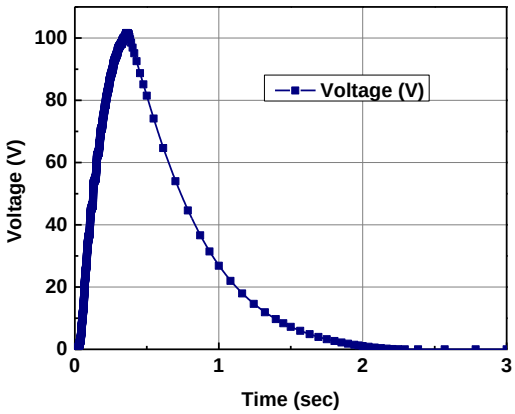

d) Voltage(V) Vs Time(sec)

Figure 5.15 The Quench Results of B2B diodes plus resistor as a Quench Protection circuit across the coil

This circuit is similar to resistor as a Quench Protection circuit with added advantage over boil-off and fast current decay with minimum peak voltage compared to both resistor and back-to-back diode circuits. The temperature of the coil is within the safety limit, hence this circuit can be used as a quench protection circuit.

5.3 The Comparison of results of above three circuit configuration

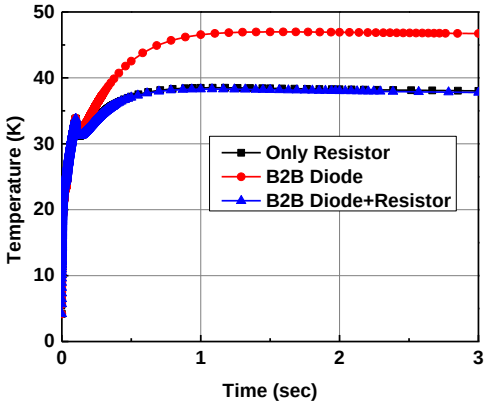

a) Temperature(K) Vs Time(sec)

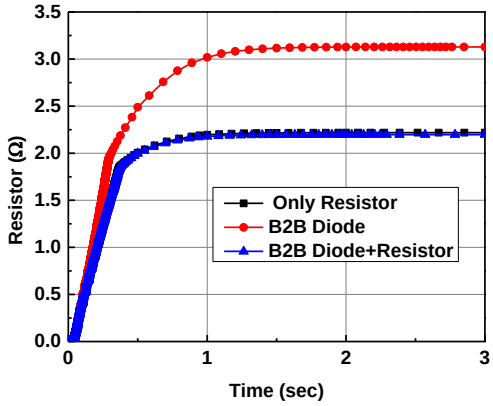

b) Resistance(Ω) Vs Time(sec)

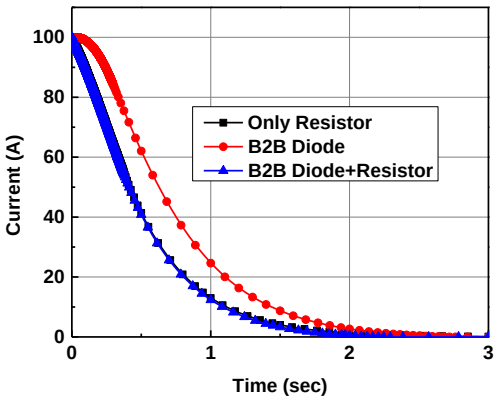

c) Current(A) Vs Time(sec)

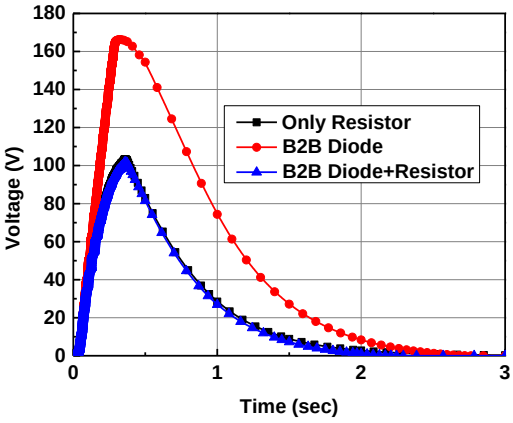

5.16-d) Voltage(V) Vs Time(sec)

Figure 5.16 comparison of the results of the 1.a) resistor, 2) B2B Diode and 3) B2B Diode + R as a quench protection circuit

In all three cases, the quench initiation heater input is same and it controls on 0.1 sec by shooting the temperature in the range of 33 to 34 K as plotted in the figure 5.16-a). The final temperature and growth of resistive zone is independent of the heater power.

In case of resistor highest temperature 38.5 K and in case of B2B+R is 38.3 K. Both resistor and back-to-back diode plus resistor behaves in the same manner for quench results like the temperature rise, resistance growth, current decay and the voltage profile. In case of B2B diode case the coil absorbs whole stored energy, hence the highest temperature is 46.98 K and is 8.5 K more than the remaining two cases. Due to absence of dumping element, the growth of the resistance is to 3.1 Ω for B2B diode protection circuit which is 40% more resistive than remaining both cases as plotted in the figure 5.16-b). The graphs 5.16-c) & d) shows that the current decays at slower rate in case of B2B diode as a protection circuit with much faster growth in resistive zone subjects to highest peak voltage 166.91 V with 60% more than the remaining two cases.

Chapter 6

6 EXPERIMENTAL TEST OF THE SINGLE COIL

In order to study and characterise the superconducting magnet and also to study the performance of different quench protection circuits, a single coil was tested in a Superconducting Test Cryostat (STC) facility at IUAC. The tests were aimed in recording the critical operational parameters of the coil such as temperature rise and voltage generation during quench, total resistive volume, current decay parameters etc.

6.1 Experimental Setup

The tests were carried out in the STC facility. The equipment consists of a 70 L liquid helium vessel under which the magnet vessel carrying the superconducting coil is connected. The helium vessel is protected from radiation heat transfer using an active copper shield cooled using the helium boil-off vapours. The magnet vessel sits much lower than the shield and thus is cooled by a LN_2 shield. The current leads for the magnet are vapour cooled and thus heat transfer to the system through the current leads are minimised. The whole system is placed in a vacuum jacket to protect the setup from any conduction or convection heat transfer. The vacuum vessel is initially pumped using a roughing pump and then a turbo pump backed by a rotary pump is used to obtain and maintain a much higher vacuum level. The top lid of the vacuum vessel is connected to the helium vessel through multiple ports such as those for helium filling, instrumentation, helium recovery and pumping. The schematic of the Test vessel is shown in figure 6.1. The helium vessel is supported from the top lid using G10 rods.

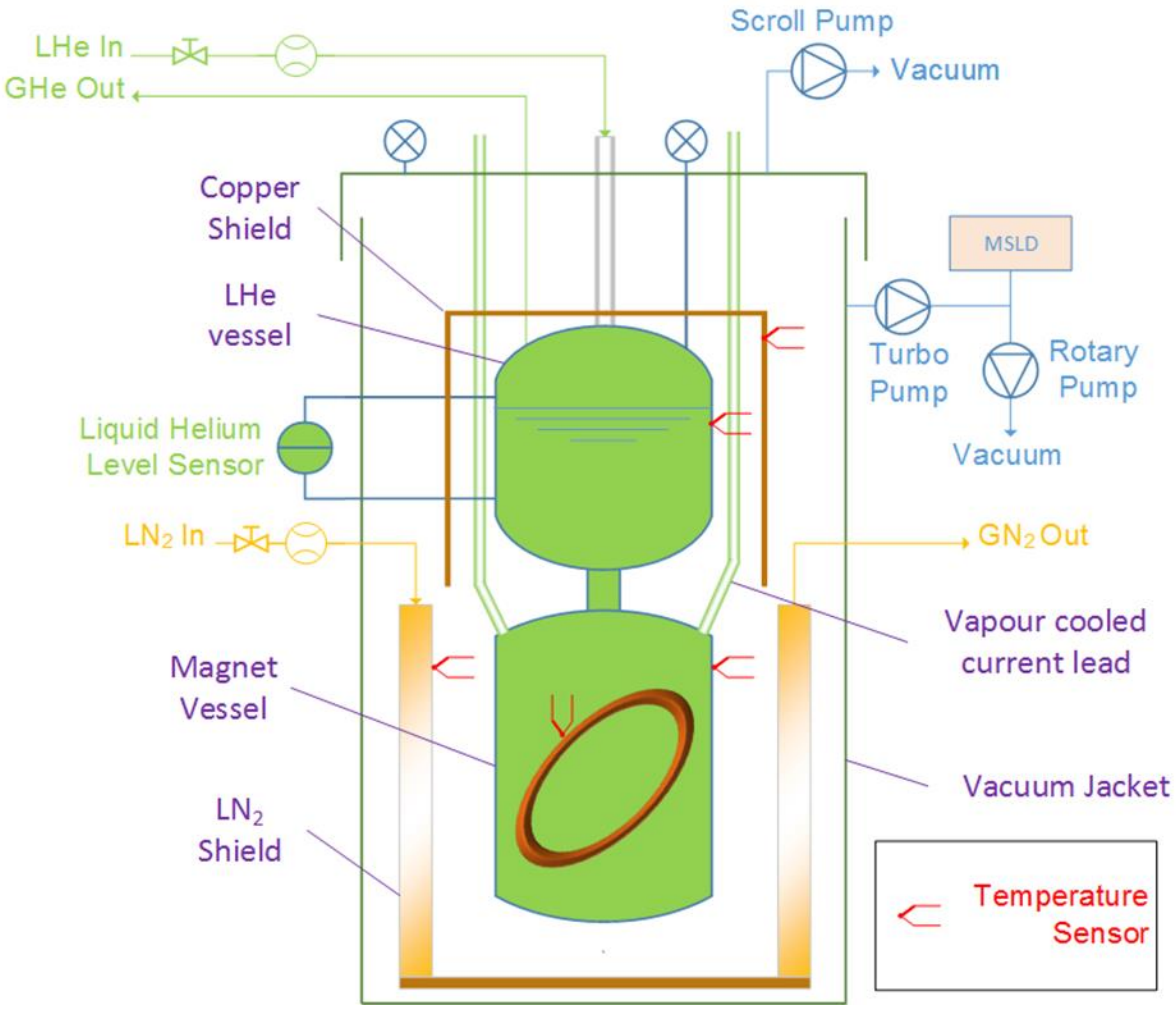

Figure 6.1 Schematic of the experimental test set up for the single superconducting coil.

6.2 Leak Testing of the experimental setup

When working with liquid helium, the heat transfer rate into the system is a critical factor. It can be seen from calculations that 1 W of heat can evaporate 1.4L of helium. To obtain least amount of heat transfer it is necessary to ensure a good vacuum around the test vessel. There are various methods to perform leak test such as using soap solution, acetone spraying, etc. In the vacuum level used here the most common method is using a mass spectrometry leak detector (MSLD) for helium. Initially the LHe vessel is tested for any leaks formed due to handling, such as cracks in welds, joints etc. The LHe vessel was found to have a leak rate of 5×10^{-7}mbar/l.s which is in the acceptable range for a vessel of large volume. Then the magnet vessel is connected to the helium vessel using CF flanges and indium groove joints.

The assembly is then tested to find the total leak rate. The effectiveness of the joints were further tested in vacuum condition using MSLD by spraying He gas at critical areas. The vessel was found to have a leak rate of 2.5 X 10^{-5} mbar/l.s. The joints were also tested under pressure using the sniffer mode of the MSLD apparatus and it also settled to 2.5 X 10^{-5} mbar/l.s whose sensitivity mostly dependent on the background helium content.

After an acceptable range of vacuum sealing is obtained, the vessel is placed inside the vacuum vessel and a global leak test is conducted at a vacuum level of 2.8 x 10^{-5} mbar and helium vessel pressure of 5 psi. A global leak rate of 2.4 x 10^{-8} mbar/ l.s was finally obtained for the assembly.

6.3 Instrumentation

In order to monitor the operation of the test facility temperature monitors are provided on the helium vessel, magnet vessel and shields. Calibrated silicon diodes from Lakeshore (DT-670) are used for temperature monitoring. A temperature sensor was also placed on the coil to monitor the coil temperature. A superconducting level sensor is placed inside the vessel to monitor the liquid helium level. Proper level of helium during experiment is a critical factor to avoid burn out of the test coil.

To measure the coil parameters such as, voltage rise, current decay through the coil etc. appropriate electrical connections are made to the circuit. All the electrical outputs are fed into a digital oscilloscope with floating grounds for real time comparisons and data recordings. The details of the electrical circuit are shown in figure. The superconducting coil used for test has already been studied and its critical current limit at 4.2 K is calculated to be 100A. To forcefully quench the coil in different conditions, such as at lower currents a heater of 10 W capacity is mounted on the surface of the stycast impregnated coil. In case of the heater the first layer was wrapped with aluminium tape to increase the heat transfer as aluminium having higher thermal conductivity. The heater and the temperature sensor placed close by are covered with Kapton tape to avoid direct contact with Liquid helium which may affect the reading of the coil temperature at the time of quench. GE varnish was applied between the coil surface and the devices to reduce the thermal contact resistance. Lakeshore temperature monitors (Model 241) is used to record the temperatures while a digital oscilloscope from Tektronic (Model 2420) is used to record all the voltage taps.

The above oscilloscope features independent floating ground terminals with up to 600 V potential differences between them. This enables us to tap voltages from different points of the circuit to the same device without shorting the ground terminals. A 1 A Keithley source meter is used to provide the DC pulse to the heater.

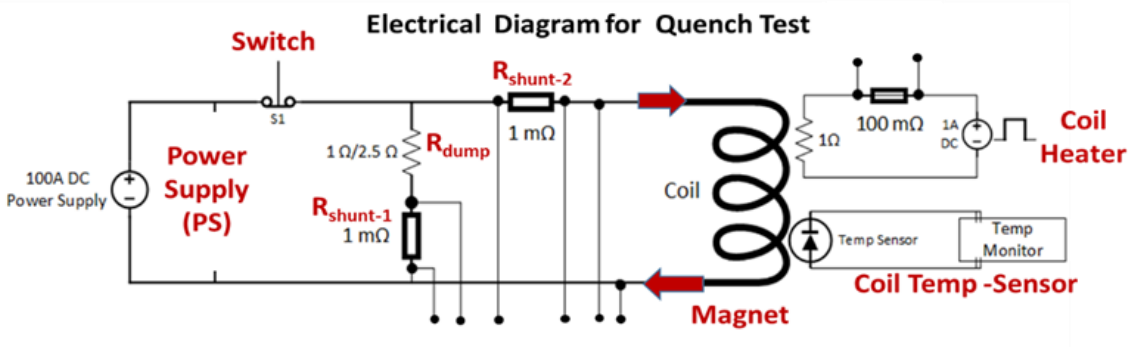

Figure 6.2 Equivalent electrical circuit diagram for the quench test at 4.2K

6.4 Energizing of the magnet coil

The high current power supply of 100 A is required to energize the coil; for that a power supply by Cryogenic ltd. with special characteristics such as ramp rate control, zero load resistance operation, quench detection etc. is used. The ramping rates used are 6A/min and 12 A/min. After quenching the power supply detects and cuts off the current supply. For the magnet current to decay a ceramic resistor of 0.91 Ω capacity rated for 100W operation is provided in the circuit.

6.5 Joining of Superconductor wire to the current lead

In order to get a proper electrical contact between the flexible vapour cooled current leads and the superconducting coil terminals potted joint method was used. The terminals are initially cleaned and deoxidised using alcohol and Zinc Chloride (ZnCl2) solution. The solder was done using 'woods metal' which is a eutectic alloy of 50% bismuth, 26.7% lead, 13.3% tin and 10% cadmium by weight. The joint consisting of copper braid (Current lead), superconducting wire and voltage taps is made and is dipped in to a bath of molten solder to ensure proper contact of solder and wires. Then the joint is placed in a pot made of aluminium sheet and the pot is filled with solder.

The joints are then cooled using jet of dry air. After cooling the aluminium pot is removed and the joints are insulated with the Kapton tape. A photograph of the potted joint is shown in figure 6.3.

Figure 6.3 Potted joining of coil with the vapor cooled current lead

6.6 LHe Cooldown of the experimental setup

The experimental setup is cooled down from room temperature to operational conditions. After ensuring proper vacuum, the nitrogen shield is first cooled down and then filled with liquid nitrogen. Then the helium vessel is cooled down and filled with liquid helium up to required level. The cool down of the apparatus after filling the shield with nitrogen is shown in figure 6.4. Before cool down, the system is purged multiple times using helium gas to remove any other gas which may freeze in liquid helium temperatures. The total chill down was completed in 3 hours while another 4 hours was required to reach thermal equilibrium.

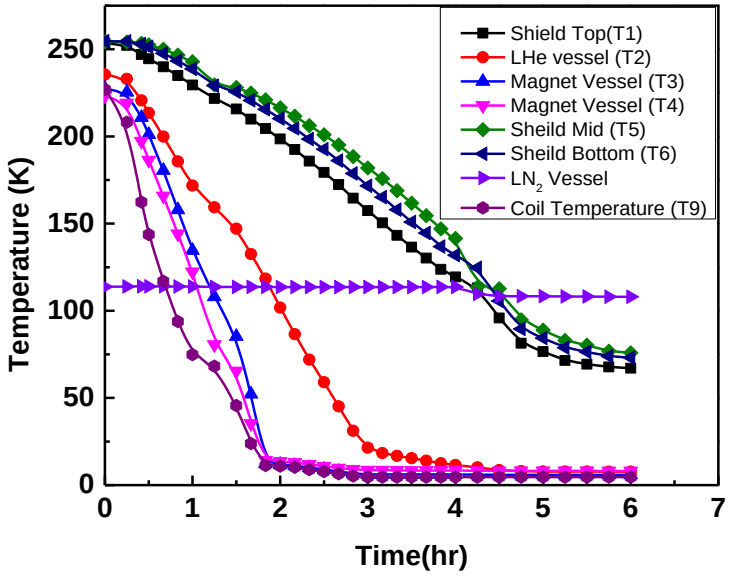

Figure 6.4 LHe Cooldown profile of the magnet and different components of the cryostat.

Case 1. Charging and discharging of the magnet with different ramp rate

Initial tests carried out in the coil were to confirm the inductive behaviour of the coil and to study the voltage generation during charging due to the inductance. The voltage developed across the coil is the slope of the coil current, multiplied by a factor equal to the inductance of the coil. At constant charging rate, i.e. when the slope of current curve during both charging and discharging is linear, a constant voltage is expected across the coil throughout the duration. The same has been verified by charging the coil at different rates and measuring the voltage. Figure 6.5 and 6.6 shows the current and voltage curves during charging. The two ramping rates 0.1 and 0.2 A/s shows respective voltages of 150 and 300 mV.

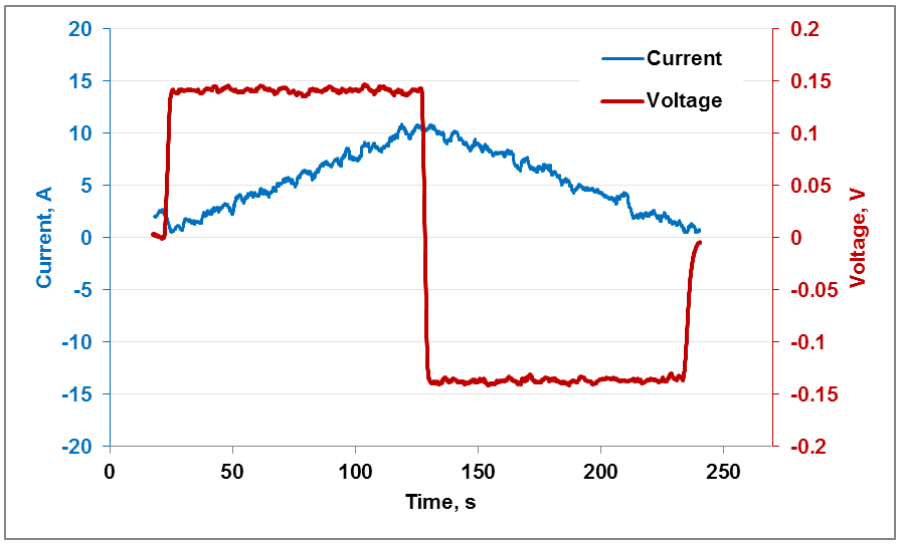

Figure 6.5 Charging Discharging curve at 0.1 A/s up to 10 A

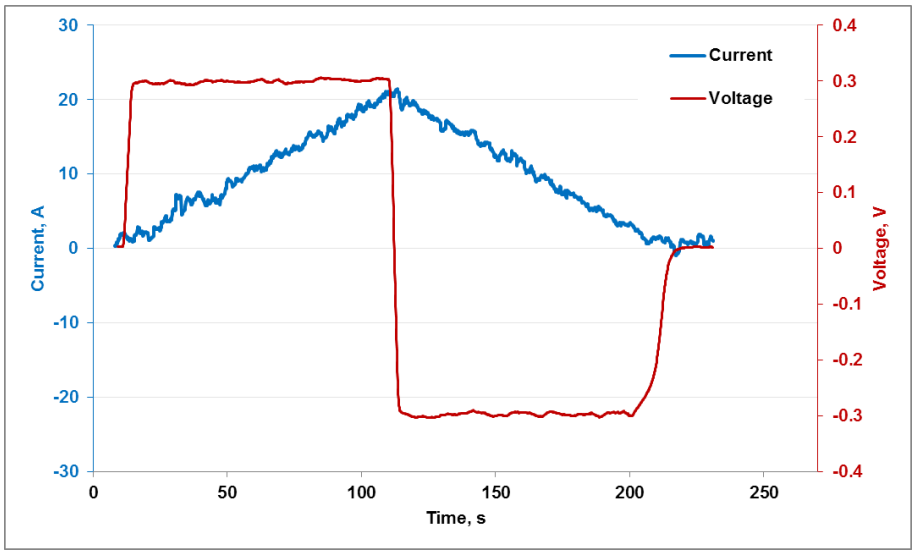

Figure 6.6 Charging Discharging curve at 0.2 A/s up to 20 A

Case 2. Power supply OFF and Power supply cut-off

The second set of experiments were carried out to study the effects for the power supply during quench. Literature shows that the power supply detects the quench and cuts off the current, but the power supply is not physically cut off causing the power supply to be present as a passive component in the quench circuit. The current can pass through the power supply and can damage the internal components. To study these characteristics, the power supply was isolated from the circuit using a circuit breaker and the current decay is compared with the case when the power

supply is directly switched off. The case when power supply is switched off is shown in figure 6.7, which shows that a sudden voltage spike of -0.6 V occurs and which then starts decreasing linearly till -0.3 V after switching OFF the power supply. After 0.3 V, the decay rate suddenly drops, creating sudden drop in voltage. This mode of operation is due to the presence of a protecting diode in the power supply which started conducting and the current is decaying through diode up to its forward voltage limit. After voltage drops below the forward bias voltage, the diode stops conducting and an exponential decrease in the voltage which happens through the dumping resistor in L/R_D manner. It concludes that if quench happens, then the maximum energy will decay in the coil as diode is providing is low resistance path to the current by bypassing of the dumping resistor.

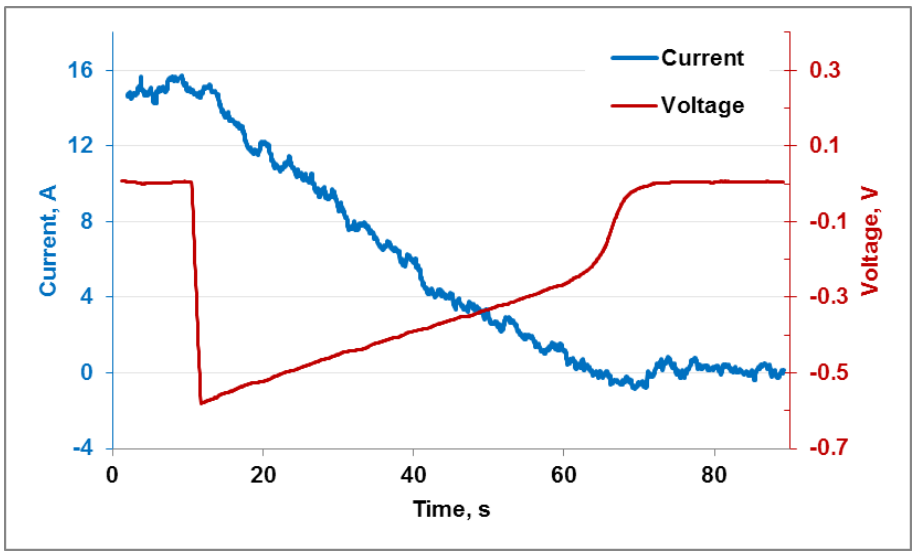

Figure 6.7 15A Power Supply Off

Above case shows that the power supply is present in the circuit even after it is switched off and leads to the necessity of physically removing the power-supply after quenching to characterize the actual behaviour of the current decay when it is protected by the dumping resistor as a protection circuitry. The circuit breaker isolates the power from the main electrical circuit. The cut off of the power supply causes sudden jump in the voltage across the voltage tap as shown in figure 6.7. Then the exponential decay associated with an L-R circuit can be observed. In which time constant is calculated as $\tau_C = 1.648$. It is to be noted that in this case the voltage developed is much higher since there are no components like diodes restricting the voltage growth.

Case 3. Quenching of the coil at 80A with a dump resistor of 1 Ω for Protection

The heater input pulse of 10W is ~2.8 sec through the Keithley Source Meter with input of 1A current to 10 Ω heater mounted on the coil. As the heater switches ON, coil becoming resistive with indication in the power supply as "Quenched" due to the generation of quench voltage in to the coil, the recorded data shows that the power supply send the current in to coil till it reaches voltage limit set by the user. On the pressing of the isolation nob, circuit breaker isolates the power supply along with its quench state circuitry. As power supply is cut-off from the circuit, the polarity of the voltage changes instantly with spike of 60 V as shown in figure 6.9. The shunt resistor R_{sh_D} in series with dumping resistor also shows jump of ~65 A in the current flowing through it after cut-off. The coil current and shunt current shows same profile of the decay as whole current is passing through the dumping resistor. From the back calculation, the quenched coil resistor R_Q is 0.6 Ω as it takes 1.5s less compared to non-quench circuit measured for the cut-off case. Figure 6.8 quenched time temperature data is recorded in temperature monitor and it shows that peak temperature rise is about 17 K and again comes back to LHe bath temperature.

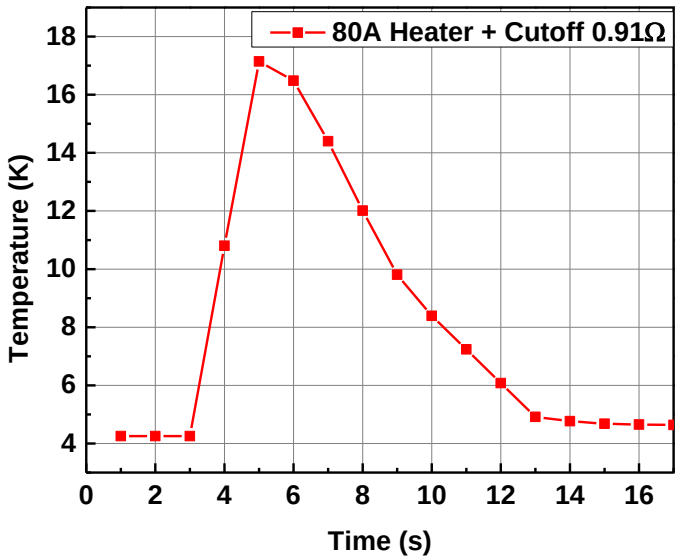

Figure 6.8 Temperature of the coil (T9, K) Vs Time (s)

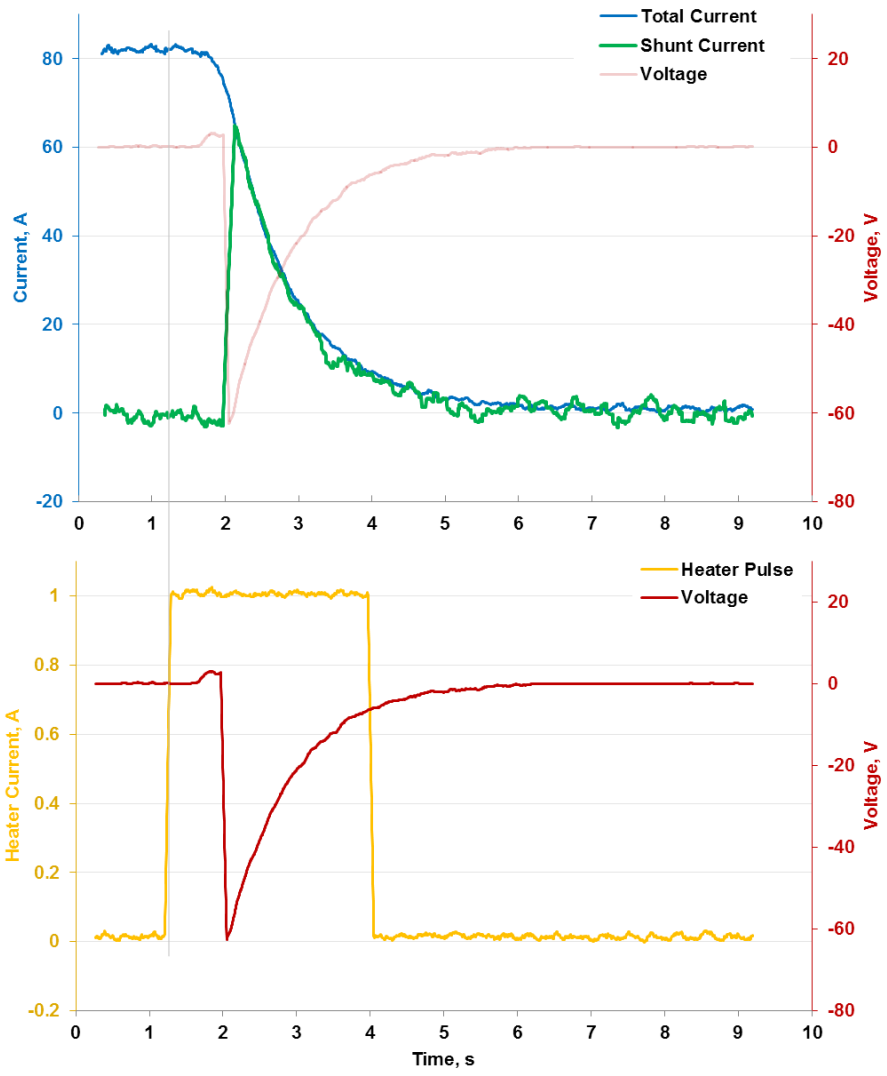

Figure 6.9 80A Heater + Cut-off, 0.91Ω Resistor

Case 4. Quenching of the coil with (26 80A Heater + Cut-off) 2.5Ω dumping Resistor as the protection circuit

In this case the dumping resistor is of 2.5Ω and heater pulse is ON throughout the decay of the coil current as shown in figure 6.10. The quench is initiated by 10 W heater input and power supply sense the voltage generation across the coil and starts signalling as 'Quenched'. The voltage increases in the coil up to power supply set point. After crossing the limit, power supply stops sending the current by virtual cut-off from the electrical circuit. Then the voltage polarity reverses because the inductive coil started behaving like a battery and current is still flowing into the

quenched state power supply circuitry. This area shows linear decrement in the voltage through the diode action of the power supply quench mode protection. The circuit breaker comes into the picture by isolating the power supply from electrical circuit and full remaining current start decaying through the dumping resistor R_D and shunt resistor R_{sh_D} .

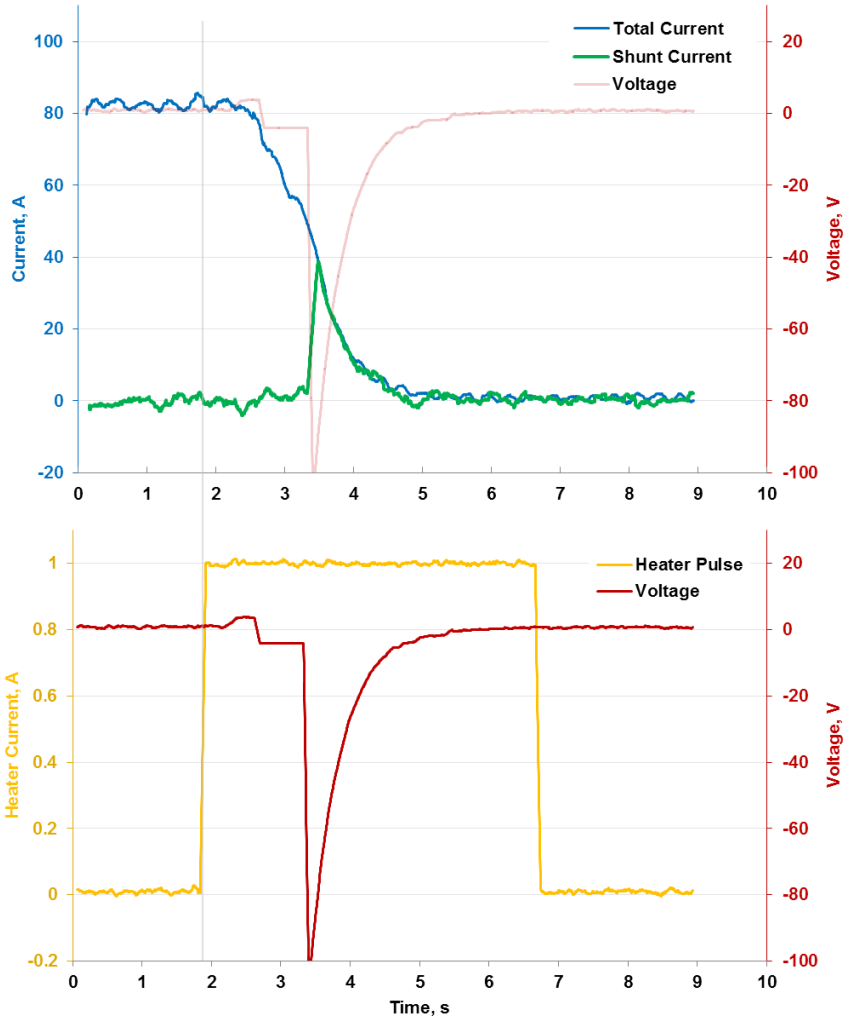

Figure 6.10 80 A Heater + Cut-off

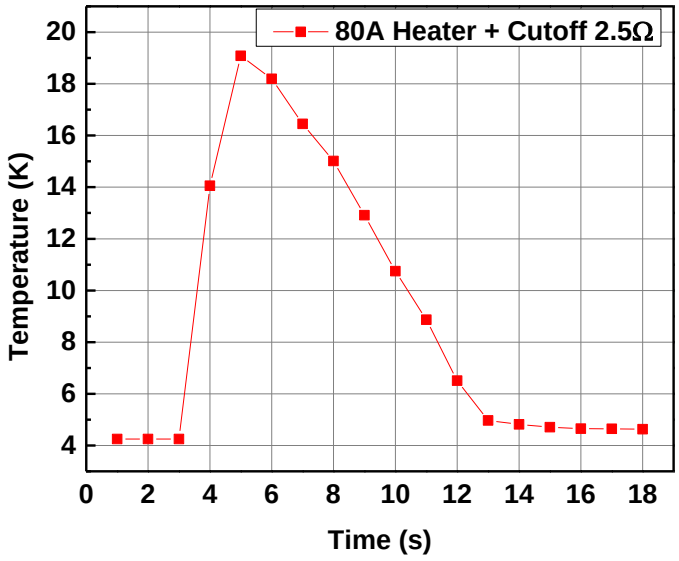

Figure 6.11 Temperature of the coil (T9, K) Vs Time (s)

Both shunt current and dumping current follow the same profile of current decay after cut-off. The voltage spike of 100 V after cut-off appears across the dumping resistor and after that the current decay is controlled by ratio of $\frac{L}{R_D+R_Q}$. The 95% of the remaining current after cut-off decays in 1.7 s, which results from the back calculation the time constant reduced to ~0.57s from 1.5s. The average rise in the quench resistance from the calculation of time constant is 0.147Ω. The high value of dumping resistor results in lower resistance in the coil by allowing the dumping path to stored energy. The peak temperature of magnet rises to nearly 19 K within 2 sec and again comes back to LHE bath temperature of 4.2 K. The profile is plotted in figure 6.11.

Case 5. Quenching of the coil with (27 80 A Quench,) 2.5Ω dumping Resistor as the protection circuit with 3W heater

For quenching purpose only energy of 100mJ is sufficient to raise the temperature above critical temperature of the coil. The heater input of 3W is given in this case and tested the coil at 80A. The heater capacity of 1W and 2W cases not able to quench the coil. This is because of infinite cooling available as coil is dipped in LHe and heater thermal contact with coil also point of concern in forceful quenching. Figure 6.12 shows that the voltage start rising up to 3V which is set voltage

limit of the power supply after that polarity changes and current decays is controlled by 'Quenched' condition protection circuitry of the power supply. The negative peak of voltage is of - 4.2 V and decays linearly till -3.5 V. Then final decay is faster through the resistor circuit as QPS.

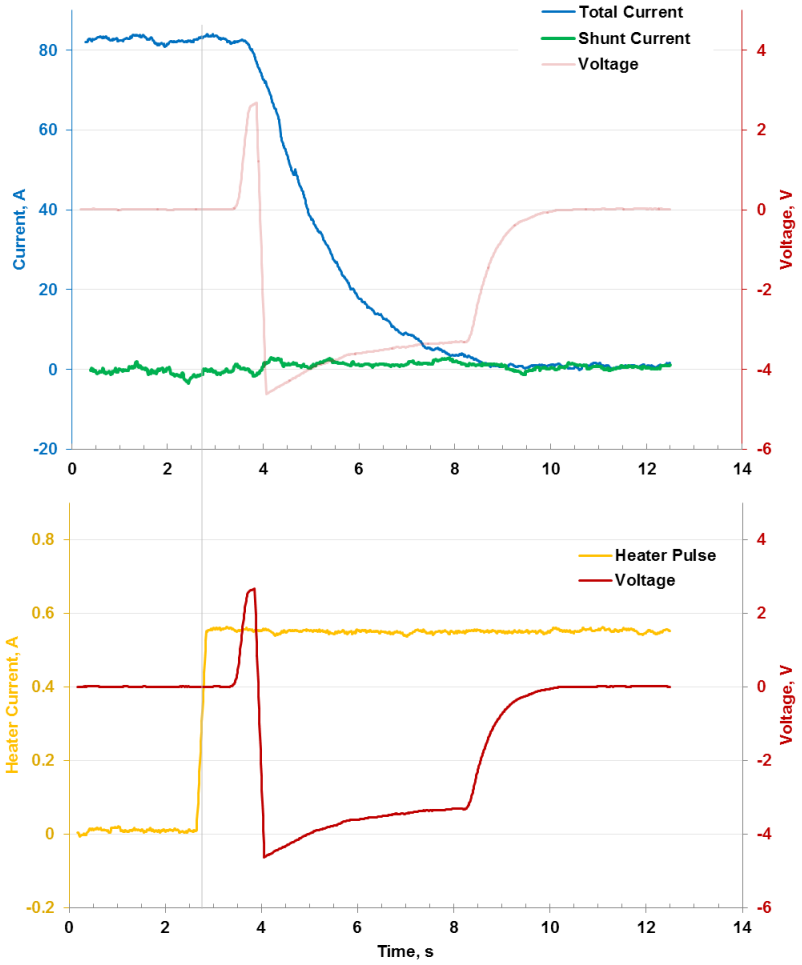

Figure 6.12 80 A Heater 3W

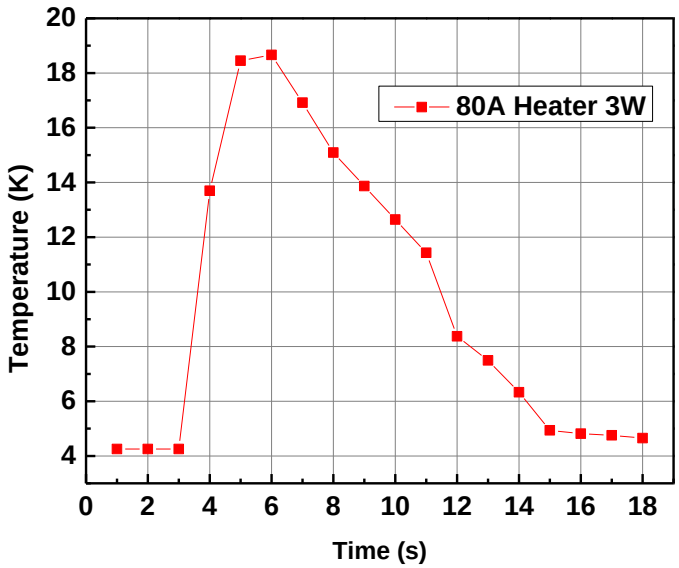

Figure 6.13 Temperature of the coil (T9, K) Vs Time (s)

The peak temperature rise of ~19 K is recorded within initial 2 s is as shown in figure 6.13. After reaching peak temperature coil decreases again to LHe bath temperature in next 10 s. this result shows that coil in self-protecting type.

Chapter 7

7 QUENCH SIMULATION OF QUADRUPOLE SINGLET STRUCTURE (QSS)

7.1.1 SELF AND MUTUAL INDUCTANCE OF QSS

The QSS has four coils which are connected in series with the superconducting joints. The LCR meter is used to find out the inductance of QSS. The measurement is taken out with the connection of LCR meter at the coil terminals. The measured inductance values are used in the QUENCH programme in the OPERA-3D [ref.no.]. Table 7.1 shows the inductance matrix of the QSS.

Table 7.1 Inductance matrix

L1	M12	M13	M14
M21	L2	M23	M24
M31	M32	L3	M34
M41	M42	M43	L4

=

1.7	0.225	-0.06	0.225
0.225	1.7	0.225	-0.06
-0.06	0.225	1.7	0.225
M41	-0.06	0.225	1.7

The OPERA-QUENCH code permits to perform quench with the all possible boundary conditions. A heat flux boundary condition is used to initiate the quench in QSS. Figure 7.1 shows the QSS model in OPERA-3D.

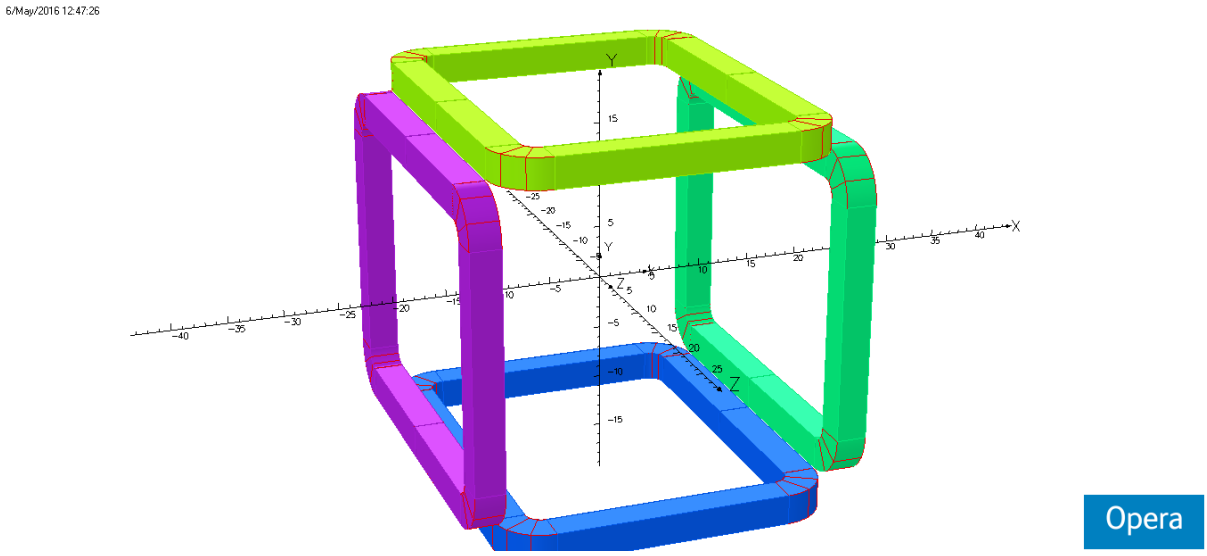

Figure 7.1 Modelling of the singlet structure in opera modeller for the Quench tool

The intentional quenches for QSS are simulated with the different protection configuration. Here each singlet can be protected against the quench by following ways:-

I. Subdivision of the QSS coils.
II. Simple protection across the QSS.

The quench simulations have been done with different ways, which are discussed below.

Case 1. Back-to-back diode with resistor across each individual coil

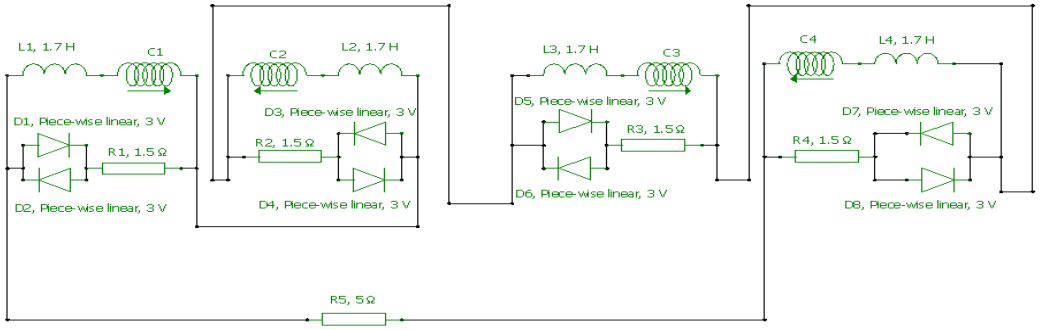

Figure 7.2 Electrical circuit of B2B+R across individual coil

The back-to-back diode (3V) with resistor (1.5 Ω) across each coil is an ideal circuit in case of subdivision in which diode threshold voltage stops the current flow at the time of magnet charging through the resistors. A dump resistor is also attached across the QSS to dump some amount of energy into it to reduce heating of the coil after quenching. The value of main dumping resistor is5 Ω, as shown in Figure 7.2. The initial time step of 0.0001 s with 10% error in time stepping and the equation tolerance limit of 10^{-6} is used for all the simulations of the QSS. For each time steps, the results are recorded and plotted as follows for quench temperature rise, the resistive zone growth, the current decay in coil and the voltage profile.

The propagation of the normal zone during quench in the coils is shown in figure 7.3 for the different time conditions.

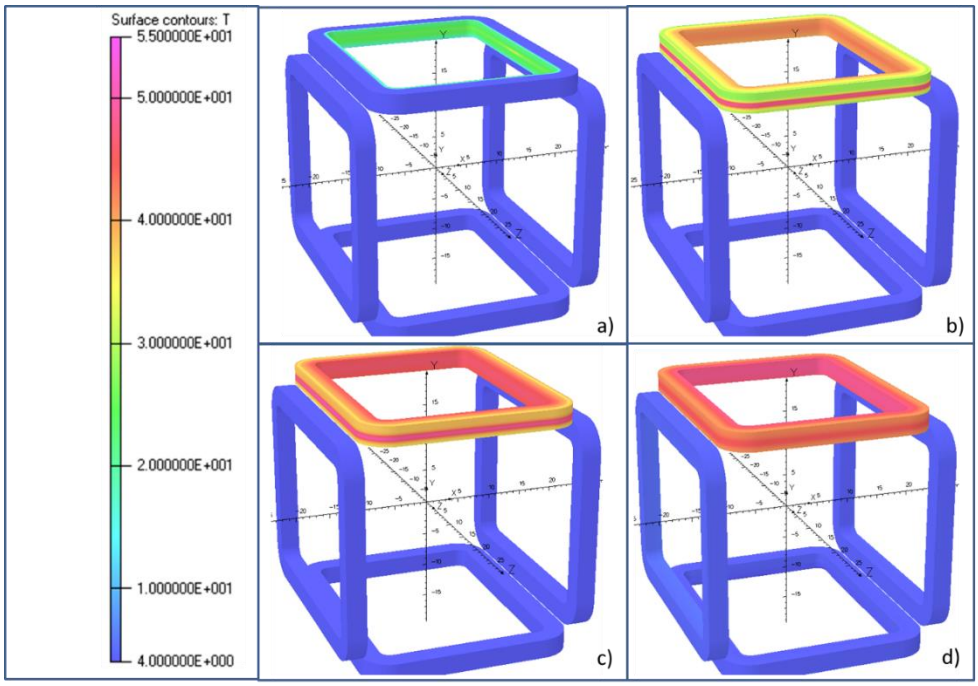

Figure 7.3 Temperature contours of the coil for B2B Diodes + Resistor across each coil as Quench Protection circuit at the different time steps a) t=0.1s, b) t=0.5s, c) t=1s and d) t=5s

The heat flux of 50 W/cm^2 in area of 0.2 X 0.2 cm^2 is provided to initiate the quench by supplying localised heat of 2 W into the coil 1 (C1). Figure 7.3 a) shows that as coil 1 quenches, the heat started spreading from the heal flux region through the conduction The quench propagates in outer layers as time goes on due the stored energy started dumping as the joule heating because of substantial rise of resistance within the coil is shown figure 7.3 b) and c). Till the end of 5 s the whole coil will become resistive, rest of the remaining three coils are in superconducting state without any sign of resistance increment throughout the simulation time period as shown in figure 7.3 d).

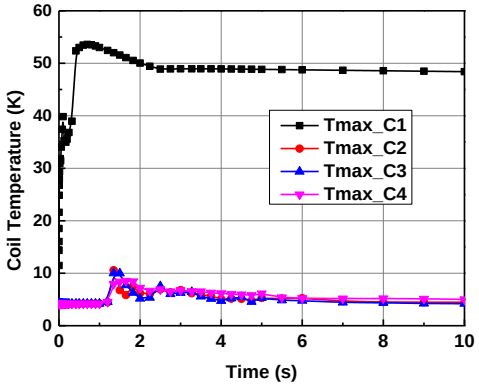

a) Temperature(K) Vs Time(s)

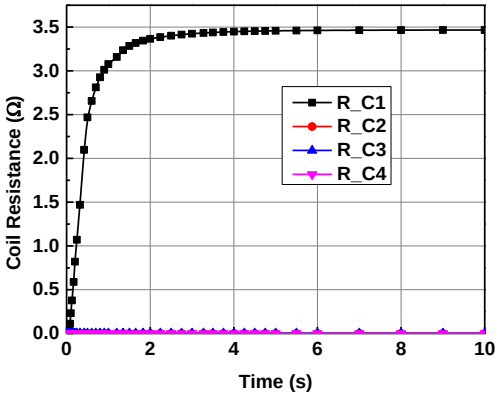

b) Resistance(Ω) Vs Time(s)

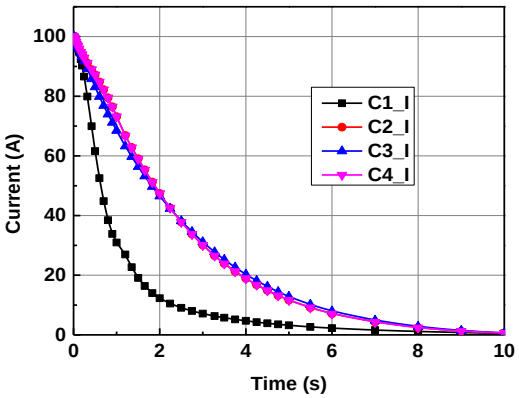

c) Current(A) Vs Time(s)

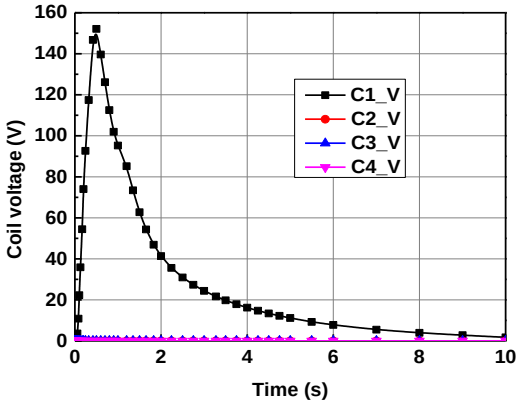

d) Voltage(V) Vs Time(s)

Figure 7.4 The Quench simulation results of B2B Diodes + Resistor across individual coil as a Quench Protection circuit across the coil

As the heater pulse initiates the temperature shoots up in the coil 1. At 0.0003 s coil temperature rises to 14.35 K, it shows the sign of first quench as there is rise in the resistance value of 2.3 X 10^{-6} Ω and current starts decaying. From figure 7.4 a) till the heater pulse is in ON condition, the temperature rises up to 39.83 K with coil quench resistance of 0.23 Ω and current value of 96.35 A. As heater comes to OFF mode, the resistive zone starts propagating with rapid increment in the coil quench resistance till 1s and it reaches to 3.07 Ω as shown in figure 8.4 b), whereas the coil temperature reduces to 34.96 K and again starts rising as coil becoming more resistive with 69.04 % decay of the current in 1sec. The maximum temperature of the coil is 53.6 K, which is quite

acceptable and will not cause any damage in the winding. After 1 sec both coil temperature and coil resistance shows the flattening nature with slow increment in the coil resistance and slow decrement in the coil temperature. The peak voltage across the coil 1 is 152.12 V at 0.5 s. and again decreases to zero as resistance increment and current decrement in coil 1 as shown in figure 7.4 c). The final resistance rise in coil is 3.47Ω at end of the 10 s.

Case 2. Back-to-back diode across each individual coil

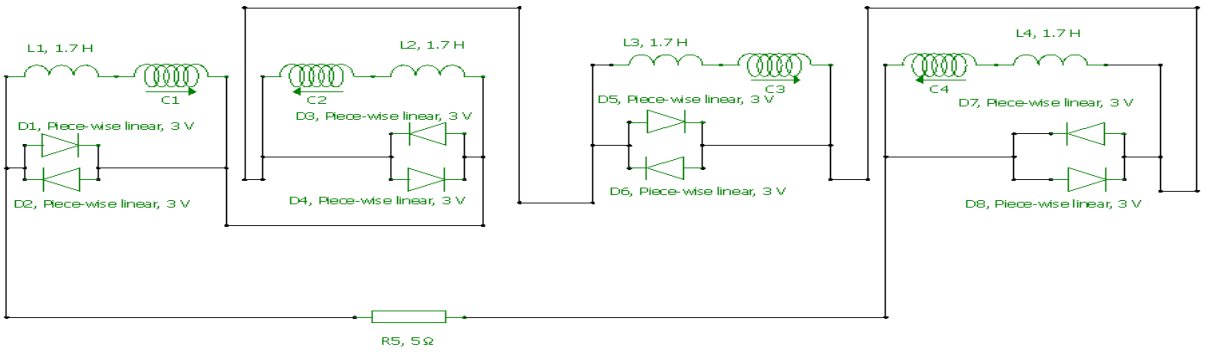

Figure 7.5 Electrical circuit of the B2B Diode across individual coil

In figure 7.5, the series resistors are not included with the diodes, the diodes are triggered as their forward voltage is generated across the coil. Diode protects the coils through bypassing the flowing current. The dumping resistor of 5Ω is also attached as discussed previously.

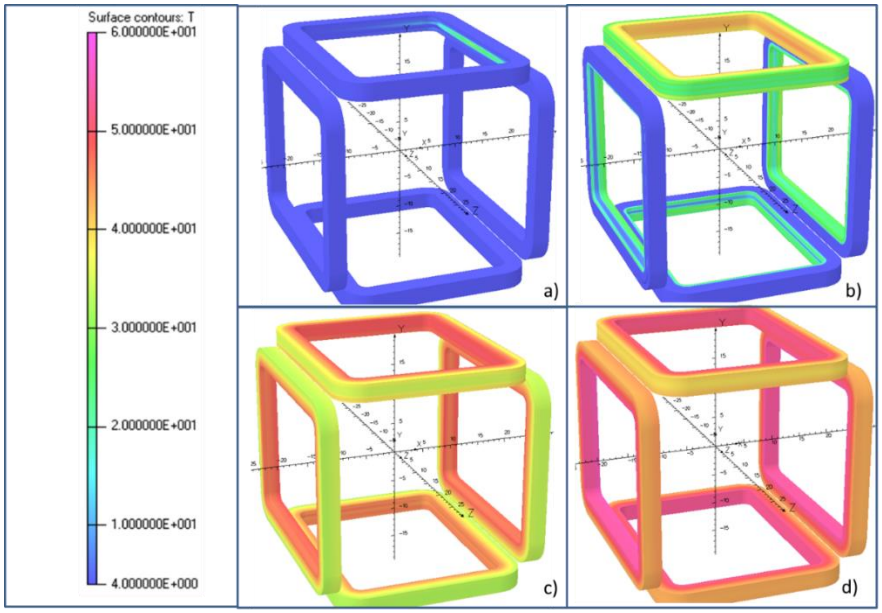

Figure 7.6 Temperature contours of the coil for B2B Diodes across individual coil as Quench Protection circuit at the different time steps a) t=0.1s, b) t=0.5s, c) t=1s and d) t=5s

The propagation of the normal zone in the coils is shown as follows for the different time conditions are shown in figure 7.6. Heater of 2 W capacity for 0.1 s initiate quenching in coil 1. Heater inner layer becomes resistive at starting as shown in figure 7.6 a) and after it spreads over the time to outer layers 7.6 b) with quench induction into the other 3 coils due to mutual coupling between them. At end of 10 s, whole singlet becomes a resistive with maximum temperature rise is shown in figure 7.6 b) and d).For each time stepping the results are recorded and plotted in figure 7.7 for quench temperature rise, the resistive zone growth, the current decay in coil and the voltage profile.

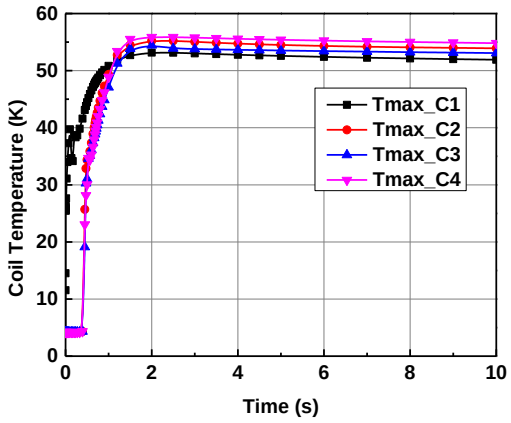

a) Temperature(K) Vs Time(s)

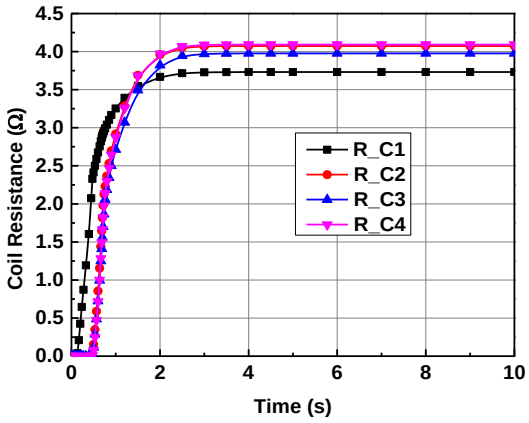

b) Resistance(Ω) Vs Time(s)

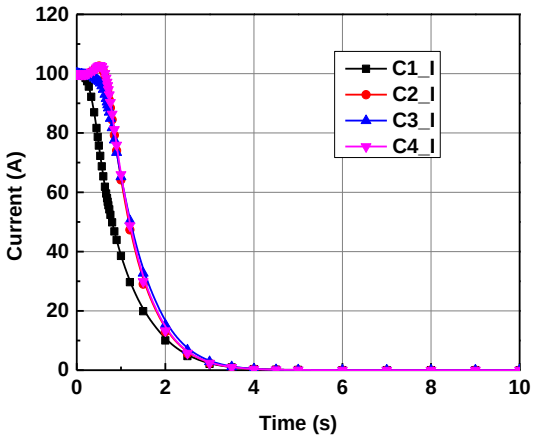

c) Current(A) Vs Time(s)

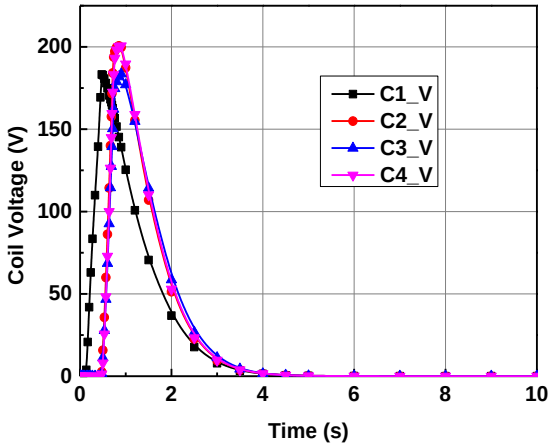

d) Voltage(V) Vs Time(s)

Figure 7.7 The Quench simulation results of B2B Diodes across individual coil as a Quench Protection circuit across the coil

As quench initiates in the coil1, then current starts decay in coil 1 and due to mutual coupling current in other coils increase to maintain the flux related to singlet. In first 0.1 s coil 1 reaches to 39.73 K temperature with resistance of 0.00065Ω. After 0.4476 s all coils become resistive in nature with peak hump in their operating temperature at condition coil 1 with 81.68A, 2.073Ω and 169.3 V. Coil 2 temperature rises to 25.71 K from 4.32 K, coil 3 temperature increases to 19.1 from 4.32 K and coil 3 temperature increases to 23.05 K from 4.34 K. The peak voltage in coil 1

is 183.24 V at 0.473 s and maximum temperature is 55.86 K at 2.5 s. The peak voltage in coil 2 is 200.5V at 0.8 s and maximum temperature is 55.23 K at 2s. The peak voltage in coil 3 is 183.59 V at 0.9s and maximum temperature is 54.4 K at 2 s. The peak voltage in coil 4 is 200.6 V at 0.9 s and maximum temperature is 55.78 K. The current decay in coils 2, 3 and 4 lags behind coil and within 10 s the current in all coil decays to zero. In end of 10 s, coils 1, 2, 3 and 4 reaches to resistance value of 3.732Ω, 4.073Ω, 3.977Ω and 4.093Ω respectively. The current decays is within 4 s to zero as all coils are resistive and energy is dumping into it only.

Comparison of singlet simulation between case 1 and 2

In case 1 and 2, except the Quench Protection System (QPS) across individual coil other all parameter are same. In case 1, only coil 1 becomes resistive after quenching till the end of simulation. But in case 2, all coils become resistive in nature because of absence of resistor across each coil with B2B diodes. The peak voltage is 152.12 V for coil 1 in case 1 and for case 2 the peak voltage is 200.6 V in coil 4. The coil 1 gets heated with highest temperature of 55.86 K in case 2 and in case 1 coil1 gets heated to maximum temperature of 53.6 K. The current decays with rapid manner in case 2 than case 1, because of more resistance offered by all quenched coil.

Case 3. Resistor across each individual coil

a) 5Ω resistor as a dumping path for coils having 1.5 ohm resistor across each coil

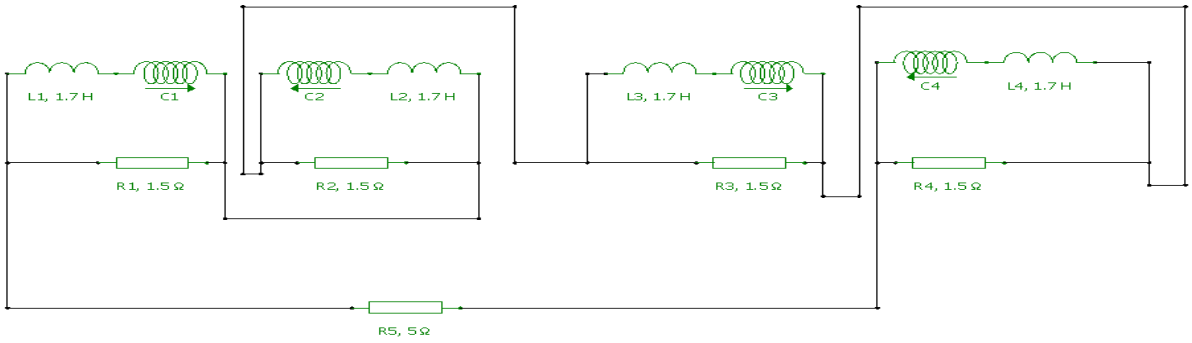

Figure 7.8 Electrical circuit for the resistor as a protection circuit across individual coil

The resistor across each individual coil allows fraction of stored energy to be dumped through it after quenching. But this circuit as shown in figure 8.8 has boil-off problems of liquid helium at

the time of charging due to inductive voltage generation as ramping rate associated coil inductance. The back-to-back diode plus resistor case is exact similar to this circuit with charging time advantage.

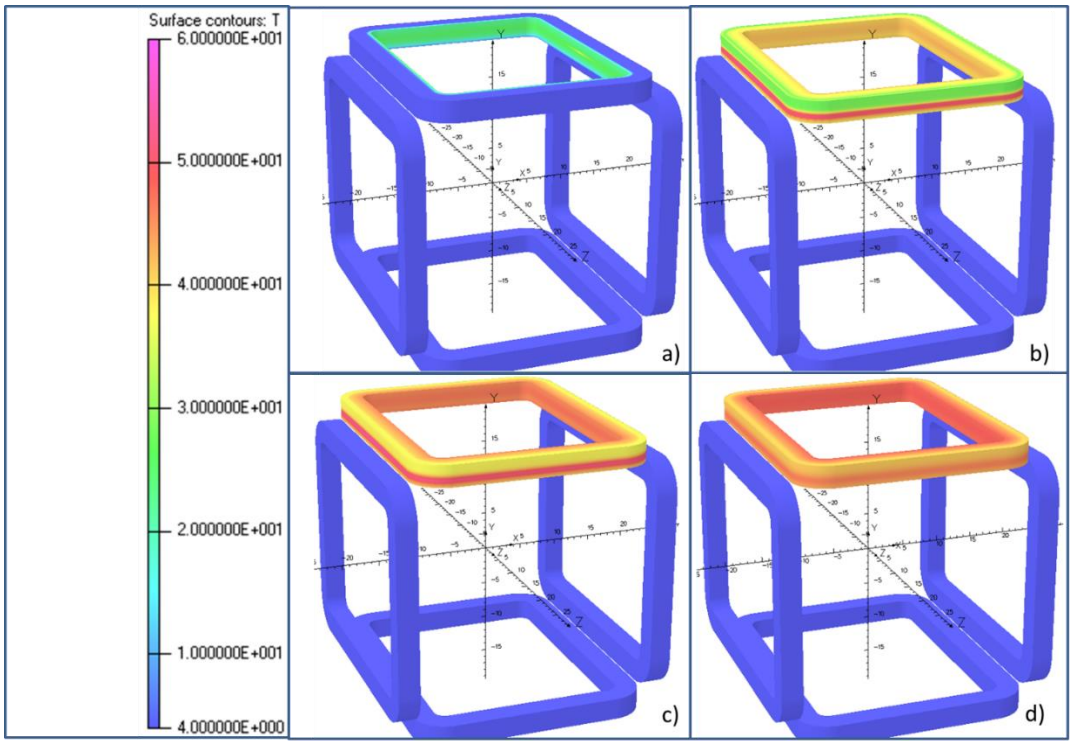

Figure 7.9 Temperature contours of the coil for Resistor across individual coil as Quench Protection circuit at the different time steps a) t=0.1s, b) t=0.5s, c) t=1s and d) t=5s

The propagation of the normal zone the coils at the different time conditions are shown in figure 7.9. The normal zone starts spreading in inner layer of coil 1 within 0.1 s, further time periods, this normal zone propagates to outer layers and full coil 1 becomes resistive in nature. Rest coils; 2, 3 and 4 remain in its superconducting state. The temperature profile in figure 7.10 a) describes about heater domination for initial 0.1 s and after that joule heating drives it to full resistive nature. The maximum temperature is 55.47 K at 0.7 sec and it settles down to 47-48 K range within 10 s. The resistance in coil 1 increases as temperature increases linearly and after 1 s there is small change in resistance with temperature is plotted in figure 7.10 b). The highest resistance in the coil 1 is 3.424Ω. Figure 7.10 c) shows that the current decays in coil 1 from 100 A to 0.5 A within 10 s, all remaining coil three coils having current of 2 A due to mutual inductance. The voltage peak is of 153.6 V is at 0.5 s and it further decreases as resistance and temperature curves start flattening and

current is also decaying through QPS. For each time stepping the results are recorded and plotted as follows in figure 7.10 for quench temperature rise, the resistive zone growth, the current decay in coil and the voltage profile.

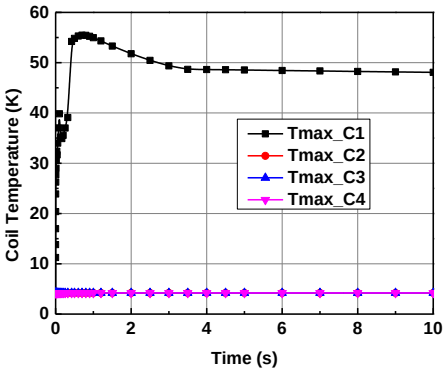

a) Temperature(K) Vs Time(s)

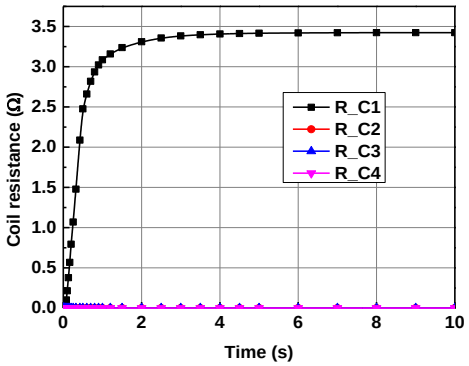

b) Resistance(Ω) Vs Time(s)

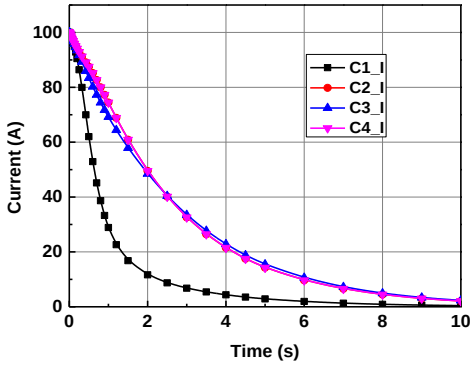

c) Current(A) Vs Time(s)

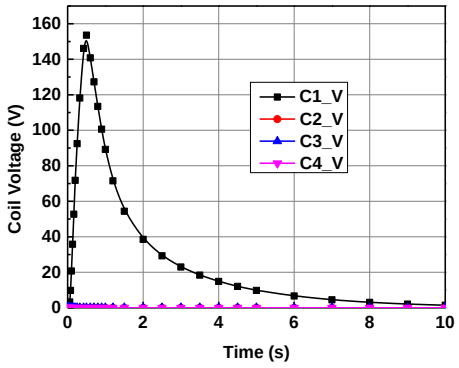

d) Voltage(V) Vs Time(s)

Figure 7.10 The Quench simulation results of Resistor across individual coil as a Quench Protection circuit across the coil

Comparison between cases 1 and 3 a)

As both cases having same resistor across each coil for dumping the energy shows similar nature of the quenched parameters. The initially case 1, after quench in coil 1 the voltage rises faster up to diodes forward voltage limit of 3V and then it starts decaying through resistor. The maximum temperature in case 1 and 3 is 53.6 K and 55.47 K respectively. The resistance and

voltage peaks are nearly of same values. The B2B+R has only charging time advantage which eliminates helium boil-off problem of case 3.

b) **Back to back diode across QSS with resistor across each coil.**

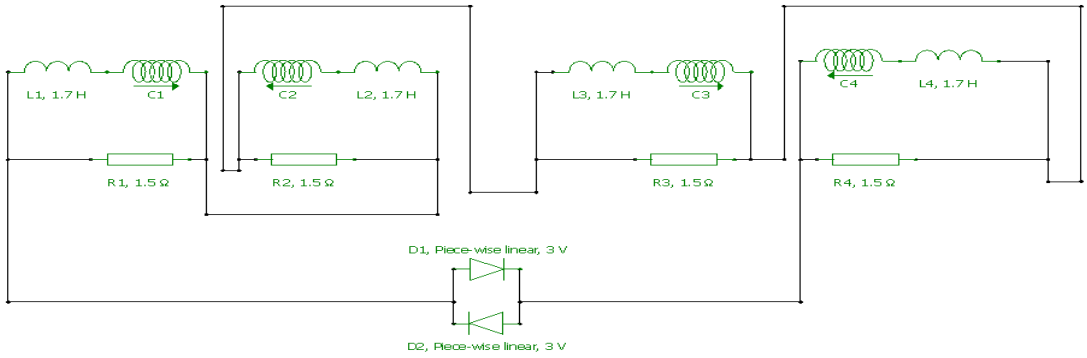

Figure 7.11 Electrical circuit for the resistor as a protection circuit across individual coil with back-to-back diodes across the singlet

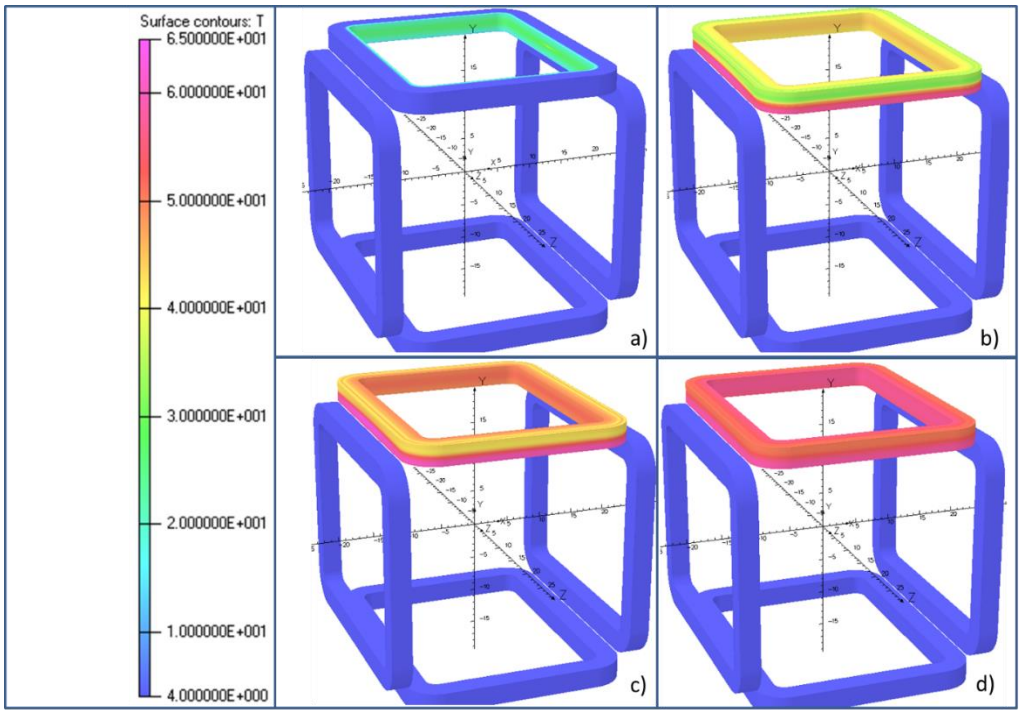

Figure 7.12 Temperature contours of the coil for only Resistor across individual coil with back-to-back across the singlet as Quench Protection circuit at the different time steps a) t=0.1s, b) t=0.5s, c) t=1s and d) t=5s

The resistor across each individual coil as QPS and back-to-back diode across the singlet is used as quench protection circuit for this case. From previous case, only difference is that the dumping resistor across the singlet is replaced by back-to-back diodes. In figure 7.12 a) shows initiation of quenching in coil 1 due to heater and other contour shows that the propagation of normal zone from inner layer to outer layer of coil 1.

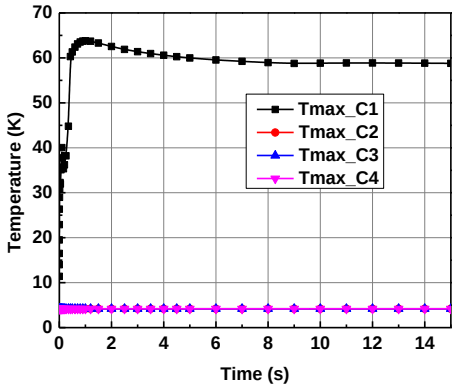

a) Temperature(K) Vs Time(s)

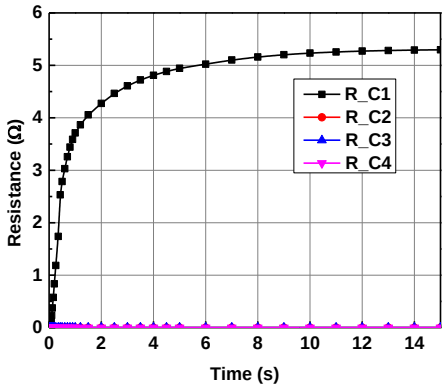

b) Resistance(Ω) Vs Time(s)

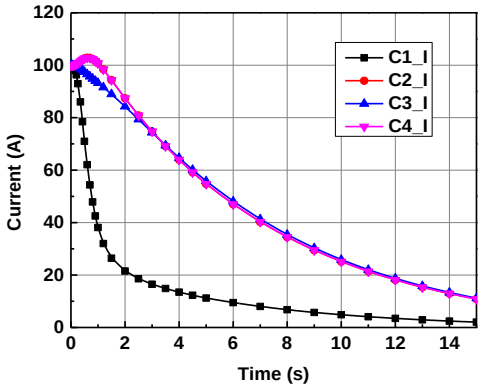

c) Current(A) Vs Time(s)

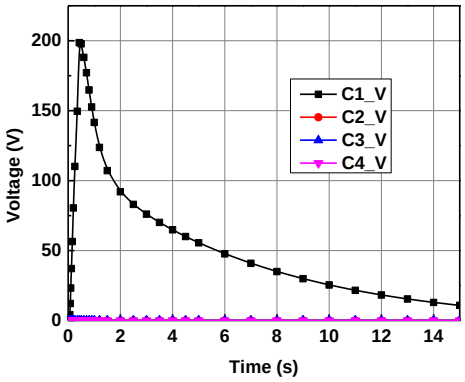

d) Voltage(V) Vs Time(s)

Figure 7.13 The Quench simulation results of Resistor across individual coil with back-to-back across the singlet as a Quench Protection circuit across the coil

In this case, figure 7.13 a) shows that the temperature reaches to maximum value of 63.78 K at 1 s and it settle to 58 K in next 10 s. Current in coil 1 starts decays, due to flux adjustment increment in current occurs in coils 2 and coil 4 to 102.77 A and 101.65 A respectively. Current decays early

in coil 1 to 5 A in 15 sec as it become resistive only and all other coils still carrying 10A of remaining current as shown in figure 7.13 c). The voltage peak of 198.62 V at 0.425 s and it reduces further as current decays as plotted in figure 7.13 d). Coil 1 is subjected to linear increment in resistance with temperature and it reaches to highest resistance of 5.29 Ω is shown in figure 7.13 b).

c) B2B diode plus resistor as a dumping path for the coils having 1.5 ohm across each

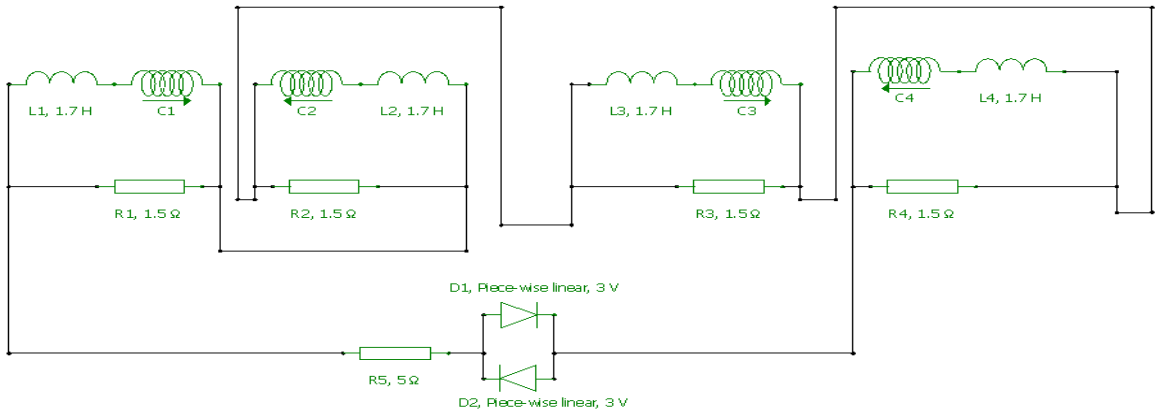

Figure 7.14 Electrical circuit for the resistor as a protection circuit across individual coil with back-to-back diodes plus resistor across the singlet

The resistor across each individual coil as QPS and back-to-back diode across the singlet is used as quench protection circuit for this case. From previous case, only difference is that the back-to-diodes across the singlet is replaced by back-to-back diodes and resistor. This case is also shows similar propagation of normal zone as in case 3 a) in the coil1.

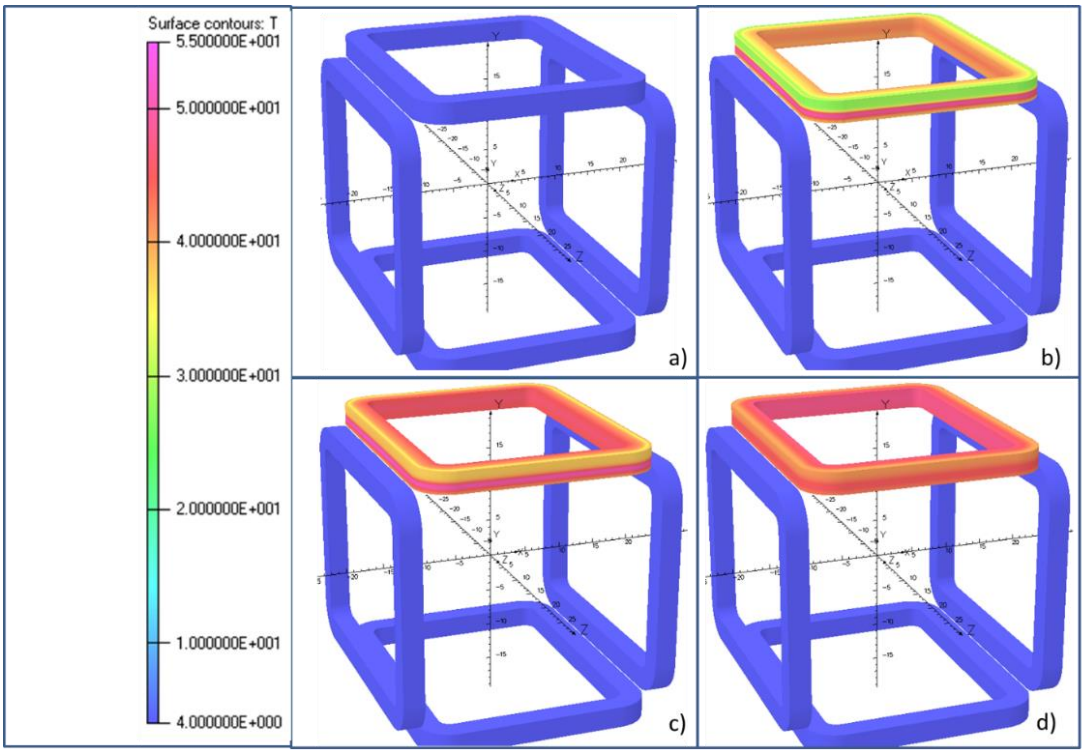

Figure 7.15 Temperature contours of the coil for only Resistor across individual coil with back-to-back plus resistor across the singlet as Quench Protection circuit at the different time steps a) t=0.1s, b) t=0.5s, c) t=1s and d) t=5s

In this coil 1 is in quenched state and all remaining coils are in superconducting state. Figure 7.16 a) shows that the maximum temperature of coil 1 is 54.15 K at 0.7 s and it settles to 48 K in next 10 s. The peak voltage rises to 153 V at 0.5s and further decreases as current decays as plotted in figure 7.16 d). The current decays to 0.3 A in 10s in coil 1 and in remaining coils it is ~3 A due to lag in current decay caused by mutual inductance as shown in figure 7.16 c).

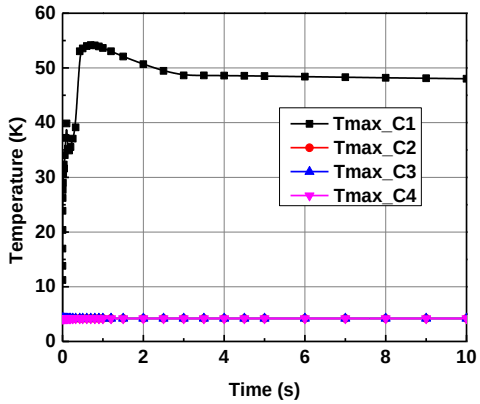

a) Temperature(K) Vs Time(s)

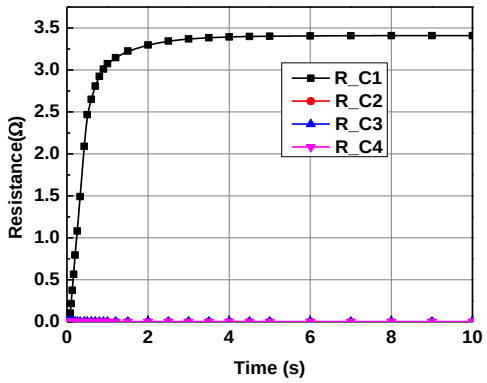

b) Resistance(Ω) Vs Time(s)

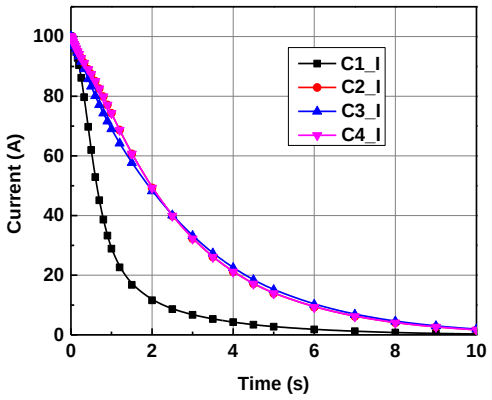

c) Current(A) Vs Time(s)

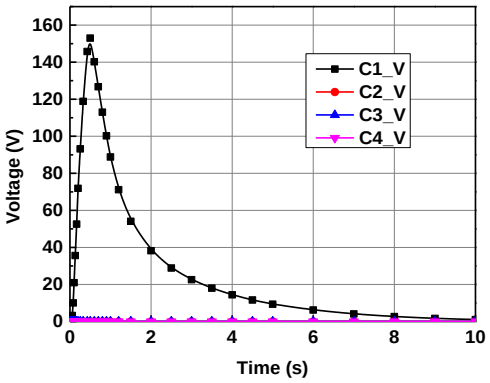

d) Voltage(V) Vs Time(s)

Figure 7.16 The Quench simulation results of Resistor across individual coil as a Quench Protection circuit across the coil

Comparison between 3. a), b) and c)

Case 3 a) and c) are similar in nature with almost same temperature rise of 54.15 and 55..47 K respectively with peak voltage of 153 V at 0.5 s. Case 3 b) takes longer time to decay the initial current with respect to case a) and c). The voltage rise 198.62 V and maximum temperature 63.78 K is also higher in case b) compared to case a) and c).

Case 4. Only Dumping resistor as the protection circuit across the singlet

a) Dumping resistor of 5Ω across the singlet as QPS

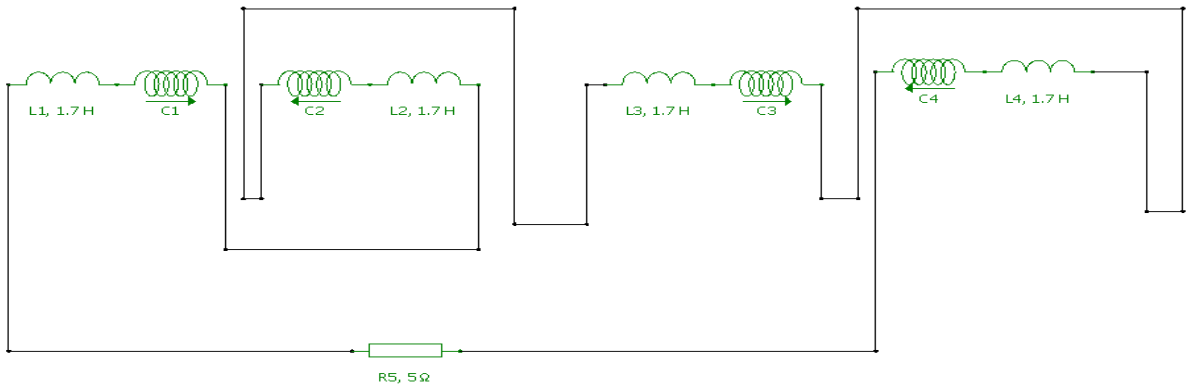

Figure 7.17 Electrical circuit for the dumping resistor of 5 Ω as the protection circuit for singlet

All coils are series with current direction resistor parallel to power supply is used to dump the part of the stored energy which becomes series component to coils after quenching so as to complete the circuit is shown in figure 7.17. The dumping resistor of 5Ω is across the singlet. The propagation of the normal zone the coils is shown as follows in figure 8.18 for the different time conditions. The quench is initiated in inner layer of coil 1 and over the period of 10s full coil becomes resistive in nature.

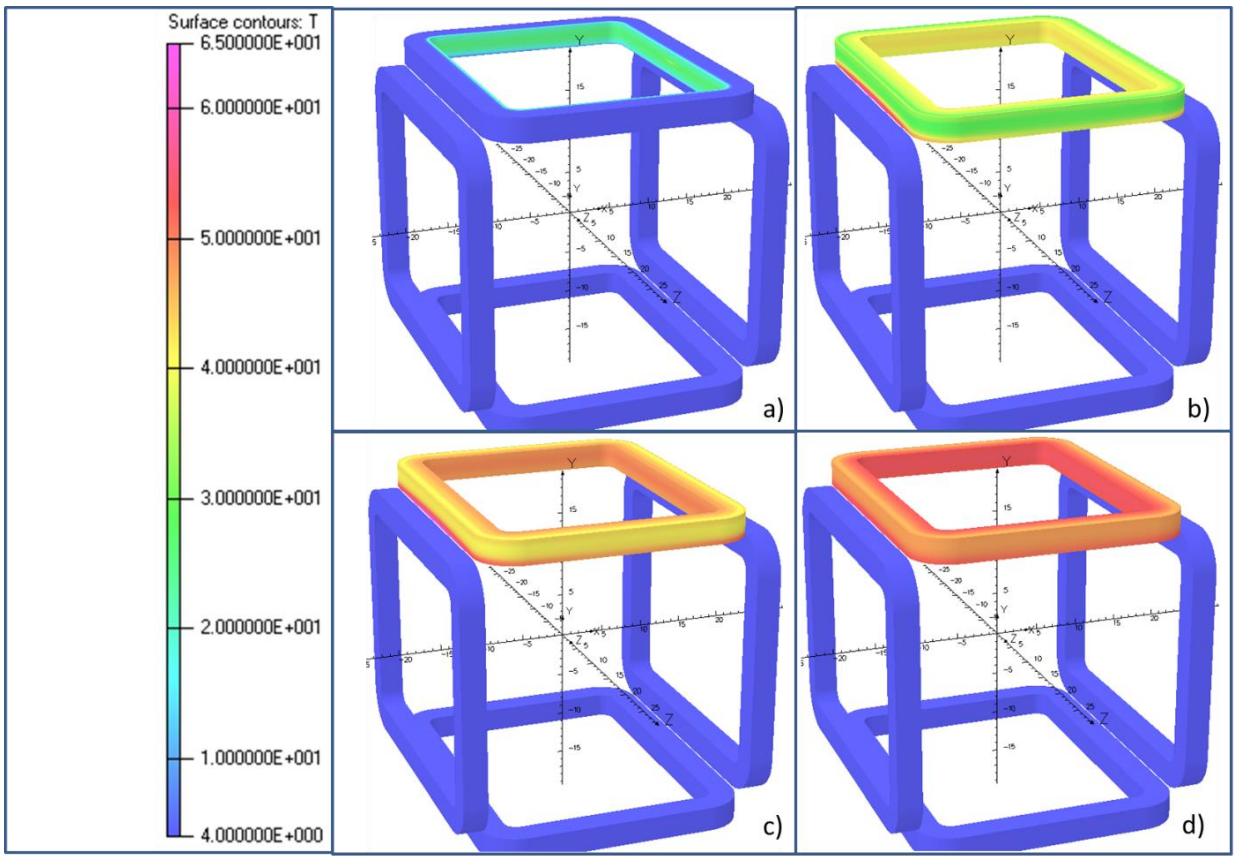

Figure 7.18 Temperature contours of the coil for the dumping resistor of 5Ω as the protection circuit for singlet at the different time steps a) t=0.1s, b) t=0.5s, c) t=1s and d) t=5s

For each time stepping the results are recorded and plotted in figure 7.19 for quench temperature rise, the resistive zone growth, the current decay in coil and the voltage profile. Figure 8.19 a) shows that the maximum temperature of 63.43 K at 1.5s is achieved in coil 1 and all other coil remains in superconducting state with no rise in temperature. The peak voltage rise is 172.66 V at 0.5 s and coil 1 reaches highest resistance of 4.25Ω in 10 s is shown in figure 7.19 b) and d). Current decays simultaneously in all coil as change in flux due to current decay is directly linked to all coils without any subdivision type is shown in figure 7.19 c).

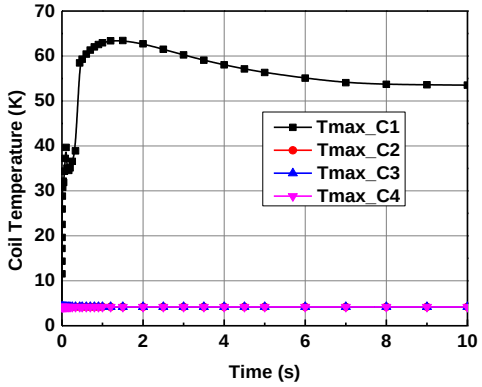

a) Temperature(K) Vs Time(s)

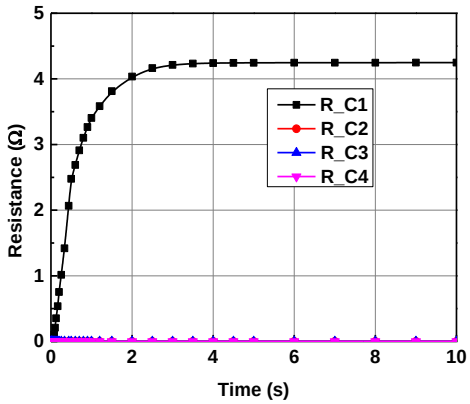

b) Resistance(Ω) Vs Time(s)

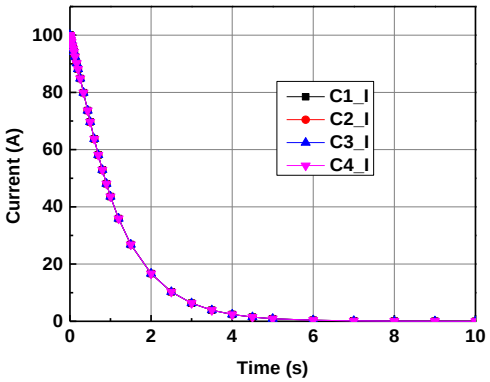

c) Current(A) Vs Time(s)

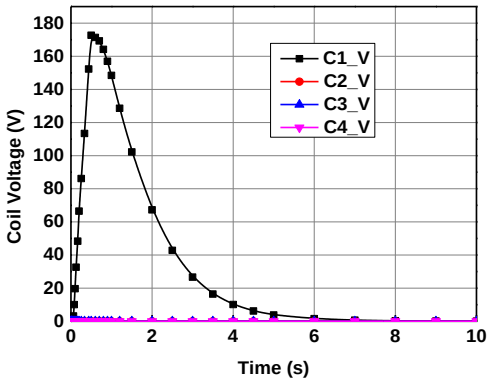

d) Voltage(V) Vs Time(s)

Figure 7.19 The Quench simulation results of the dumping resistor 5Ω as the protection circuit for singlet

b) Dumping resistor of 1.5Ω across the singlet

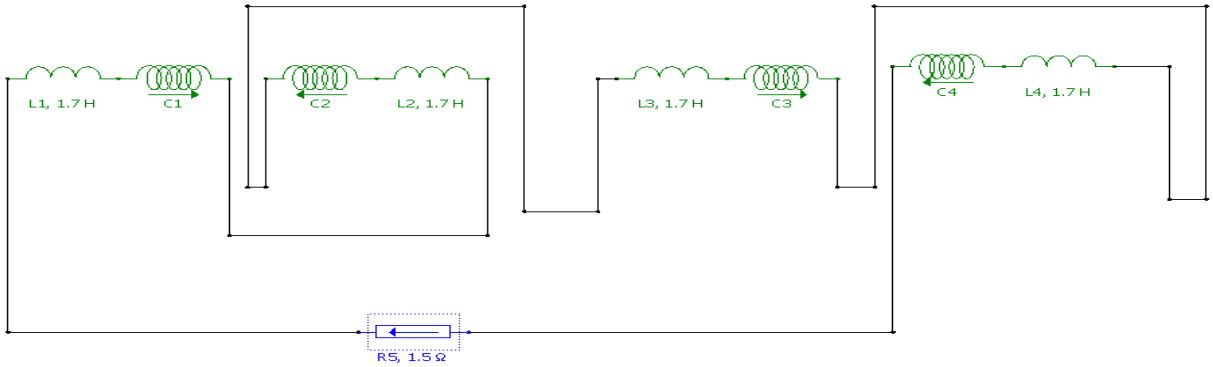

Figure 7.20 Electrical circuit for the dumping resistor of 1.5 Ω as the protection circuit for singlet

All coils are series with current direction resistor parallel to power supply is used to dump the part of the stored energy which becomes series component to coils after quenching so as to complete the circuit as shown in figure 7.20. The dumping resistor of 1.5Ω is across the singlet. The propagation of normal zone from inner layer to outer layer of coil 1 is contoured in figure 7.21 for different time steps.

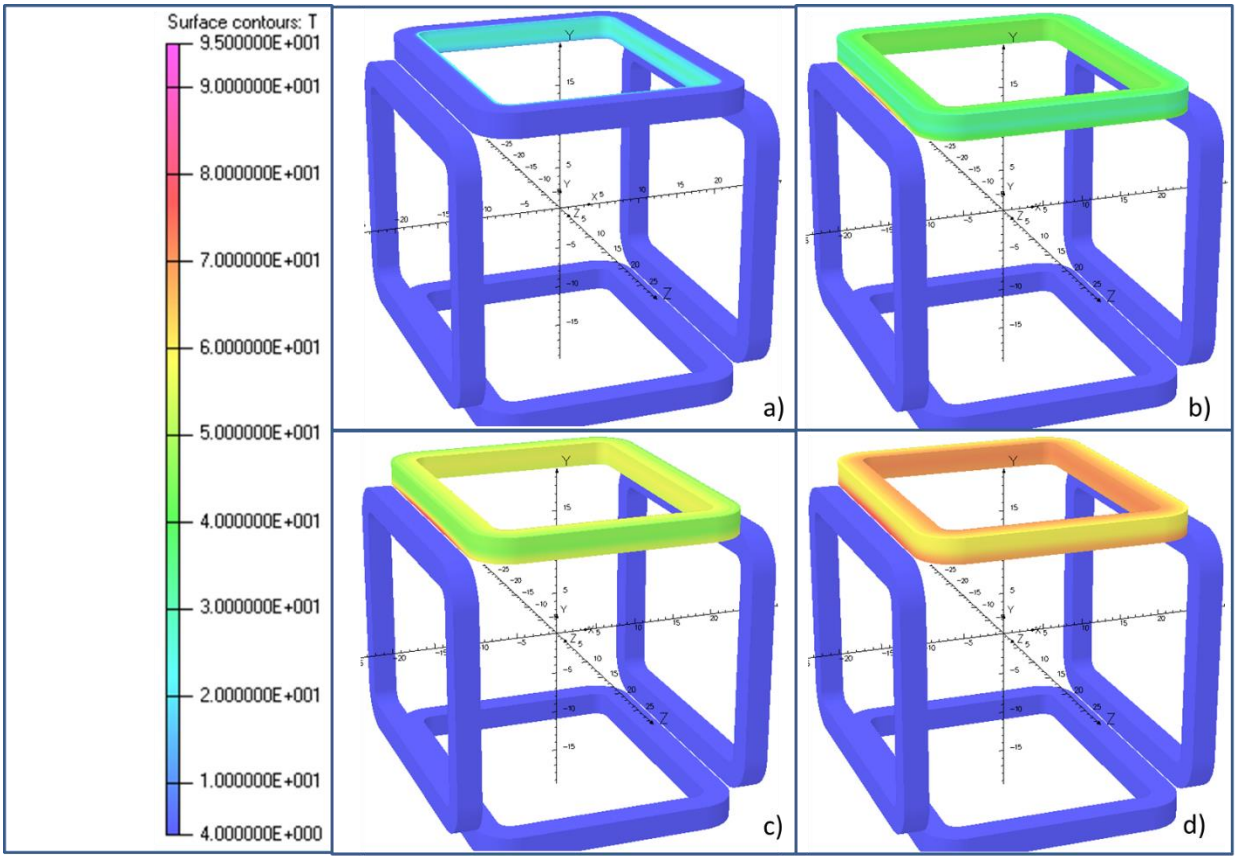

Figure 7.21 Temperature contours of the coil for the dumping resistor of 1.5Ω as the protection circuit for singlet at the different time steps a) t=0.1s, b) t=0.5s, c) t=1s and d) t=5s

The nature of temperature rise, resistance growth, current decay is similar to case 4 a). Due to smaller dumping resistor value more amount energy will dump into the magnet coil instead of dumping in to the resistor as QPS. The coil is subjected to maximum temperature of 91 K and peak voltage of 286.75 V is shown in figure 7.22 a) and c). Coil reaches to resistance of 7.605Ω because of dumping of energy within it. It is near to safety limit of 100 K which causes strain in coil above permissible limit of 0.1 %.

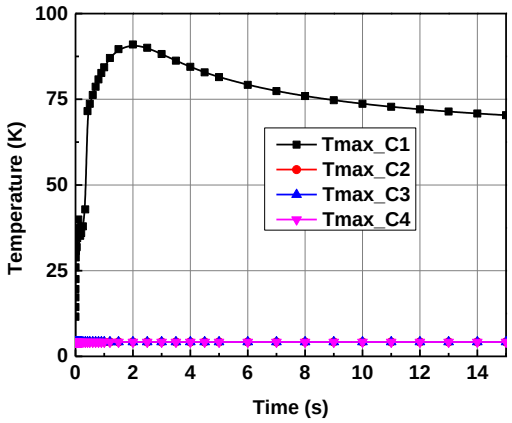

a) Temperature(K) Vs Time(s)

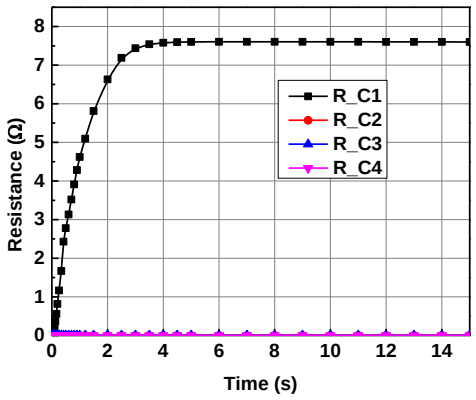

b) Resistance(Ω) Vs Time(s)

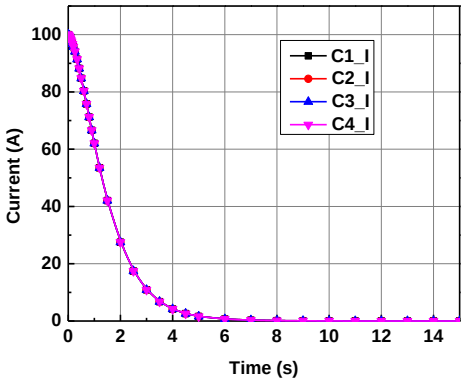

c) Current(A) Vs Time(s)

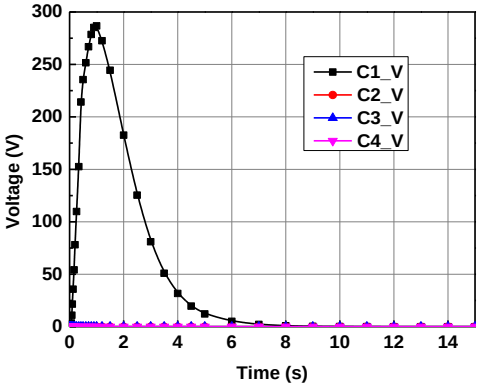

d) Voltage(V) Vs Time(s)

Figure 7.22 The Quench simulation results of the dumping resistor of 1.5Ω as the protection circuit for singlet

Comparison between case 4 a) and b)

The smaller value 1.5 Ω over 5Ω of dumping resistor causes to higher temperature of 91 K over 64 K, which is almost near to safety limit of 100 K. Peak voltage is 172.6 V and 286.75 V for 5 Ω and 1.5 Ω dumping resistor respectively. In case 1.5 Ω dumping resistor, coil 1 subjected to almost twice resistance growth as more amount energy is dumped in it compare to 5Ω dumping resistor case.

Case 5. Only Back-to-back diodes across the whole singlet structure

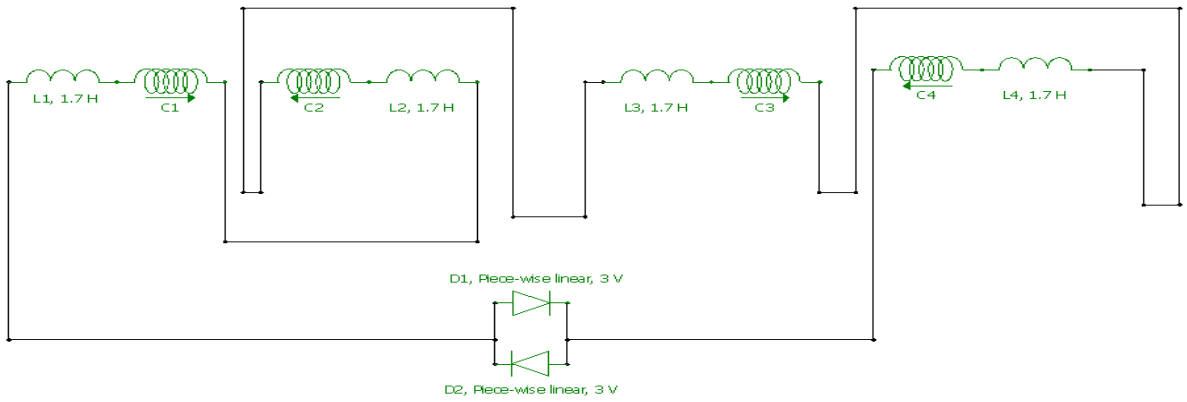

Figure 7.23 Electrical circuit for the back-to-back diode as protection circuit across the singlet

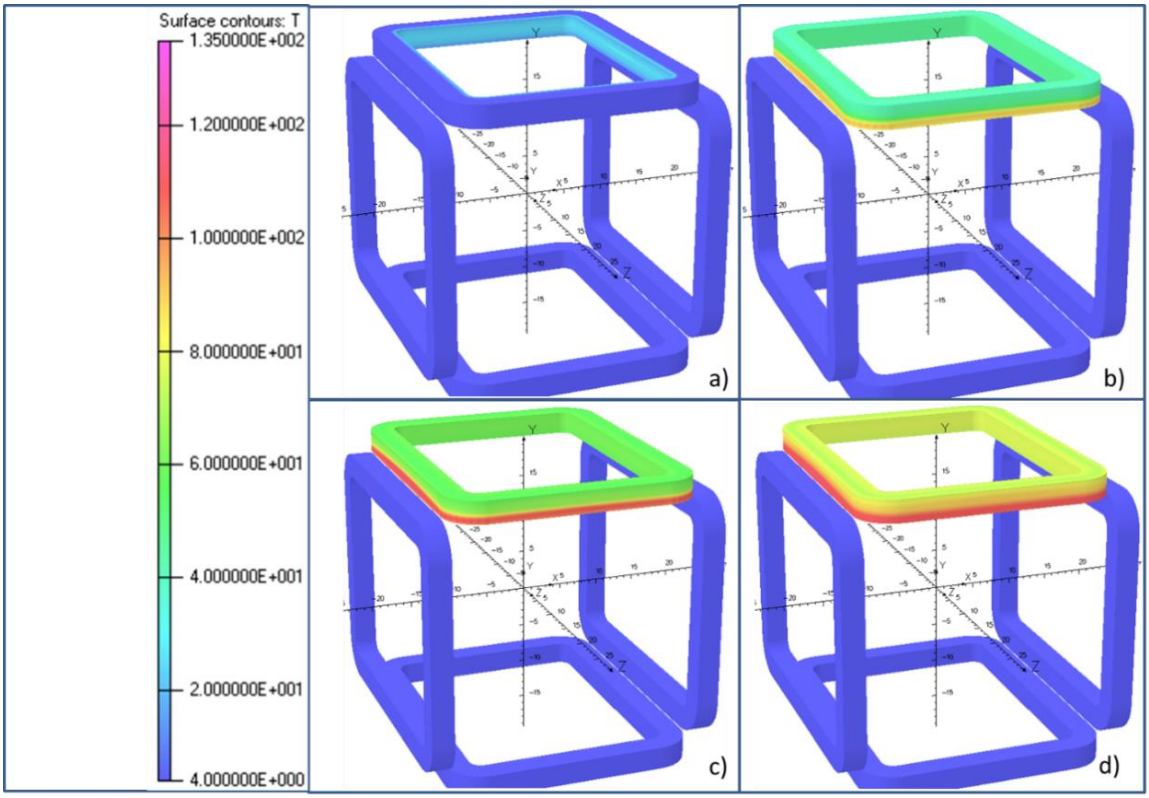

Figure 7.24 Temperature contours of the back-to-back diode as protection circuit across the singlet at the different time steps a) t=0.1s, b) t=0.5s, c) t=1s and d) t=5s

In figure 7.23, the back-to-back to diode decides the energizing ramping rate of magnet to achieve the designed current operating condition. The back-to-back diodes provides safety in any polarity of the current supply. It does not allow the current to flow still it forward voltage to be breakdown by the voltage generation across the singlet terminals. No dumping element is present in this circuit to share the stored energy, hence the singlet structure is subjected to whole stored energy to be dumped into the quenched coil which results in higher temperature of quenched coil with highest resistance value.

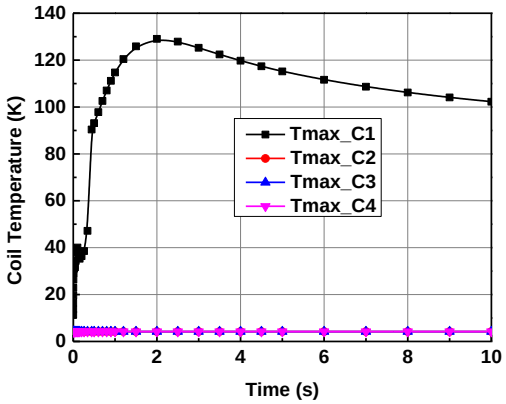

a) Temperature(K) Vs Time(s)

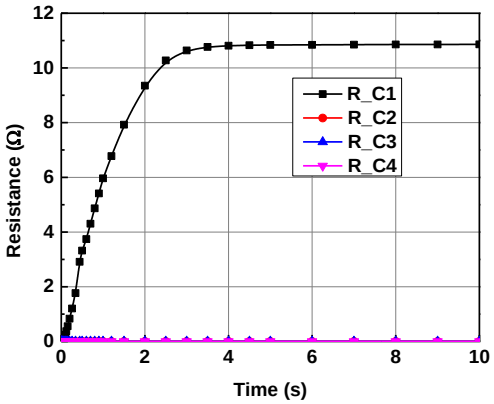

b) Resistance(Ω) Vs Time(s)

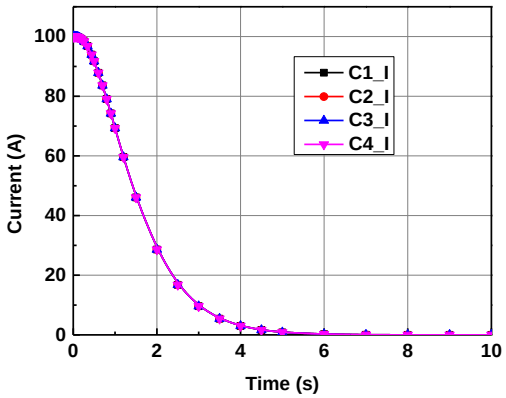

c) Current(A) Vs Time(s)

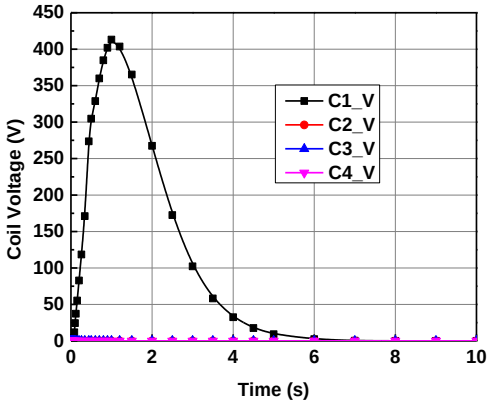

d) Voltage(V) Vs Time(s)

Figure 7.25 The Quench simulation results of the back-to-back diode as protection circuit across the singlet

The propagation of the normal zone from inner layer to outer layer of the coil 1 is shown in figure 7.24 for the different time conditions. For each time stepping the results are recorded and plotted as follows in figure 7.25 for quench temperature rise, the resistive zone growth, the current decay in coil and the voltage profile.

In this no dumping resistor is present into the circuit means full stored energy of the magnet will s=dump in to magnet itself after quenching. Hence coil is subjected to highest temperature of 129.07 K at 2sec which is above the safety limit of 100 K is shown in figure 7.25 a). Peak voltage

rise in coil 1 is 413.2 V which also large compared to other cases is shown in figure 7.25 d). The current decays in all coils in similar fashion as shown in figure 7.25 c). The maximum resistance is of 10.86Ω at the end of 10s is shown in figure 7.25 b).

Case 6. Back-to-back diode plus resistor as a protection circuit across the singlet

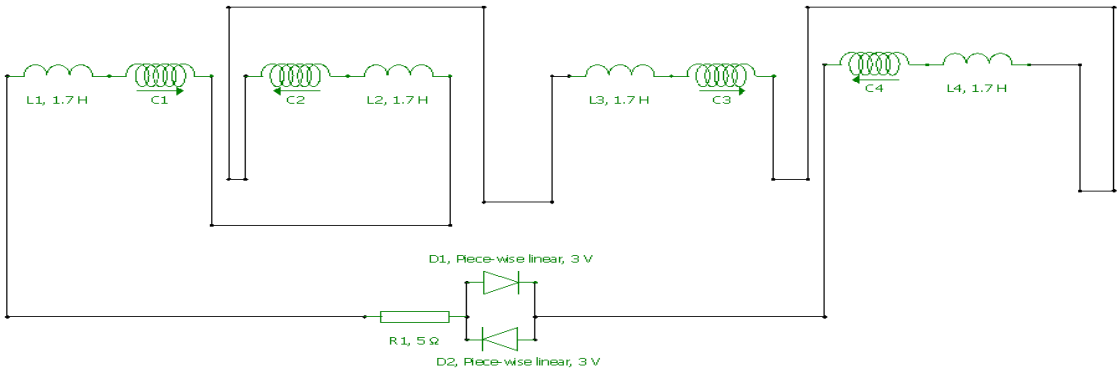

Figure 7.26 Electrical circuit for the back-to-back diode plus resistor as a protection across the singlet

The back-to-back diode plus resistor across singlet structure as a protection circuit allows the protection in both charging as well as in quench condition. At the time of charging, diodes decides the ramping voltage and restrict the current to flow through the resistor which does not allow boil-off of the liquid helium. And at the quench condition, diode start conducting with permission of dumping of the stored energy into the resistor.

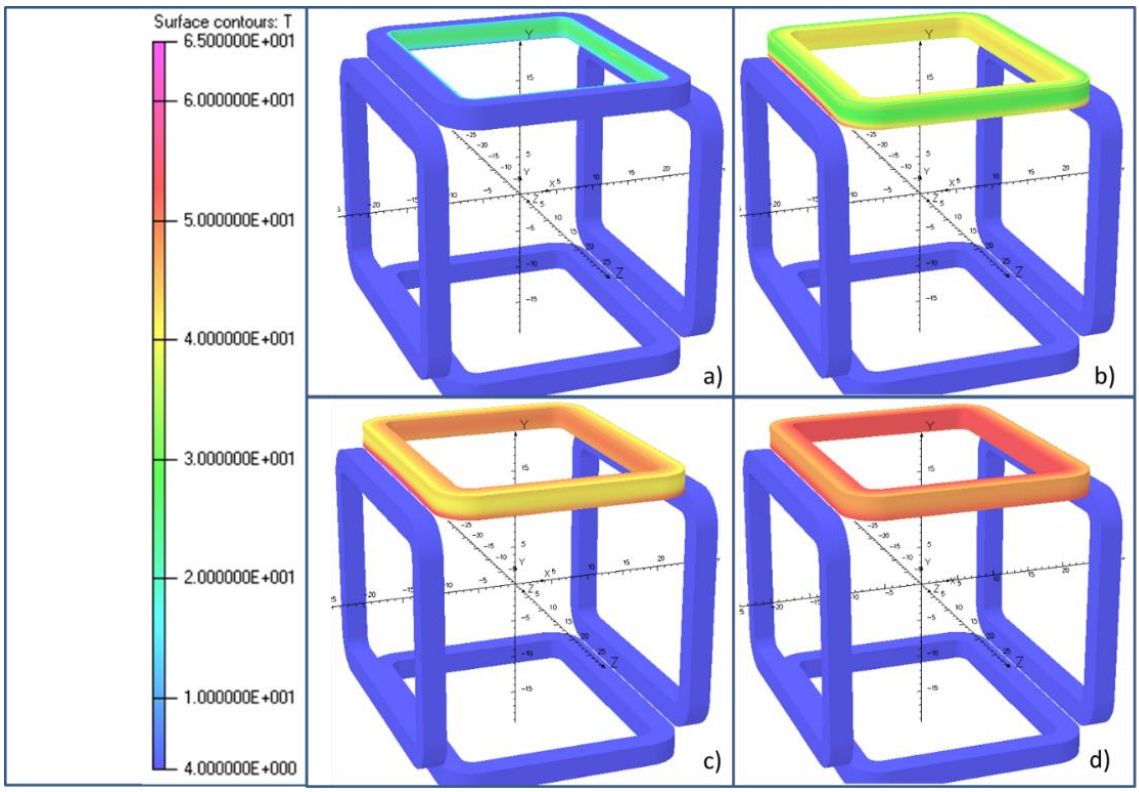

Figure 7.27 Temperature contours of the back-to-back diode plus resistor as a protection across the singlet at the different time steps a) t=0.1s, b) t=0.5s, c) t=1s and d) t=5s

The propagation of the normal zone from inner layer to outer layer the coil 1 is shown figure 7.27 for the different time conditions. For each time stepping the results are recorded and plotted as follows in figure 7.28 for quench temperature rise, the resistive zone growth, the current decay in coil and the voltage profile. Coil 1 reaches to maximum temperature of 63.2 K AT 1.5 s and peak voltage is 172.2 V at 0.5 s with resistance increment from superconducting state to 4.22Ω in 10 s is plotted in figure 7.28 a), d) and b) the decays simultaneously in all coils as shown in figure 7.28 c).

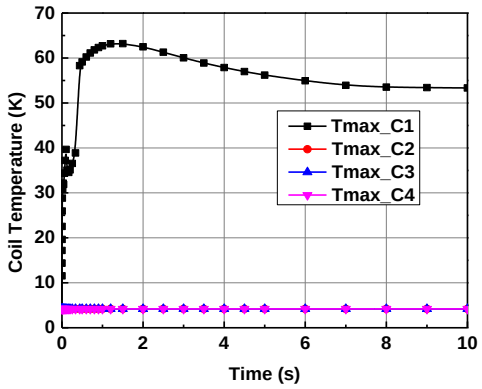

a) Temperature(K) Vs Time(s)

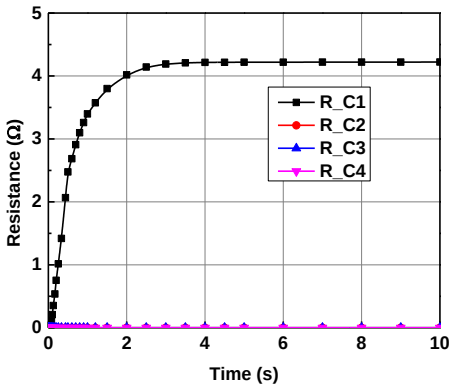

b) Resistance(Ω) Vs Time(s)

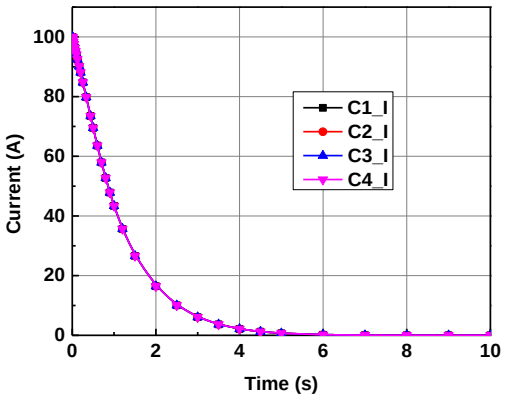

c) Current(A) Vs Time(s)

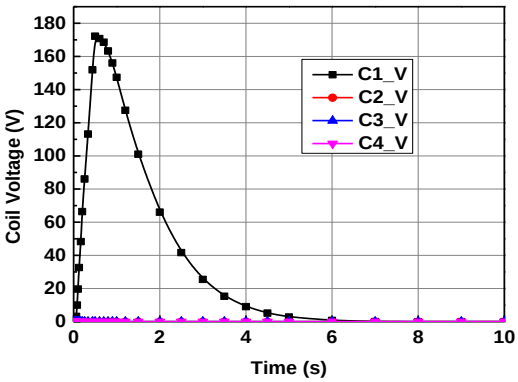

d) Voltage(V) Vs Time(s)

Figure 7.28 The Quench simulation results of the back-to-back diode plus resistor as a protection across the singlet

Comparison between case 4 a), 5 and 6

Case 4 a) and case 6 are shows almost similar behaviour for the quench parameters as both are having dumping resistor of 5Ω to dump the stored energy after quenching. In case 5, whole magnet energy dumped within the coil causes highest temperature rise of 129 K and peak voltage of 413.2 V which is above the safety limit of 100 K. While case 4 a) and 6 the maximum temperature rise is 63.43K and 63.2 K respectively. Coil 1 is subjected to resistance of 10.86Ω in case 5, while in case of 4 a) and 6 the highest resistance in coil 1 is 4.25Ω and 4.22Ω respectively. In all three cases, except coil1 all other remains at same temperature. And current decays in all coils in similar fashion in respective cases.

Chapter 8

8 DESIGN OF TEST CRYOSTAT FOR SUPERCONDUCTING QUADRUPOLE DOUBLET STRUCTURE

The basic function of a cryostat is to house and thermally insulate a superconducting device, while providing all the interfaces for its reliable and safe operation such as cryogen feeding, powering, diagnostics instrumentation, safety devices, etc. It is a metallic container, generally made of metals, to maintain the cryogenic environment. The cryostat is composed of the following components

- Vacuum jacket
- Thermal radiation shield
- Liquid helium (LHe) vessel
- Supporting systems.
- Venting systems
- Instrumentation

The quadrupole doublet structure (QDS) is going to be used in HYRA for beam focusing. Before directly putting into the operation with main cryostat assembly, this structure will be tested in LHe bath based test cryostat. Various quench protection systems and other operational parameters will also be tested in the test cryostat. In this design, nitrogen cooled thermal shield is not considered, instead MLI superinsulation is used to reduce the heat load to the LHe bath. The vacuum jacket of an existing facility will be used for this, while the helium vessel with the support structure have to be designed separately.

The design of the test cryostat consists of two sections as follows

1). Mechanical Design

2). Thermal Design

8.1 Material selection for the test vessel design

The LHe vessels are normally made of austenitic steels, since at cryogenic temperature austenitic structure doesn't show any ductile to brittle transition. Austenite is also stable at high magnetic field as it is non-magnetic in nature. For special applications SS316LN is preferable, where field effect should not alter the material properties at cryogenic temperature and provides non-corrosiveness, formability as well as ductility but from a cost reduction point of view SS304L is the better choice, which is a lower grade austenitic material over SS316LN. To hold the LHe vessel at some height from the bottom of the vacuum jacket, support structures are required and they should be capable of taking the load of QDS while providing minimum conduction heat load from ambient atmosphere to LHe vessel. The support structure is made of G10 material which is a laminated composite of thermosetting epoxy and glass fiber and provides high strength as well as good thermal insulation [22].

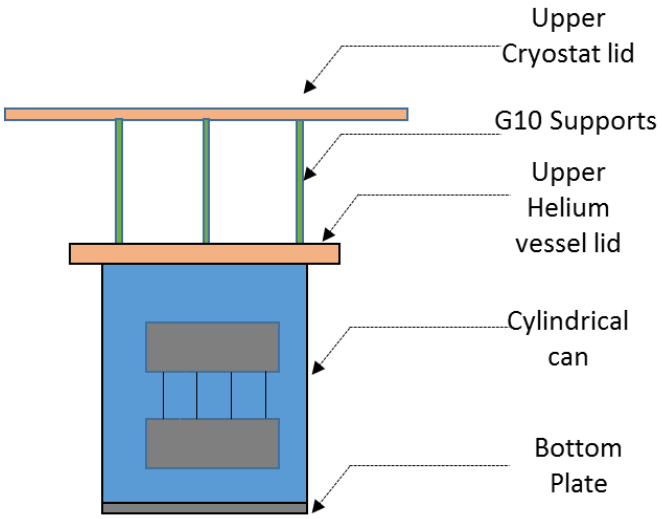

Figure 8.1 Schematic of the test cryostat for QDS testing

8.2 Mechanical Design

The cryogenic grade vessels are mostly considered as thin shells, with thickness variation in between 1-15mm range of sheet construction. The mechanical design should be within safety limit such that the designed component should bear the maximum operating load without any kind of failure. The design calculations of different parts are as followed.

8.2.1 Cylindrical CAN of LHe vessel

The CAN is subjected to gaseous helium pressure at the time of magnet operation and also vacuum loading at the time of evacuating. The CAN should have enough thickness to obtain the hoop stress and axial stress well below its material yield strength.

The cylinder hoop stress will be subjected to internal pressure P_i is given by

$$\sigma = \frac{P_i\, r_i}{t_c} \qquad (8.1)$$

Similarly, the longitudinal stress will be experienced along the length is given by

$$\sigma = \frac{P_i\, r_i}{2\, t_c} \qquad (8.2)$$

Where, P_i is internal pressure, r_i is internal radius ($r_i =$ 420 mm) and t is thickness of the CAN.

The hoop stress is normally kept below 50% of the yield strength of the material used. The longitudinal stress is half the hoop stress, hence a longitudinal joint running the length of the vessel needs to be twice as strong as a transverse joint. But for vacuum, the inverse of the internal pressure situation, the outer pressure will try to implode the CAN, rather than exploding it. To provide strength against buckling that a more conservative safety margin used to limit the hoop stress within 20-25% of the material's annealed yield strength [23].

Yield strength of SS304L (S_{yt}) at room temperature is 240 MPa. So, the permissible hoop stress is

$$\sigma_p = \frac{S_{yt}}{4} = = 60 \text{ MPa}$$

$$60 = \frac{0.1013 * 420}{t_c}$$

$$t_c = 0.71\ mm$$

But when subjected to external pressure, CAN must be designed against the radial buckling, which can lead to sudden collapse of the cylinder as it exceeds critical pressure.

For a thin vessel of infinite length, the critical pressure is given by

$$P_{cr} = \frac{E_e}{(1-\mu^2)} * \left(\frac{t_c}{r_i}\right)^3 \qquad (8.3)$$

From the general thumb rule$\left({}^{t_c}/_{r_0}\right) \geq 0.012$. So,

$$t_c \geq 5.05\ mm$$

Considering factor $f = 1.5$ for homogeneity purpose. So $f \times 5.05 = t_c$

$$t_c = 7.5\ mm$$

So critical pressure for safety margin,

$$P_{cr} = \frac{195 * 10^9}{(1-0.3^2)} * \left(\frac{0.0075}{0.42}\right)^3$$

$$P_{cr} = 3.0505\ bar$$

A CAN will be able to sustain up to 3.0505 bar pressure in radial buckling.

8.2.2 Bottom plate of the LHe vessel

The bottom plate is subjected to the weight of full Quadrupole Doublet Structure with plates for concentricity and the weight of liquid helium in the LHe vessel.

Table 8.1 the static load of Superconducting Quadrupole Doublet Structure

	Component	Number	Mass, kg
1	300 mm pole tip	4	200
2	250 mm pole tip	4	160
3	300 mm yoke	1	680
4	250 mm yoke	1	570
5	Intermediate connecting ring	1	50
6	Support Plates	2	120
7	Coils	8	80
8	Aluminium fixtures for coil	10	140
	Total mass of QDS		2000

8.2.2.1 Circular plate with concentric loading

The formula for calculation of bending stress for circular disk with edges simply supported is given by [24]

$$\sigma = \frac{6M}{{t_1}^2} \tag{8.4}$$

t_1 =Thickness of bottom plate

$$M = \frac{W}{4\pi} * \left[(1+\mu)\ln\left(\frac{r_i}{e}\right) + 1\right] \tag{8.5}$$

$$M = \frac{2000 * 9.81}{4\pi}\left[(1+0.3)\ln\left(\frac{0.42}{0.28}\right) + 1\right]$$

$$\sigma_{max} = \frac{S_{yt}}{2} = 120\ MPa$$

$$t_1 = 11\ mm$$

Where, M is bending moment acting on the plate, e is eccentricity in between centre of the plate and point of load application.

8.2.2.2 Circular plate with uniform loading

Bending stress at centre of plate due to uniform pressure (for simply supported edges) is given by [24]

$$\sigma_{max} = \frac{3(3+\mu)}{8{t_1}^2} * {Pr_i}^2 \qquad (8.6)$$

$$\sigma_{max} = \frac{1.238}{{t_1}^2} * 1.013 * 10^5 * 0.42^2$$

$$t_1 = 13.6\ mm$$

From above calculation bottom plate thickness with uniform loading condition is higher than the concentric loading condition, so t_1= 13.6 mm is preferred. As per the standard thickness of the bottom plate is $t_1 = 15\ mm$.

8.2.3 Upper Lid of LHe vessel

The LHe vessel is to be suspended inside cryostat at the end of G10 supports. The upper lid having four ports such as vent, current lead, instrumentation and safety port. These holes are main reason to weak the plate. Considering one big port is at centre, and designing the upper lid as a Circular Flat Plate with central hole, concentrated load at hole, simply supported at outer edge [24].

Table 8.2 k_1 and k_2 Rectangular Flat Plate, concentrated load at centre, edge clamped

a/b											
1.25		1.5		2		3.3		4		5	
k_1	k_2	k_1	k_2	k_1	k_2	k_1	k_2	k_1	k_2	k_1	k_2
0.341	0.1	0.519	1.26	0.672	1.48	0.734	1.88	0.724	2.17	0.704	2.34

$$\sigma_m = K_2 \frac{P}{{t_2}^2} \qquad (8.7)$$

$$t_2 = 21.43\ mm$$

We are taking standard size of t_2 = 25 mm.

8.2.4 Design of G10 support

The main reason of using G10 strips is to reduce the thermal load coming from the ambient. G10 is good insulator having good mechanical strength. The ultimate tensile strength at break for G10 is ~310 MPa. The G10 strips are subjected to tensile load. Generally these materials break at high load, so as per safety consideration factor of safety is 6, so permissible stress is 50 MPa.

$$\sigma_t = \frac{W}{A} \qquad (8.8)$$

Here 4 supports are used to hold the LHe vessel. So if the tensile load is 2500*9.81N then tensile stress is,

$$\sigma_t = \frac{2500 * 9.81}{4 * 20 * 20 * 10^{-6}}$$

$$\sigma_t = 15.33\ MPa$$

The tensile stress is within the permissible limit.

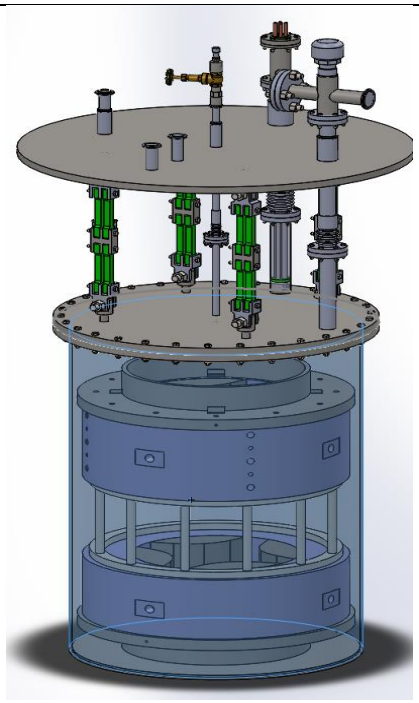

Figure 8.2 Isometric view the test cryostat

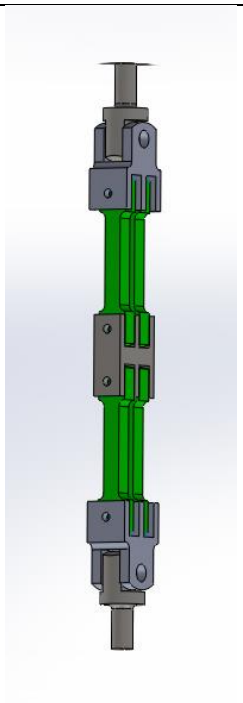

Figure 8.3 G 10 support structure

8.2.4.1 Simulation of the Support Structure

The support structure of the LHe vessel with upper lid of vacuum vessel and top plate of LHe vessel is simulated in static structural simulation environment in ANSYS R14.5. The simulated structure has shown in figure 8.2. The G10 support structure as shown in figure 8.3 goes under bending, whereas initial positioning is required to maintain LHe vessel's concentricity and height inside the vacuum jacket. To avoid the bending of G10 support which is more hazardous to break, universal joint are designed to ensure the movement in both lateral and transverse direction. The maximum principle stress (MPS) is 23.5 MPa and generated at the site of support structure attachments both at LHe vessel and Vacuum vessel plate. Figure 8.4 the MPS is well below permissible stress limit, so this design is acceptable.

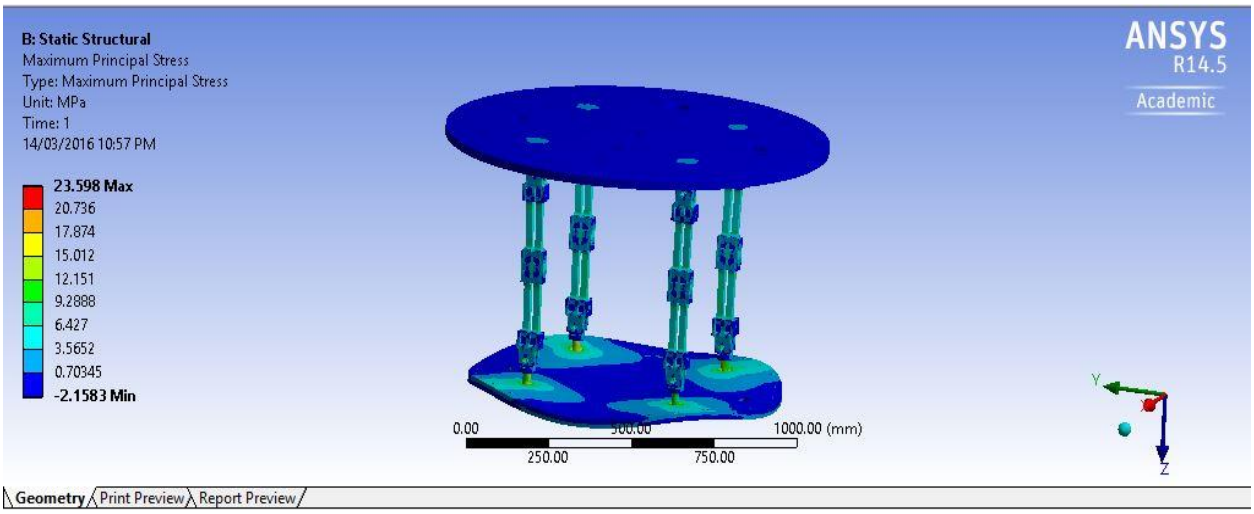

Figure 8.4 stress analysis of the support structure assembly

8.3 Thermal Design

8.3.1 Radiation Load

The radiation heat transfer from hot surface to cold surface is given by

$$q_{1-2} = \sigma . \varepsilon . A_1 (T_1^4 - T_2^4) \qquad (8.9)$$

The outer jacket is setting at atmosphere condition of 300 K and LHe vessel is at 4.2 K. The large temperature difference is there, so as to reduce radiation heat load on cold mass multi-layer insulation is used (IUAC has tested 30 layers of MLI gives heat load about

$$q = 2\ W/m^2).$$

Heat load due to radiation,

$$H_1 = q * A_{surface} \qquad (8.10)$$

Where, $A_{surface}$ is cold mass area = 4.5m^2.

$$H_1 = 9\ W$$

8.3.2 Conduction load

8.3.2.1 Conduction through the pipes

The pipes and bellows of all ports are of SS304L [25].

$$\int_{4.2\ K}^{300\ K} k\ dT = 3047.7 \frac{W}{m}\ (for\ the\ SS)$$

For the length of 600 mm,

The conduction heat load from each port is,

$$H_{21} = \left(\left(\frac{A}{L}\int_{4.2\ K}^{300\ K} k\ dT\right)_{current\ lead} + \left(\frac{A}{L}\int_{4.2\ K}^{300\ K} k\ dT\right)_{safety\ port} + \left(\frac{A}{L}\int_{4.2\ K}^{300\ K} k\ dT\right)_{vent\ port} + \left(\frac{A}{L}\int_{4.2\ K}^{300\ K} k\ dT\right)_{filling\ port}\right) \qquad (8.11)$$

$$H_{21} = 4\ W$$

8.3.2.2 Conduction Load through G10 Supports

Conduction load through four G10 support is,

$$\int_{4.2\ K}^{300\ K} k\ dT = 101.873 \frac{W}{m}\ (for\ the\ G10)$$

$$H_{22} = 0.272\ W$$

Total Heat load through the conduction is

$$H_2 = H_{21} + H_{22} = 4.272\ W$$

8.3.2.3 Heat load through the vapour-cooled current lead

To enhance the surface contact between the copper rods and upward moving helium gas. The SS tubes are welded inside the current lead port to guide the gas. As this lead of 600-700 mm in length, these are difficult to make them efficient as perfectly vapour cooled. Each lead is giving the load of 200 mW/A.

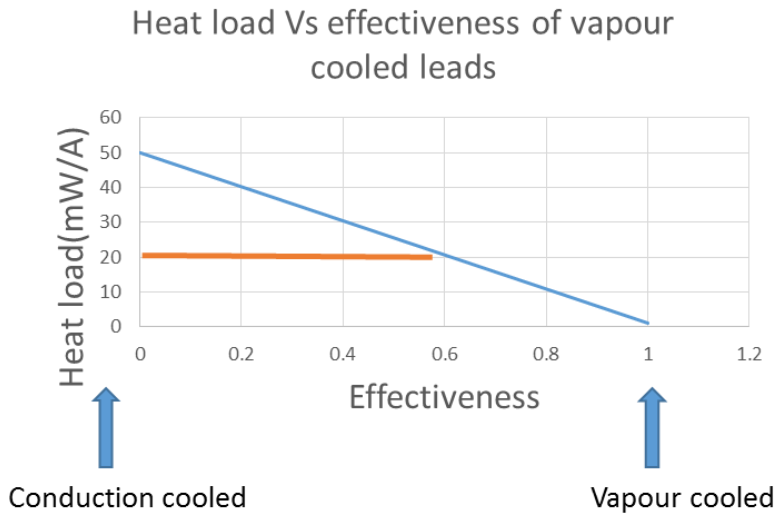

Figure 8.5 Head load Vs effectiveness of the vapour cooled current leads

The load due to 4 vapour cooled current lead working at 100 A current supply,

$$H_3 = 200 * 4 * 100 = 8\,W$$

8.3.3 The Total thermal load

The net heat load on the cold mass is summation of above two.

$$H_T = H_1 + H_2 + H_3 = 21.272\,W$$

8.3.4 Design of the vent port on the basis of heat load

The vent port should be designed to maximum heat load, so that any malfunction happens the gas from vessel can come out as fast as possible (chocking condition). For chocking condition of vent tube,

$$A_{vent} = \frac{H_T}{h_{fg}\rho_{vap}}\sqrt{\frac{m}{\gamma RT}} \qquad (8.12)$$

$$d_{vent} = 28\,mm\ (Standard\ availaible\ size)$$

8.3.5 The requirement of LHe for Test

The height of the Liquid inside the LHe vessel should be 1.1 m to fully deep the Superconducting QDS.

$$V_{LHe} = V_{1.1\,m} - V_{structure} = 0.386\ m^3 = 386\ l$$

$$M_{LHe} = \rho_{LHe} * V_{LHe} = 48.25\ kg$$

Chapter 9

9 CONCLUSION

1) The iron structure is able to shape the magnetic field lines within itself by exposing minimum fringe field to the surrounding cryostat environment and enhances the field at pole centre by providing minimum resistance path to flow these line.
2) The weak points such as pole tips, where magnetic field is concentrated are identified through magneto-static simulation.
3) The simulated results of the quench at higher operating current is prone quench early is validated with the tested coil result and heater is only for quench initiation purpose in simulation as well as in liquid helium dipped case.
4) To dump energy in the dump resistor or to decay post –quench current through the dump resistor, it is mandatory to physically isolate the Magnet power supply.
5) These Quadrupole coils are self-protected, hence temperature rise is well below the higher limit of temperature.
6) Very high voltage generation should be avoided. As arcing can damage the magnet.
7) The mutual coupling between the four single coils in Superconducting Quadrupole Singlet are studied with different quench protection circuits, which are going to be tested in designed test cryostat.

10 REFERENCES

[1] http://www.iuac.res.in/

[2] N MADHAVAN et al, "Hybrid recoil mass analyser at IUAC — First results using gas-filled mode and future plans", Pramana – J. Phys., Vol. 75, No. 2, August 2010

[3] Carl L. Goodzeit (Retired BNL, SSCL), Jan 2001, Lecture on "Superconducting Accelerator Magnets- An Introduction to Mechanical Design and Construction. Methods".

[4] http://www.cyberphysics.co.uk/topics/electricity/higher_electricity/superconductivity.htm

[5] Bernd T. Matthias, "MAGNETIZATION CURVES OF SUPERCONDUCTORS--TYPE I, TYPE II AND TYPE III", University of California http://lss.fnal.gov/conf/C721010/p90.pdf(1981)

[6] Dr. Soumen Kar, Lecture Note on "Cryogenics and Superconductivity-Ph.D. Course", Inter University Accelerator Centre, New Delhi.

[7] Ramesh Gupta, Lecture on "Superconducting Accelerator Magnets", US Particle Accelerator School , University of California – Santa Barbara June 23-27, 2003, BNL website

[8] Martin N. Wilson, "Superconducting Magnets", Clarendon Press, Monographs on Cryogenics(book)

[9] X. L. Guo et al, "Quench protection for the MICE cooling channel coupling magnet" Year:2009 Month:06 Volume:19 Issue:3 PAGE NO-1360-1363

[10] K.E. Robins et al, "SUPERCONDUCTING MAGNET QUENCH PROTECTION FOR ISABELLE" IEEE-1977 Volume:24 Issue:3

[11] Yamamoto, S. et al, "Quench protection of persistent current switches using diodes in cryogenic temperature", Year:1988, Page no.-321-325, IEEE PESC '88 Record., 19th Annual IEEE Power Electronics Specialists Conference - Kyoto, Japan (11-14 April 1988)]

[12] M.A.Green, “Quench Protection and Design of the high current density superconducting magnet” IEEE TRANSACTIONS ON MAGNETICS, VOL. MAG-17, NO. 5, SEPTEMBER 1981, Page no.1793-1798

[13] Yi Li et al, “A Passive Quench Protection Design for the 9.4 T MRI Superconducting Magnet,” IEEE TRANSACTIONS ON APPLIED SUPERCONDUCTIVITY, VOL. 24, NO. 3, JUNE 2014

[14] S. S. Chouhan et al, “Voltage Characteristics of Diodes Used for Passive Quench Protection of Low-Current Magnets”, IEEE TRANSACTIONS ON APPLIED SUPERCONDUCTIVITY, VOL. 25, NO. 3, JUNE 2015

[15] Lake Shore Cryotronics, Inc., “Lake shore cryotronics specification for a DT-670 silicon diode temperature sensor,” Westerville, OH, USA, 2016. [Online] Available: www.lakeshore.com

[16] Hongseok Lee et al, “Electromagnetic characteristics of a Superconducting Magnet for 28GHz ECR Ion Source according to the Series Resistance of a Protection Circuit” (Submitted on 11 Aug 2015) Physics > Accelerator Physics, Cornell University library

[17] P Schmuser, “Superconducting magnets for particle accelerators”, 1991,Reports on Progress in Physics, Volume 54, Number 5

[18] R. Carcagno et al, “Studies of the coild protection diodes”, Superconducting super collider laboratory” , Springer-Supercollider 2, Vol-2, Page no-25-38,1990

[19] M.A. Green et al, “Protecting the leads of a powered magnet that is protected with diodes and resistors” IEEE TRANSACTIONS ON APPLIED SUPERCONDUCTIVITY, VOL. 22, NO. 3, JUNE 2012

[20] Yi Li et al, “Quench protection design of an 8-T magnet built with low-and high-temperature superconducting coils,” IEEE TRANSCTIONS ON APPLIED SUPERCONDUCTIVITY, VOL.22,NO.5, OCTOBER2012

[21] M. A. Hilal et al, “Self-protection of high current density superconducting magnets” , IEEE Transactions on Magnetics (Volume:25 , Issue: 2), Mar 1989, Page no-1604-1607

[22] V. Parma, “Cryostat Design”, CERN Yellow Report CERN-2014-005, pp.353-399

[23] Jack Ekin, “Experimental Techniques for Low-Temperature Measurements: Cryostat Design, Material Properties and Superconductor Critical-Current Testing”(book)

[24] Richard G. Budynas et al, “ Roark’s Formulas for Stress and Strain”, eighth edition November 2011(book)

[25] THERMAL CONDUCTIVITY OF SOME SOLIDS, NBS Circular 556